THE DESIGN OF ELECTROSTATICALLY AUGMENTED MOVING BED GRANULAR GAS FILTERS

GERRIT KORNELIUS

A thesis submitted in fulfilment of the requirements for the degree of

PHILOSOPHIAE DOCTOR (ENGINEERING)

in the

SCHOOL OF ENGINEERING,

FACULTY OF ENGINEERING, THE BUILT ENVIRONMENT AND INFORMATION TECHNOLOGY

UNIVERSITY OF PRETORIA

November 2003

Magnificat anima mea Dominum
Et exsultant spiritus in Deo salutari meo.

For Petra and the girls in gratitude, and to my parents.

The following students are acknowledged as contributors to this work:

Jannie Lourens
Jeanne du Randt
Ken Bouchinger
Leon Kamffer
Danie Jacobs
Gerrit van de Pypekamp
Faffa du Preez
Theuns Venter
Werner Kruger
Joe Botha

while dr Gerrit Genis is thanked for enlightening discussions, especially on measurement error and its effect on parameters calculated from experimental results.

CONTENTS

SUMMARY

Title: **The design of electrostatically augmented moving bed granular gas filters.**
Author: **Gerrit Kornelius**
Supervisor: **Professor UHJ Grimsehl**
Department: **Chemical Engineering**
University: **University of Pretoria**
Degree: **Philosophiae Doctor (Engineering)**

Granular gas bed filters have been used in industry for a considerable period and mathematical descriptions of dust capture have allowed rigorous design of static beds. Provision for bed movement and electrostatic augmentation, which allows much thinner continuous beds to be used, requires adaptation of design methods for these phenomena.

Design methods that allow for this are developed for a cross-flow bed with vertical bed movement and a number of granule and dust types. Direct current charging is applied to the bed itself and to the particles before they enter the bed. In the case of electrostatic augmentation, it is shown that simple models of spherical particles describe the mechanism adequately. The advantages of pre-charging dust particles before they enter the bed are indicated by calculation and proved experimentally. Parameters to describe the enhancement of filtration efficiency by the collected dust are obtained experimentally.

It is shown that the factors controlling re-entrainment vary with particle size. For the dust particles less than 1,5 micrometers in size, re-entrainment is linked closely to the electrostatic capture mechanism which is dominant in that size range. For particles approaching 10 micrometer, re-entrainment can be neglected as the impaction efficiency, which is dominant for particles of this size and larger, approaches unity. A complex situation exists between these particle sizes as the magnitude and predominance of capture mechanisms in this region are determined by a number of operational parameters.

It did not prove possible to develop predictive equations for re-entrainment efficiency using the results of this study. A number of heuristics are however developed that allow rational design by the use of the empirical parameters found, and that will be valid for the range of parameters used in this work.

Key words: Granular beds, moving granular beds, filtration efficiency, electrostatic augmentation, gas filtration, re-entrainment.

Symbols used.

Symbol.		First used	Unit
a	Granule radius	Eq 3.2	[m]
B	Particle mobility	Eq 3.17	[s kg^{-1}]
B(ε)	Function of porosity	Eq 3.5	
C	Cunningham correction factor $=1+2\lambda_m/d_p[1,26+0,40\exp(-0,55d_p/\lambda_m)$	Eq 3.12	-
C_{bed}	Local dust concentration in bed	Eq 3.35	[kg m^{-3}]
C_{in}	Dust concentration at bed inlet	Eq 3.1	[kg m^{-3}]
C_{out}	Dust concentration at bed outlet	Eq 3.1	[kg m^{-3}]
d_g	Granule diameter	Eq 3.11	[m]
d_p	Particle diameter	Eq 3.10	[m]
D	Diffusivity of particle	Eq 3.11	[m^2 s^{-1}]
e	Charge of a single electron=$1,62.10^{-19}$C	Eq 3.26	
E	Bed filtration efficiency	Eq 3.1	-
E_0	Field strength	Eq 3.24	[V m^{-1}]
f(ε)	Function of porosity	Eq 3.3	
F_1	Function indicating increase in efficiency	Eq 3.27	
F_2	Function indicating increase in pressure drop	Eq 3.28	
g(ε)	Function of porosity	Eq 3.13	
k	Mass transfer coefficient	Eq 3.10	[m s^{-1}]
k_B	Boltzmann's constant = $1,380622.10^{-23}$	Eq 3.12	[J K^{-1}]
k_1	Constant	Eq 3.13	-
K_c	Constant	Eq 3.16	-
K_E	Electrostatic capture parameter	Eq 3.17	-
K_1	Constant	Eq 3.1	-
ℓ	Unit cell size	Para 3.2	[m]
L	Bed depth/width	Eq 3.2	[m]
m	Specific deposit	Eq 3.37	[kg m^{-3}]
n	Number of electron charges	Eq 3.26	
N_{Pe}	Peclet number = $d_gU_0/\mathbf{D}$	Eq 3.11	-
N_R	Interception parameter = $d_p/2a$	Eq 3.3	-
N_{Re}	Reynolds number of granule = $d_gU\rho/\mu$	Table 3.1	-
N_{Sh}	Sherwood number of particles = $kd_p/\mathbf{D}$	Eq 3.10	-
N_{St}	Stokes number of particle = $C\rho_p d_p^2 U_0/9\mu d_g$	Eq 3.5	-

N_{St}^{*}	Modified Stokes number = $B(\varepsilon).N_{St}$	Eq 3.5	-
N_{St}^{+}	Modified Stokes number = N_{St}/ε	Eq 3.8	-
N_0	Ionic density of gas	Eq 3.24	$[m^{-3}]$
P	Bed penetration	Eq 3.1	-
$q_{p,d}$	Charge of particle due to diffusion charging mechanism	Eq 3.26	[C]
$q_{p,f}$	charge of particle due to field charging mechanism	Eq 3.24	[C]
$q_{p,f,s}$	saturated particle charge due to field charging mechanism	Eq 3.24	[C]
T	Temperature	Eq 3.12	[K]
U_0	Superficial gas velocity	Eq 3.11	$[ms^{-1}]$
U_∞	In-bed flow field gas velocity	Eq 3.17	$[ms^{-1}]$
v	Local bed velocity	Eq 3.30	$[ms^{-1}]$
V	Average ionic velocity	Eq 3.26	
w_j	volume fraction of the *j*th size fraction=σ_j/σ		
x	Horizontal position in bed	Eq 3.34	[m]
y	Vertical position in bed	Eq 3.34	[m]
Z	Electrical mobility of ions	Eq 3.24	$[m^2\ V^{-1}\ s^{-1}]$
α_1,α_2	Parameters to calculate collection efficiency increase for monodisperse particles	Eq 3.27	-
$\alpha_{1(kj)},\alpha_{2(kj)}$	Parameters to calculate the efficiency increase for the *k*th size fraction in a bed loaded with the *j* th fraction of polidisperse particles	Eq 3.29	
β_1,β_2	Parameters to calculate increase in pressure drop	Eq 3.28	
ε	Bed porosity	Eq 3.1	-
ε_c	Relative di-electric constant of collector (granule)	Eq 3.17	-
ε_p	Relative di-electric constant of particle	Eq 3.20	
ε_0	Gas permittivity	Eq 3.25	$[F\ m^{-1}]$
ε_m	Relative di-electric constant of the bed matrix	Eq 3.18a	
η	Single granule efficiency	Eq 3.1	-
$\eta_{0,d}$	Efficiency of clean granule due to diffusion	Eq 3.13	-
$\eta_{0,E}$	Efficiency of clean granule due to electrostatic mechanisms	Eq 3.19	-
$\eta_{0,i}$	Efficiency of clean granule due to interception	Eq 3.3	-
$\eta_{0,imp}$	Efficiency of clean granule due to impaction	Eq 3.7	-
κ	Efficiency coefficient	Eq 3.23	

λ_m	molecular free path length	Symbols list	[m]
λ	Filter coefficient of filter after elapsed time	Eq 3.27	[m^{-1}]
λ_0	Filter coefficient of clean filter	Eq 3.27	[m^{-1}]
μ	Gas viscosity	Eq 3.12	[Pa.s]
ρ_d	Bulk density of dust	Eq 3.37	[kg m^{-3}]
ρ_g	Gas density		[kg m^{-3}]
ρ_p	Particle density	Symbols list	[kg m^{-3}]
σ	Specific deposit of collected dust	Eq 3.28	[m^3 m^{-3}]
σ_j	Specific deposit of the *j*th size fraction of collected dust	Eq 3.29	
φ_g	Sphericity of granule	Eq 3.15	
φ	Collector polarisation coefficient=$(\varepsilon_c-1)/(\varepsilon_c+2)$	Eq 3.17	
ω	Bed di-electric parameter=$3+\varepsilon(\varepsilon_c-1)$	Eq 3.22	

CHAPTER 1.
INTRODUCTION

1.1 SCOPE OF THE THESIS

This thesis reports the results of a study on the efficiency of a moving granular bed used for air pollution control. The study was prompted by the advantages which this type of gas cleaning apparatus offers in special applications where the conventional types show certain shortcomings. The objective is to find generally applicable and robust design methods for moving granular beds, including the effect of applied electrostatic fields on the efficiency of such beds.

Equipment for the engineering control of particulate air pollution can be divided into four broad classes (Boegman 1979)

- mechanical separators mainly applied for the removal of large particles, which in this context means particles larger than say 10 micrometers - this type of equipment, which usually has a low capital cost and a relatively low pressure drop is often used as a precleaner to reduce the load on the following three classes -
- electrostatic precipitators which can handle large gas volumes at a low pressure drop
- bag filters which can produce very low outlet concentrations
- wet scrubbers for hot or combustible gas streams.

Each of these main types has certain limitations. Wet scrubbers for instance have a high energy consumption and reduce the gas temperature, thus limiting its atmospheric dispersion potential and creating water pollution and sludge disposal problems, while bag filters are limited in the handling of high temperature gases and "sticky" dusts (Cooper and Alley 1994). It is therefore difficult to apply equipment from the three last-mentioned classes to situations where dust has to be removed from gas at high temperature, such as would for example be required where gas from fluidized bed combustors is to be used in gas turbines (Andries 1993, Ahmadi and Smith 2002). Another problematic case is the removal of hygroscopic or water soluble salts, which tend to complicate cleaning of filter bags and cause corrosion problems in wet electrostatic precipitators or wet scrubbers. Such an application, for the filtration of particulate matter containing condensed fume particles of potassium and sodium salts from exhaust gas of a sinter plant in the South African iron and steel industrial sector (von Reiche *et al.* 1983, von Reiche *et al.* 1992) gave direct rise to the work described here. For such applications, the granular bed offers a possible solution.

1.2 GRANULAR BED DESCRIPTION

The granular bed utilises a granular medium, with the granules typically being two orders of magnitude or more larger than the particles which are to be removed. The gas stream that is to be cleaned moves through the granular bed in countercurrent, crosscurrent or cocurrent mode and the particles are removed from the gas by attachment to the granules. The bed acts as a depth filter rather than a surface filter (Rajagopalan and Tien 1979). For use on an industrial scale, the filter medium must be replaced

or cleaned. This can be done by replacement with new medium on an intermittent basis (Arras and Berz 1972) but more conveniently by removing the medium, cleaning it off-line and returning it to use in a continuous manner (Combustion Power Company 1979, Abatzoglu *et al.* 2002).

1.3 HISTORICAL OVERVIEW

1.3.1 Static granular beds

The filtration of liquids and gases through a bed of granular medium developed as an industrial process during the 19th century. A patent for the clarification of molasses in sugar factories was for example granted in 1888 (Arras and Berz *op cit.*). Early applications to gas filtration are summarized by Squires and Pfeffer (1970) and Tien (1989). A static bed was mostly used, being replaced when the pressure drop became excessive. Large-scale commercial applications followed the introduction of *in situ* cleaning methods, for example by mechanical shaking (Berz and Maus 1977) or by reverse flow together with rotating rakes (Hermann 1973). Although this arrangement required cyclical operation, it was used on large scale for the off-gas of cement clinker coolers, lime and gypsum kilns, zinc furnaces, anode coke production and for ammonium chloride fume (Hoffmann and Brachthäuser 1988)

1.3.2 Continuous granular beds

The first continuously operated granular bed filters were of the horizontal type, operated in the fluidized bed mode. Cook *et al.* (1971) and Rush *et al.* (1973) describe filters with a granular alumina medium treating emissions from electrolytic aluminium cells. They were fed mechanically and overflowed directly into the cells.

Non-fluidized continuous beds were developed during the 1950's. These are described by Kornelius and von Reiche (1984), Perry (1984) and Elvers *et al.*(1988). The medium moves vertically by gravity between Venetian blind-shaped screens. The vertical flow rate is controlled by rotating valves or pneumatic removal of the medium at the bottom of the bed. In the configuration designed by the Combustion Power Company (1979) the medium was cleaned during vertical pneumatic transport back to the top of the bed (Storms *et al.* 1983), but bucket hoists have also been used. The Lurgi company has marketed a cyclically operating version of the pneumatically regenerated vertical bed (Lurgi 1986)

.

A number of review articles have appeared indicating that, under carefully chosen operating conditions, gas from fluidised bed combustors, even where lime or dolomite is used for desulphurisation, may be cleaned to gas turbine inlet specification at up to 800°C and 1 MPa. (Henry *et al.* 1982 and 1985, First 1985, Shaw 1986, Zakkay *et al.* 1989, Pitt 1989, Andries 1993, Zevenhoven 1992, Zevenhoven *et al.* 1992, 1993a, 1993b)

1.3.3 Electrostatic augmentation

Pilney and Erickson (1968) first described the improvement in the filtration efficiency of a bed of polystyrene beads caused by the tribo-electric charging of the granules. This was subsequently confirmed through measurement of the granule charges by Tardos *et al.* (1979,1983). The Combustion Power Company was first to utilize the phenomenen commercially (von Reiche 1983, Guillory *et al.* 1981). As not all bed materials are electrostatically charged or polarised and the field strength developed without an applied field is difficult to control, the electrostatic driving force in the commercial application was created by applying an electric direct current potential between an electrode placed vertically in the centre of the bed and the containing screens. Dust particles are charged tribo-electrically and by the applied field and migrate under the influence of the field, thus augmenting the mechanical filtration mechanisms. A parametric study by Snaddon (1985) shows that with the application of a sufficiently intense field (> 10^5 Volt/m) the particles may be charged within the bed to such an extent that electrostatic capture mechanisms become predominant. This type of filter was applied to particulate control in wood-fired boilers and in sinter plants in the metallurgical industry. In both cases, particles of approximately 0,5 micrometer in diameter, which due to their high potassium content are "sticky" and therefore not amenable to removal in bag filters are successfully captured (von Reiche *et al.* 1992). Parallel bed versions of the vertically-moving type, with a fast-moving first stage to prevent blinding and a slower moving (and thicker) second stage to provide dust holding capacity have been described (Sundstrom and Leith 1982, Zahedi and Alexander 1983, Jordan and Lindner 1988)

Kallio and Dietz (1980) and Kallio *et al.*(1980) have argued that electrostatic augmentation has limited effect at temperatures exceeding 500°C. This is due to the increase in conductivity of the medium so that a sufficiently strong field can not be established. It thus seems that this temperature represents an upper limit to the utility of electrostatic augmentation.

1.3.4 Particle charging

It has been shown theoretically by Henry *et al* (1985) and confirmed by Mazumder and Thomas (1967) and Nielsen and Hill (1976a, 1976b, 1981) that charging of dust particles before these enter the bed may considerably improve the filtration efficiency, especially when the bed is thin and allows only a limited retention time for particle charging within the bed. Kornelius *et al.* (1987), Kornelius (1991),Kornelius and von Reiche(1993) and de Haan (1985) demonstrated experimentally that this was in fact the case in static beds composed of commercially available granular media, and this effect is included as part of this study.

1.4 THIS STUDY

The cross-flow vertically moving gravel bed with an applied electric field is the configuration that has found the most application. It has a low pressure drop with a concomitant low energy consumption. However, no rigorous design equations have appeared in the literature for this specific configuration. It is the purpose of this study to propose design equations for such filters and test them using a laboratory scale apparatus. Due to the advantages obtained in respect of filtration efficiency when dust particles are precharged, particular attention will be given to the effects of this phenomenen.

Chapter 2 describes the mechanisms of particle capture and release that operate in a granular bed, and how these mechanisms are modified by the loading and movement of the bed. Chapter 3 gives the mathematical description of the mechanisms which together make up the design equations. Chapter 4 describes the experimental apparatus and its operation. Chapter 5 gives experimental results, compares them to theoretical values and proposes modifications to the design equations. Chapter 6 gives conclusions and proposes further areas of research.

1.5 REFERENCES

Abatzoglu, N. *et al.* (2002): US Pat. 6 436 161: Mobile granular filtration apparatus for hot gas conditioning.

Ahmadi, G., Smith, D.H. (2002). Analysis of Steady-state Filtration and Backpulse Process in a Hot-Gas Filter Vessel. Aerosol Sci. Tech. **36** p 665-677

Andries, J. (1993). *FBC research at the Delft test rig.* Delft University of Technology Laboratory for Thermal Power Engineering Internal report GRANOFOR.WB1

Arras, K., Berz, W. (1972). Gravel bed filters for clinker coolers. IEEE Conf. Rec. P.229

Berz, W.M., Maus, W. (1977). Entwicklungstand des Schüttschichtfilters. Zement-Kalk-Gips **30** (1) pp.3-6

Boegman, N. (1979) *The development of a national policy for the control of air pollution in South Africa.* Ph D thesis, University of the Witwatersrand.

Combustion Power Company (1979) *The Electroscrubber*™ Menlo Park, California

Cook, C.C. *et al.* (1971). Operating experience with the Alcoa 398 process for fluoride recovery. J. APCA **21** (8) pp. 479-483

Cooper, D.C., Alley, F.C. (1994) . *Air pollution control: A design approach.* 2nd ed. Prospect Heights, Illinois: Waveland Press

De Haan, P.H. (1985) . Een geëlektrificeerd korrelbedfilter als vliegasfilter voor kolengestookte installaties. Energiespectrum Jan pp. 23-29

Elvers, B. *et al.* (eds)(1988) *Ullmann's Encyclopedia of Industrial Chemistry* 5th ed. Vol B2 pp. 13.25 -13.29 VCH, Weinheim.

First, M. (1985) Gas cleaning systems for the high temperature high pressure fluidized bed coal combustor. J.APCA **35** (12) pp. 1286-1297

Guillory, J.L. *et al.* (1981) . Electrostatic enhancement of moving bed granular filtration. Env. Int. **6** pp. 387-395

Henry, R.F. *et al.* (1982). Gas cleanup systems for fluidized bed coal combustors. Filt.Sep. Nov/Dec pp. 502-506

Henry, R.F. *et al.* (1985) A review of electrostatically augmented gas cleaning devices for particulate removal IEEE Trans. Ind.Appl. **IA-21** (4) pp. 959-949

Hoffmann, H., Brachthäuser, M. (1988). Neuartiges Schüttschichtfilter für die Heissgasreinigung. Chem.-Ing.-Tech. **60** (1) pp. 36-38

Hermann, G. (1973). Die Entstaubung der Schacht- und Drehrohröfen in der Kalk- und Zementindustrie. Zement-Kalk-Gips **26** (9)

Jordan,S., Lindner,W. (1988) Betriebserfahrungen mit einem Querschnitt-Schüttschichtfilter. Chem.-Ing.-Tech. **60** (1) pp. 34-35

Kallio, G.A., Dietz, P.W. (1980). *Image charge collection of fine particles in granular beds.* General Electric Rep 80CRD096

Kallio, G.A. *et al.* (1980). Theoretical and experimental filtration efficiencies in electrostatically augmented granualr beds. Proc 2nd Symp. On Transfer and Utilization of Particulate Control Technology Vol 3 pp. 344-362

Kornelius, G., von Reiche, F.V.K. (1984). The applicability of gravel bed filters in air pollution control. Proc. 6th Int Conf on Air Pollution, Pretoria, South Africa.

Kornelius, G. *et al.* (1987). Gasfiltrasie deur gruisbeddens met aanwending van 'n elektriese veld. Clean Air Journal (SA) **7** (3) pp. 15-20

Kornelius, G. (1991) Elektrostatiese gruisbeddens vir gasfiltrasie: Die invloed van partikellading op doeltreffendheid. Proc. SAIChE Nat.Conf., Durban

Kornelius, G., von Reiche F.V.K. (1993) Gravel bed filters with electrostatic augmentation: Laboratory and plant experience. Proc. CHISA 1993, Prague

Lurgi South Africa (Pty) Ltd (1986). *The new granulate-tube-filter.*(sales brochure)

Mazumder, M.K., Thomas, K.T. (1967). Improvement of the efficiency of particulate filters by superimposed electrostatic forces. Filt.Sep. Jan/Feb pp. 25-30

Nielsen, K.A., Hill, J.C. (1976a). Collection of inertialess particles on spheres with electrical forces. Ind. Eng .Chem. Fund **15** (3) pp. 149-157

Nielsen, K.A., Hill, J.C. (1976b). Capture of particles on spheres by inertial and electrical forces. Ind. Eng. Chem.Fund. **15** (3) p 157-163

Nielsen, K.A., Hill, J.C. (1976c). Collection of inertialess particles on spheroids and spheres with electrical forces and gravitation. Chem. Eng .Comm. **12** pp. 171-193

Perry, R. H., Green, D.W. (eds.) (1984).*Chemical Engineers' Handbook* 6th ed. p 20.104-20.105. New York, N.Y.: McGraw-Hill

Pilney, J.P., Erickson, E.E. (1968). Fluidized bed fly ash filter. J APCA **18** (10) pp. 684-685

Pitt, R.U. (1989). Heissgasentstaubung. Brennstoff-Wärme-Kraft **41** (3) pp. L4-L9

Rajagopalan, R, Tien, C. (1979). Trajectory analysis of deep-bed filtration with the sphere-in-cell porous media model. AIChE J **22** (3) pp. 523-533

Rush, D. *et al.* (1973). Air pollution abatement on primary aluminium potlines: Effectiveness and cost. J. APCA **23** (2) p 98-104

Shaw, G.D.H. (1986). *The engineering assessment of the moving granular bed filter.* Energy Research Institute, University of Cape Town Report 109

Snaddon, R.W.L. (1985). Electrically enhanced collection of respirable aerosols in granular bed filters at low Reynolds numbers. IEEE Trans. on Industrial Applications **IA-21** (2) pp. 501-506

Squires, A.M., Pfeffer, R. (1970). Panel bed filters for simultaneous removal of fly ash and sulfur dioxide: 1. Introduction. J APCA **20** (8) pp. 534-538

Storms, S.R. *et al.* (1983). Weyerhaeuser's experience with Electroscrubber™ filters on its large wood and multifuel boilers: Case studies for the Longview, Columbus and Plymouth mills. Proc. TAPPI Environment Conf., Atlanta, Georgia

Sundstrom, G., Leith, D. (1982). High efficiency collection of fly ash in a parallel bed filter. Filt.Sep Jan/Feb. pp. 34-36

Tardos, G.I.*et al.* (1979) Triboelectric effects in filtration of small dust particles in a granular bed Ind. Eng. Chem. Fund. **18** (4) pp. 433-435

Tardos, G.I. *et al.* (1983). Filtration of airborne dust in a tribo-electrically charged fluidized bed. Ind.Eng. Chem. Fund. **22** (4) pp. 445-453

Tien, C. (1989) *Granular filtration of aerosols and hydrosols.* Boston, Mass. : Butterworths

von Reiche, F.V.K. *et al.*(1983). Application of the Electroscrubber™ filter to Iscor's alkali-controlled iron ore sintering plants. Proc. EPA Symposium on Iron and Steel Pollution Abatement Technology. Chicago, Illinois

von Reiche, F.V.K. *et al.*(1992). South African ironmaking experience with high-alkali fine iron ore. Proc. Annual Conf. of the National Association for Clean Air. Vereeniging, South Africa

Zakkay, V. *et al.* (1989) Particulate and alkali capture from PFBC flue gas utilizing granular bed filters. Combust. Sci.&Tech.**68** pp. 113-130

Zahedi, K., Alexander, J.C. (1983) US patent 4374652: Filter apparatus and method for collecting fly ash and fine dust.

Zevenhoven, C.A.P. (1992) *Particle charging and granular bed filtration for high temperature application.* Ph.D thesis, Technical University of Delft.

Zevenhoven, C.A.P. *et al* .(1992) The filtration of PFBC combustion gas in a granular bed filter. Filt.Sep. May/June pp. 239-244

Zevenhoven, C.A.P. *et al.* (1993a) High temperature gas cleaning fot PFBC using a moving granular bed filter. Proc. 2nd Int. Symp. on gas cleaning at high temperatures, Univ. of Surrey.

Zevenhoven, C.A.P. *et al.* (1993) The filtration of PFBC combustion gas in a granular bed filter. Proc. 6th World Filtration Congrass, Nagoya

CHAPTER 2
INTERACTION BETWEEN FILTRATION MEDIUM AND PARTICLES: MECHANISMS

2.1 INTRODUCTION

The design of gravel bed filters requires that the mechanisms that capture, retain and release particles be understood to the extent that a quantitative description is possible using a minimum of empirical parameters. Such a description is complicated by

- the simultaneous operation of a number of capture mechanisms
- the change in dominant mechanism with changing particle and filter parameters
- the possible interaction between the mechanisms
- the influence of bed loading of the bed
- the removal of dust from the bed granules due to movement of the bed.

These factors, and others that require consideration in the design process, will now be individually discussed.

2.2 CAPTURE MECHANISMS

Simple mechanical collectors such as cyclones or settling chambers, which are not subject to the operational difficulties mentioned earlier, will readily collect particles whose diameter exceeds 10 micrometers. They are in fact often used as pre-collectors (Patterson 1984). On the other hand, particles smaller than 0,1 micrometers make up a neglible mass fraction of dusts found in typical industrial applications. In the following discussion, only those mechanisms operating on particles between these sizes will therefore be described in detail.

The gravel bed filter acts as a depth filter and the normal surface filter equations do not apply. Mechanisms that have been identified as playing a role in depth filtration are the following:

2.2.1 Gravity

Dust particles fall from the gas on to the surface of the granule in a gravitational field (Paretsky *et al.* 1971, Lee 1981, Patterson 1984). The mechanism is important only for relatively large particles ($\approx$ 50 micrometer) for which normal mechanical separators are adequate, and will therefore not be considered further in this work.

2.2.2 Direct interception

The dust particles follow a gas streamline that passes the granule within a distance of half a particle diameter or less ("grazing distance") and is captured (Patterson 1984). It has been shown by Kimura *et al.* (1985) that deviation from a perfect spherical shape of granule, as may be expected in full-scale installations, influences the efficiency for this mechanism positively.

2.2.3 Inertial interception

The inertia of a particle is such that it leaves the streamline where the latter changes direction to pass around the granule, and hence the particle impacts on the granule surface (Knettig and Beeckmans 1974, Tardos and Pfeffer 1980, Walters 1982, Patterson 1984).

Both the latter mechanisms are important for the particle sizes considered here (‹ 20 micrometer), although Tien (1989) states that direct interception is of major importance only when inertial interception is negligible.

2.2.4 Diffusion

A dust concentration gradient exists between the bulk of the gas and the granule surface. This gradient causes a particle flux towards the granule surface (Tardos *et al.* 1983, Tardos and Snaddon 1984). The mechanism is of importance mainly for particles ‹ 1 micrometer in size and is therefore considered here.

2.2 5 London- or van der Waals forces

Short-term asymmetry in molecular structures may cause temporary attraction due to dipoles (Spielman and Fitzpatrick 1973, Prieve and Ruckenstein 1974). A parametic study by the latter authors shows that these forces may be neglected as a collection mechanism for the parameters obtaining in this study. Similarly, thermal precipitation, where particles move in the thermal gradient between the gas and the granule (Pilat and Prem 1976) may be neglected under the steady state assumptions in this work.

2.2.6 Electrostatic capture

Electrostatic forces may take a number of forms (Knutson 1975; Nielsen and Hill 1976a, 1976b; Self *et al.* 1981; Shapiro *et al.* 1983, 1986)

(i) Both granule and particle may be electrostatically charged and thus experience Coulombic forces (Tardos and Pfeffer 1979, Pfeffer and Tardos, 1981).

(ii) Similarly, the charged particle may experience a Coulombic force due to its movement in an electrostatic field (Shapiro *et al.* 1983), termed the external electrostatic field force. The field lines are distorted by the presence of granules and, for the correct combination of polarity of the particle charge and the electrostatic field are drawn inwards to the granule. The work of Barker *et al.* (1991) on liquid filtration makes provision for the gradual collection of charge by the granules and the resultant reduction in the net attractive force on the particles, but it is shown by Zahedi and Melcher (1976), Dietz and Melcher (1978) and Dietz (1981) that the assumption of no net charge on the granules is appropriate to the conditions pertaining in gas

filtration in fixed (as opposed to fluidized) beds. This mechanism, with the assumption of no net granule charge, is therefore the dominant one in granular beds.

(iii) A charged particle in a homogeneous cloud of similarly charged particles in the vicinity of a neutral granule experiences an uneven space-charge distribution resulting in a net repulsion force from the cloud towards the granule. Dietz (1981) has shown that, unless the concentration of charged particles is extremely high, the effect is negligible.

(iv) A charged dust particle may induce charge polarization in a neutral granule. This is called the image force and may lead to attraction or repulsion (Kallio and Dietz 1980). It has been shown by Self *et al.* (1981) and Shapiro *et al.* (1983) that the image force need be considered only for very small (< 0,01 micrometer) particles. It is therefore neglected in this study.

(v) A charged particle experiences differential forces at its poles in a non-homogeneous electrostatic field. The non-homogeneity may be present in the external field, or may be induced by the presence of charges on the granule. This force is described as the dielectrophoretic force. Similarly, an uncharged particle in an inhomogeneous electrostatic field may experience an induced dipole and a resultant force. Shapiro *et al.* (1983) and Self *et al.* (1981) have shown that these forces are at least an order of magnitude less than the Coulombic forces in the particle size range of interest here (< 20 micrometer) and they are therefore not considered further in the present study.

2.3 INTERACTION BETWEEN CAPTURE MECHANISMS

Many authors have accepted as self-evident that the different capture mechanisms should be additive. (Self *et al.* 1981, Pendse and Tien 1982a, Tien 1982). For the mechanisms of direct interception, impaction and diffusion, Gutfinger and Tardos (1979) demonstrated by calculation that the results of rigorous particle trajectory calculations and simple addition of the mechanisms differ only marginally. Previously, Prieve and Ruckenstein (1974) showed the same for the combination of diffusion, impaction, interception, gravity and London forces. On the other hand, Peters *et al.* (1985) argue that at least direct interception, impaction and electrostatic mechanisms should be regarded as independent events, for which the penetrations should be multiplied instead of efficiencies being added.
In practice, the results according to the above-mentioned summation methods differ by small margins only. This is due to two reasons

- Under given conditions of flow velocity, size ratio between particle and granule, and other process parameters, one of the mechanisms is dominant
- Efficiencies calculated for single granules are often relatively small so that simple addition is a reasonable approximation (Coury *et al.* 1987)

2.4 PARTICLE RETENTION

A number of authors have indicated that not all particles that collide with a granule are retained (Dahneke 1971, Hiller and Löffler 1980, Löffler 1983). Retention of particles is due to van der Waals

forces or, in the case of electrostatically enhanced beds, to Coulombic forces (MacLean 1972), and if the energy associated with plastic deformation during collision exceeds the retention energy, the particle will not be retained. Prediction methods for specific pairs of materials (of the granule and the particle) based on this approach have met with limited success (Hiller and Löffler *op.cit.*). Similarly, efforts to correlate lack of retention with the Stokes number (and thus particle momentum) show no direct correlation (Yoshida and Tien 1985, Clift 1984, Kalinowski and Leith 1983), indicating incomplete understanding of the physical processes. In addition, as bed porosity is reduced by deposition of dust on the granules, interstitial gas velocity may increase to the extent that drag forces cause re-entrainment of particles (Yuu and Oda 1983), but the onset of this phenomenon will be determined by specific conditions of bed loading and filtration velocity.
An additional mechanism for the release of particles from granule surfaces operates in moving beds. This is the mechanical force generated by slippage between granules (Kalinowski and Leith *op cit.*). The magnitude of this force will be determined by the same variables that determine shear stresses within the bed such as bed depth, intra-bed friction coefficients and the pressure drop caused by gas flow.

2.5 BED LOADING

Deposition of dust on bed granules influences both bed efficiency and pressure drop. The effect is not the same for stationary and moving beds.

For stationary beds, it was shown by trajectory calculations by Payatakes *et al.* (1974) and Pendse and Tien (1982b) that deposition does not occur as a uniform coating on the granules, but as a combination of a uniform coating and dendrites or "tree growths" on the granules. This has a profound influence on the porosity of the deposit and requires empirical determination of the influence of the parameters (Takahashi *et al.* 1986, Peukert and Löffler 1991, Jung 1991, Friess and Yadigaroglu 2002) although generally a monotonously increasing relationship is observed between efficiency and specific deposition (Sundstrom and Leith 1982, Walata as cited by Tien 1984, Choo and Tien 1993) until an upper limit in improvement is approached, probably due to particles being re-entrained as the interstitial gas flow increases in velocity (Tien 1982, Wada *et al.* 1984, Peters *et al.* 1985).

For moving beds, Shaw (1986) has noted a deterioration in moving bed efficiency from an initial clean condition as the bed becomes more loaded. Tsubaki and Tien (1988) have shown that this eventually reaches an equilibrium condition, independent of the downward velocity of the bed.

2.6 PARTICLE CHARGING

Forced electrostatic charging of particles taking place both in the pre-charger and in the bed itself has been studied in considerable detail because of its importance in the design of electrostatic precipitators,

especially for the electric power industry. Standard texts have appeared (White 1963, Bohm 1982, White 1984). It is generally agreed that charging takes place by two mechanisms:

- For particles less than approximately 0,1 micrometer in diameter, particle charging occurs predominantly by diffusion of ions (generated by electrical discharge at a negative electrode and diffusing at a rate commensurate with their position in the thermal energy distribution) to the surface of the particle. As ions accumulate on the particle, a repulsive field is set up and the charging rate slows down because increasingly higher thermal energy is required to overcome this.
- For particles above approximately 1 micrometer in diameter, the particles are sufficiently large to act as targets for the ions moving in the electrostatic field between the (negative) discharge electrode and the positive one. Charging occurs by impaction of charged ions on the particles and is described as field charging. Collection of ions by the particle ceases when the field set up by the cumulatively collected ions prevents further impaction. This condition is referred to as a saturation charge.

Between the two particle sizes, neither of the mechanisms is predominant and both have to be taken into account. As the resulting differential equations are awkward to solve analytically, approximate or numerical methods with an acceptable accuracy have been developed (White 1984).

2.7 REFERENCES

Barker, R.E. *et al.* (1991) Granular Electrofiltration. Sep. Technology **1** p 166-174

Bohm, J. (1982) *Electrostatic precipitators.* Amsterdam, Elsevier.

Choo, C-u., Tien,C.(1993) Transient-state modelling of deep bed filtration. Wat. Sci. Tech. **27** (10) p 101-116

Clift, R. (1983). Fundamental processes in gas filtration. Trans. Inst. Eng. Austr. **ME8**, p 181-191

Coury, J.R. *et al.* (1987). Capture and rebound of dust in granular bed gas filters. Powder Techn. **50** p 253-265

Dahneke, B. (1971). The capture of aerosol particles by surfaces. J. Colloid &Interface Sc. **37** (2) p 342-353

Dietz, P.W., Melcher, J.R. (1978) Interparticle forces in packed and fluidized beds. Ind. Eng. Fundam. **17** (1) p 28-32

Dietz, P.W. (1981). Electrostatic filtration of inertialess particles by granular beds. J. Aerosol Sc. **12** p 27

Friess, H. , Yadigaroglu, G. (2002). Modelling of resuspension of particle clusters from multilayer aerosol deposits with variable porosity. J.Aerosol Sc. **33** p 883-906

Gutfinger, C, Tardos, G.I. (1979). Theoretical and experimental investigation on granular dust filters. Atmos. Environ. **13** p 853-867

Hiller, R., Löffler, F. (1980). Influence of particle impact and adhesion on the collection efficiency of fibre filters. Ger. Chem. Eng. **3** p 327-332

Jung, Y. (1991). *Granular filtration of mono-dispersed and poly-dispersed aerosols.* Ph D dissertation, Syracuse University

Kalinowski, T.W., Leith, D. (1983). Aerosol filtration by a co-current moving granular bed: Penetration theory. Environ. Sc. Technol. **17** p 20-26

Kallio, G.W., Dietz, P.W. (1980). *Image charge collection of fine particles in granular beds.* General Electric Rep 80CRD096

Kimura, N. *et al.* (1985) Effect of particle shape on the efficiency of collection of a granular-bed filter taking into account both diffusion and direct interception. Int. Chem. Eng. **25** (3) p 143-145

Knettig, P., Beeckmans, J.M. (1974). Capture of monodispersed aerosol particles in a fixed and in a fluidized bed. Can. J. Chem. Eng. **52** p 703-706

Knutson, E. O. (1976). Approximate formulas for electrostatic collection of aerosol particles by spheroids. J. Colloid and Interface Sc.**54** p453

Lee, K.W. (1981). Maximum penetration of aerosol particles in granular bed filters. J. Aerosl Sci. **12** p 79-87

Löffler, F. (1983). Partikelabscheidung an Tropfen und Fasern. Chem. Ing. Techn. **55** (3) p 171-178

MacLean, K.J. (1977). Cohesion of precipitated dust layer in electrostatic precipitators. J. APCA **27** p100-1103

Nielsen, K.A., Hill, J.C.(1976a). Collection of inertialess particles on spheres with electrical forces. Ind. Eng. Chem. Fund. **15** (3) p 149-157

Nielsen, K.A., Hill, J.C.(1976b). Capture of particles on spheres by inertial and electrical forces. Ind. Eng. Chem. Fund. **15** (3) p 157-163

Paretsky, L. *et al.* (1971). Panel bed filters for simultaneous removal of fly ash and sulfur dioxide. J APCA **21** (4) p 204-209

Patterson, G. (1984) Particulate pollutant characteristics. *in* Calvert, S. and Englund, H.M.(eds) *Handbook of Air Pollution Technology.* New York, J Wiley, Ch 6

Payatakes, A.C.*et al.* (1974). Application of porous media models to the study of deep bed filtration. Can. J. Chem. Eng. **52** p 722-733

Pendse, H., Tien, C. (1982a). General correlation of the initial collection efficiency of granular filter beds. AIChE J. **28** (4) p 677-686

Pendse, H., Tien, C. (1982b). A simulation model of aerosol collection in granular media. J. Colloid and Interface Sc. **87** (1) p 225-241

Peters, M.H. *et al.* (1985). A dynamic simulation of particle deposition on spherical collectors. Chem. Eng. Sci. **40** (5) p 723-731

Peukert, W. and Löffler, F. (1991). Influence of temperature on particle separation in granular bed filters. Powder Techn. **68** p 263-270

Pfeffer, R, Tardos, G.I. (1980). Capture of aerosols on a sphere in the presence of weak electrostatic forces. Ind. Eng. Chem. Fund. **20** (2) p 168-171

Pilat, M. J. , Prem A. (1976). Calculated particle collection efficiencies of single droplets including inertial impaction, Brownian diffusion, diffusiophoresis and thermophoresis. Atmos. Environ. **10** (1) p 13-19

Prieve, D.C., Ruckenstein, E. (1974). Effect of London forces upon the rate of deposition of Brownian particles. AIChE J. **20** (6) p 1178-1187

Self, S.A. *et al.* (1981). Electrical augmentation of granular bed filters. Env. Int. **6** p 397-414

Shapiro, M, *et al.* (1983). Electric forces in aerosol filtration in fibrous and granular filters – a parametric study. Atmos. Environ. **17** (3) p 477-484

Shapiro, M *et al.* (1986). Electrostatically enhanced granular bed filters. Aerosol Sc. Technol. **5** p 39-54

Shaw, G.D.H. (1986). *The engineering assessment of the moving granular panel filter.* Energy Research Institute, University of Cape Town, Report 109

Spielman, L.A., Fitzpatrick, J.A. (1973). Theory for particle collection under London and gravity forces. J. Colloid and Interface Sc. **42** (3) p 606-623

Sundstrom, G. , Leith, D. (1982). High efficiency collection of fly ash in a parallel flow filter. Filt. Sep. Jan/Feb

Takahashi, T. *et al.* (1986). Transient behaviour of granular filtration of aerosols – effect of aerosol deposition on filter performance. AIChE J. **32** (4) p 684-690

Tardos, G.I ..*et al.* (1979). Experiments on aerosol filtration in granular sand beds. J. Colloid and Interface Sc. **71** (3) p 616-621

Tardos, G.I.,. Pfeffer, R. (1980). Interceptional and gravitational deposition of inertialess particles on a single sphere and in a granular bed. AIChE J. **26** (4) p 698-701

Tardos, G.I.,. Pfeffer, R. (1979). Proc. 2nd World Filtration Congress, London. p 239

Tardos, G.I. .*et al.* (1983) . Filtration of airborne dust in a tribo-electrically charged fluidized bed. Ind. Eng. Chem. Fund. **22** p 445-453

Tardos, G.I., Snaddon, R.W. L. (1984). Separation of charged aerosols in granular beds with imposed electric fields. AIChE Symp. Series **80** (234) p 60-69

Tien, C. (1982) . Aerosol filtration in granular media. Chem. Eng. Comm. **17** p 361-382

Tien, C. (1989) *Granular filtration of aerosols and hydrosols.* Boston, Mass. : Butterworths

Tsubaki, J. and Tien, C. (1988). Gas filtration in granular moving beds – an experimental study. Can. J. Chem. Eng. **66** p 271-275

Wada, K. *et al.* (1985). Study of a packed-bed dust collector. Int. Chem. Eng. **24** (1) p 135-145

White, H.J. (1963). *Industrial electrostatic precipitation.*, Reading, Mass.: Addison-Wesley

White, H.J. (1984) Control of particulates by electrostatic precipitation *in* Calvert, S., Englund H.M.(eds.) *Handbook of air pollution technology.* New York, J Wiley & Sons

Yoshida, H., Tien, C. (1983). A new correlation of the initial collection efficiency of granular aerosol filtration. AIChE J. **31** (10) p 1752-1754

Yuu, S., Oda, T. (1983). Disruption mechanism of aggregate aerosol particles through an orifice. AIChE J. **29** (2) p 191-198

Zahedi, K., Melcher, J.R. (1976) Electrofluidized beds in the filtration of submicron aerosol. J. APCA **26** (4) p 345-352

CHAPTER 3
MATHEMATICAL DESCRIPTION

3.1 INTRODUCTION

It is the purpose of this chapter to list, and develop where necessary, the equations that describe the filtration efficiency of electrostatically augmented moving granular beds. Bed efficiency has traditionally been found by calculating the efficiency of dust capture for single granules under clean bed conditions, and extending the results to granule assemblies (Paretsky *et al.*1971, Pilat and Prem 1976, Nielsen and Hill 1976, Tardos *et al.* 1978, Rajagopalan and Tien 1979, Degani and Tardos 1981, Pendse and Tien 1982, D'Ottavio and Goren 1983, Yoshida and Tien 1985, Peukert and Löffler 1991). Allowance is then made for the influence of previously collected dust (Chiang and Tien 1985a, 1985b, Walata *et al.* 1986, Fichman *et al.* 1988, Gutfinger *et al.* 1988, Jung 1991, Jung and Tien 1991, 1992, 1993, Choo and Tien 1993), which has not previously been allowed for in the presence of an electrostatic field. Lastly, the influence of bed movement must be allowed for. For this phenomenon, no directly applicable equations were found and they are therefore developed here.

3.2 BED CAPTURE EFFICIENCY DERIVED FROM SINGLE GRANULE EFFICIENCY

Single granule efficiency is calculated by dividing the number of particles captured by a granule of radius **a** by the number of all particles approaching the granule through a cross-sectional area πa^2 centered on the granule. The efficiency of the bed, **E**, or alternatively the penetration, **P**, is defined by

$$E = 1 - P = 1 - \frac{C_{out}}{C_{in}} \qquad \text{.....(3.1)}$$

(Jung, 1991) and is related to single-granule efficiency by

$$E = 1 - \exp\left[-K_1(1-\varepsilon)\frac{L}{2a}\eta\right] \qquad \text{.....(3.2)}$$

with K_1 given alternatively by 1,5 (Snaddon and Dietz 1980, D'Ottavio and Goren 1983), $1{,}5/\varepsilon$ (Paretsky *et al.* 1972, Tardos *et al.* 1974) or $(6/(\pi(1-\varepsilon)))$ (Tien and Payatakes 1979, Pendse and Tien 1982, Yoshida and Tien 1985). In the latter case, a characteristic dimension ℓ of the unit cell instead of the granule diameter 2a is used in the defining equation 3.2 . Conversion between the efficiencies calculated by different authors is therefore possible, provided that one converts η_o values obtained at one value of K_1 to those based on other values.

3.3 SINGLE GRANULE CAPTURE EFFICIENCIES

A large number of equations have been proposed for single granule efficiency. A summary and discussion is given by Jung (1991). The discussion indicates that it is necessary to obtain equations for the different mechanisms shown to be operating in different regimes of operating parameters as indicated in paragraph 2.2, and even then to analyse studies by different authors carefully for

similarities or dissimilarities in operating parameters. The following paragraphs list the equations used in this study and gives reasons for the selections.

3.3.1 Direct interception. Calculations were first carried out by Ranz and Wong (1952) for ideal or potential flow around single cylinders or spheres. For ideal flow in a bed of spherical collectors or granules, Tardos and Pfeffer (1980) use Lamb's flow field to calculate

$$\eta_{0,i} = 1{,}5\,[f(\varepsilon)]^3\, N_R^2 \quad \text{.....(3.3)}$$

with **f(ε)** approximately equal to **1,3/ε**. In the range of bed porosity of practical interest viz. 0,35<ε<0,45 values obtained differ little from the values calculated from the equation given by Paretsky (quoted by Coury *et al.* 1987) obtained using similar methods viz

$$\eta_{0,i} = 6{,}3\,\varepsilon^{-2{,}4}\, N_R^2 \quad \text{.....(3.4)}$$

or from the values calculated by Lee (1981) using Kuwabara's flow field. A similar form of equation is derived by Tien (1989) using a constricted tube model instead of the spherical collector model.

A number of authors have found empirically that the expressions for direct interception require correction from the relatively simple form given above at high Reynolds numbers. For this purpose, the free granule Reynolds number (as opposed to the actual Reynolds number as experienced by the granule in the bed) is used for ease of calculation. The proposed corrections are given below in Table 3.1, with the values obtained at Reynolds numbers of 10 and 80, which are the lower and higher values used in this work.

Table 3.1 : Correction factors for interception efficiency

Author	Correction	Value at N_{Re} = 10	Value at N_{Re} = 80
Ciborowski and Zakowski (1977)	$N_{Re}^{0,30}$	1,995	3,723
Pendse and Tien (1982)	$(1 + 0{,}04N_{Re})$	1,40	4,20
Yoshida and Tien (1985)	$7 - 6 \exp(-0{,}0065\, N_{Re})$	1,378	3,092
Kimura *et al.* (1985)	$N_{Re}^{0,25}$	1,778	2,991

It will be noted that the values of the correction factors differ relatively little from each other. The values corresponding closest to the conditions used in this work will be discussed under results in Chapter 5

3.3 2 Inertial interception or impaction. The mechanism finds application in meteorology, industrial hygiene, biology, defence research and environmental engineering and has therefore been studied by a large number of researchers (Ranz and Wong 1952, Starr 1967, Beard and Grover 1974, Knettig and

Beeckmans 1974, Pilat and Prem 1976, Degani and Tardos 1981, Fichman and Pnueli 1982, Peters *et al.* 1982,1985, Pulley and Walters 1992). A summary is given by Tien (1989). From the basic force balance equation for a particle moving in a gaseous medium, it can be deduced that the velocity vector of a particle in a flow field close to a target granule must be a function of the gas velocity vector, the ratio between particle size and granule size (Jackson and Calvert 1966) and the Reynolds number of the sphere (Gal *et al.* 1985). For direct interception and diffusion, the argument can be made that these mechanisms are influenced by the flow fields very close to the granule and that solutions calculated using creeping flow around single spheres are probably close to correct. However, impaction is more probably influenced by the entire flow field and therefore more sensitive to the assumptions made about the flow field in a granular bed. In addition, the assumption underlying the force balance that the particle follows Stokes' law, where the local relative velocity between particle and granule is used, may be an oversimplification in view of the acceleration and torque experienced in the boundary layer.

Dimensional arguments lead to the conclusion that single granule impaction efficiency must be a function of at least the dimensionless groups Reynolds number N_{Re}, Stokes number N_{St}, and, for an assembly of granules, the porosity ε. The initial correlations based on potential or viscous flow fields around single spheres (summarised by Tardos *et al.* 1978) were soon replaced by those based on models for flow fields in assemblies of spheres, for instance those of Happel (1952) for viscous flow or Neale and Nader (1974) for flow at $N_{Re} < 10$. It was found experimentally that impaction occurred at Stokes numbers (based on open bed flow) considerably lower than those predicted by this theory. As an example, Gutfinger and Tardos (1979) state that the impaction efficiency calculated by Neale and Nader's flow field becomes essentially zero at $N_{St} = 0{,}1$ while Gal *et al.*(1985) show through the use of the flow field description of Snyder and Stewart (1966) and also experimentally that impaction occurs at N_{St} as low as 0,01. This observation underscores the importance of taking into account the modification of flow that occurs around a granule contained in an assembly when compared to an isolated sphere, which was first described as a "flow intensification factor" by Snaddon and Dietz (1980), although without a systematic comparison with experimental data.

Based on this phenomenon, D'Ottavio and Goren (1983) suggest that boundary layer theory may be used at low Reynolds numbers, but with the open bed gas velocity replaced by inter-granule velocity. The reasoning is that, at low Stokes numbers, particles will follow streamlines to very close to the granule and that only the flow field in the boundary layer close to the granule need be taken into account. They then define a modified Stokes number as

$$N_{St}^{*} = B(\varepsilon)N_{St} \qquad \text{.....(3.5)}$$

$B(\varepsilon)$ is calculated for a flow field appropriate to the Reynolds number in the bed. Under the conditions discussed here, the flow field description of Schlichting (1968) is used to find

$$B(\varepsilon(\varepsilon)_{Re} >> 1) = \frac{2\left[1-\alpha^{5/3}\right]}{\left[2-3\alpha^{1/3}+3\alpha^{5/3}-2\alpha^{2}\right]} + 1{,}14N_{Re}^{1/2}\varepsilon^{-3/2} \quad \text{.....(3.6)}$$

$$\alpha = 1-\varepsilon$$

The impaction efficiency is then correlated with the modified Stokes number by

$$\eta_{0,imp} = \frac{[N_{St}^{*}]^{3,55}}{\left[1{,}67+[N_{St}^{*}]^{3,55}\right]} \quad \text{.....(3.7)}$$

For liquid aerosols these authors find very good correlation with experimental values; for solid aerosols deviations start at modified Stokes numbers of 0,5 probably due to particle bounce (See section 3.3.5).

One further modification to this efficiency equation was proposed by Coury *et al.* (1987) based on the reasoning that the form of the equation is shown to be correct by results from a number of researchers, but that the use of a modified Stokes number based on isolated spheres can be improved upon. They therefore use the modified Stokes number proposed for assemblies of spheres by Thambimuthu(cited by Coury *et al* 1987) based on the interstitial gas velocity

$$N_{St}^{+} = \frac{N_{St}}{\varepsilon} \quad \text{.....(3.8)}$$

and correlate the results of a number of researchers by

$$\eta_{0,imp} = \frac{[N_{St}^{+}]^{3,55}}{1{,}1.10^{-4}+[N_{St}^{+}]^{3,55}} \quad \text{.....(3.9)}$$

to find that this equation improves significantly on equation 3.7 in the description of the effect of bed porosity. It should be noted that equation 3.9 does not take the effect of the Reynolds number into account, as the Thambimuthu version of the Stokes number is not a function of the granule Reynolds number. For N_{Re} close to unity, equations 3.7 and 3.8 therfore yield very similar results. As N_{Re} for the conditions used in this work vary between 20 and 80 equation 3.7 was used.

3.3.3 Diffusion.

At the relatively low Reynolds number pertaining here, movement of particles to the granule surface due to a concentration gradient can be described by a mass transfer coefficient of the form

$$N_{Sh} = \frac{kd_p}{D} \quad \text{.....(3.10)}$$

which is a function of the Peclet number defined by

$$N_{Pe} = \frac{d_g U_0}{D} \quad \text{.....(3.11)}$$

$$D = \frac{Ck_B T}{3\pi\pi\mu_p} \quad \text{.....(3.12)}$$

(Coury *et al* 1987), where the diffusivity of particles much larger than the mean free path of molecules can be found from the Stokes-Einstein equation (Tardos *et al.* 1976). For particle flux from the bulk concentration to the granule surface (where the concentration is taken to be zero) in packed beds, eq 3.8 takes the form

$$N_{Sh} = k_1 g(\varepsilon) N_{Pe}^{1/3} \quad \text{.....(3.13)}$$

and the efficiency due to diffusion

$$\eta_{0,d} = \frac{8DN_{Sh}}{U_0 a} = 4k_1 g(\varepsilon) N_{Pe}^{-2/3} \quad \text{.....(3.14)}$$

by taking the particle flux over the granule surface as $\eta_0 U_0 C_0/4$ per unit surface area. A large number of values have been given for the correction factor $\mathbf{g(\varepsilon)}$. These have been summarized by Tardos *et al.*(1976, 1978), Tien (1989) and Chiang and Tien (1992) and may be extremely complicated functions of the porosity. Tardos (1976) has shown that, for practical values of ε, the correction factor may be satisfactorily approximated by a direct inverse relationship for which Wilson and Geankopolis (1966) empirically found a value of $\mathbf{k_1}$ of 1,09.

It has been shown by Kim *et al.* (2000) that the above calculation method is applicable to collection by the diffusion mechanism also for the case of poly-dispersed dust.

Fig 3.1 shows the relative values for the single-sphere efficiency due to the "mechanical" mechanisms described above under typical bed conditions in a bed of spherical granules. The logarithmic scale on the efficiency ordinate should be noted, as well as the minimum in the combined or added value that occurs at approximately 1 micrometer particle size. This minimum is a feature of all the curves for combined mechanical efficiencies and is caused by the fact that the magnitude of the different efficiencies change at different rates with change in particle size. The particle size at which it occurs will however change with filtration conditions. The calculations shown here were done for particles with a density of 2 800 kg m^{-3} in air at 100 kPa and 293 °C moving at 0,45 m s^{-1} (nominal or open-bed velocity) through a bed of 3mm spherical granules. Values for the inertial mechanism and for the total efficiency are not displayed for particles > 4 μm, as particle bounce significantly reduces the efficiency above this size under the conditions specified above. This phenomenen, and the correction that must be applied to account for it, will be covered in paragraph 3.3.5.

Fig 3.1 Calculated single-sphere efficiency of the "mechanical" mechanisms

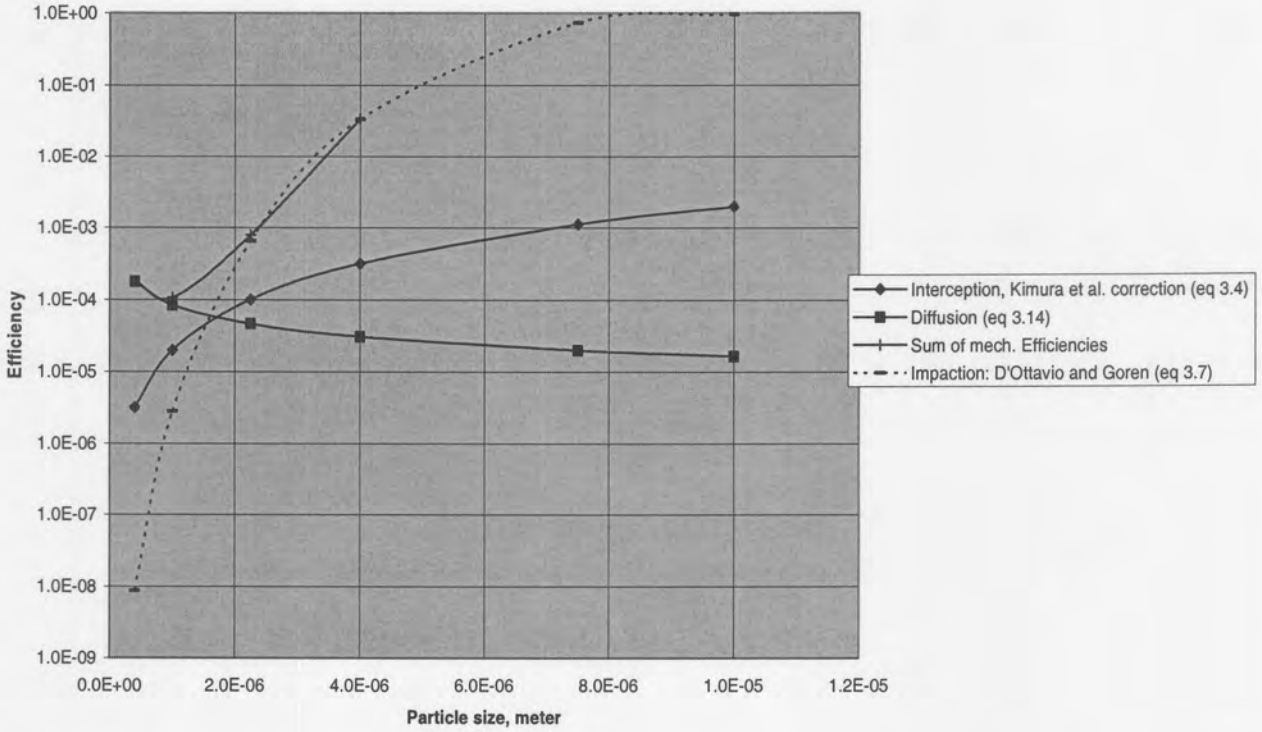

Jung (1991) has proposed an alternative method for the calculation of the combined efficiency of impaction and interception by correlating his experimental results, as well as those of previous authors, with D'Ottavio and Goren's modified Stokes number N^*_{St} and the interception parameter N_R. He finds that

$$\eta_{0,i,imp} = N_{St}^{*\,1,3437} N_R^{\,0,23} \quad \text{.....(3.14a)}$$

for the values of the Stokes number lower than the value at which particle bounce starts to occur, viz approx $N^*_{St} < 1,2$. The results of a comparison of the "addition of mechanisms" rule with Jung's proposal for filter conditions as in fig 3.1 is shown in fig 3.2. In this comparison, the value for diffusion, as calculated in eq 3.14 (for which Jung has not made allowance in his results) has been added to the value calculated from eq 3.14a.

Fig 3.2: Comparison of most recent correlations for "mechanical" efficiencies

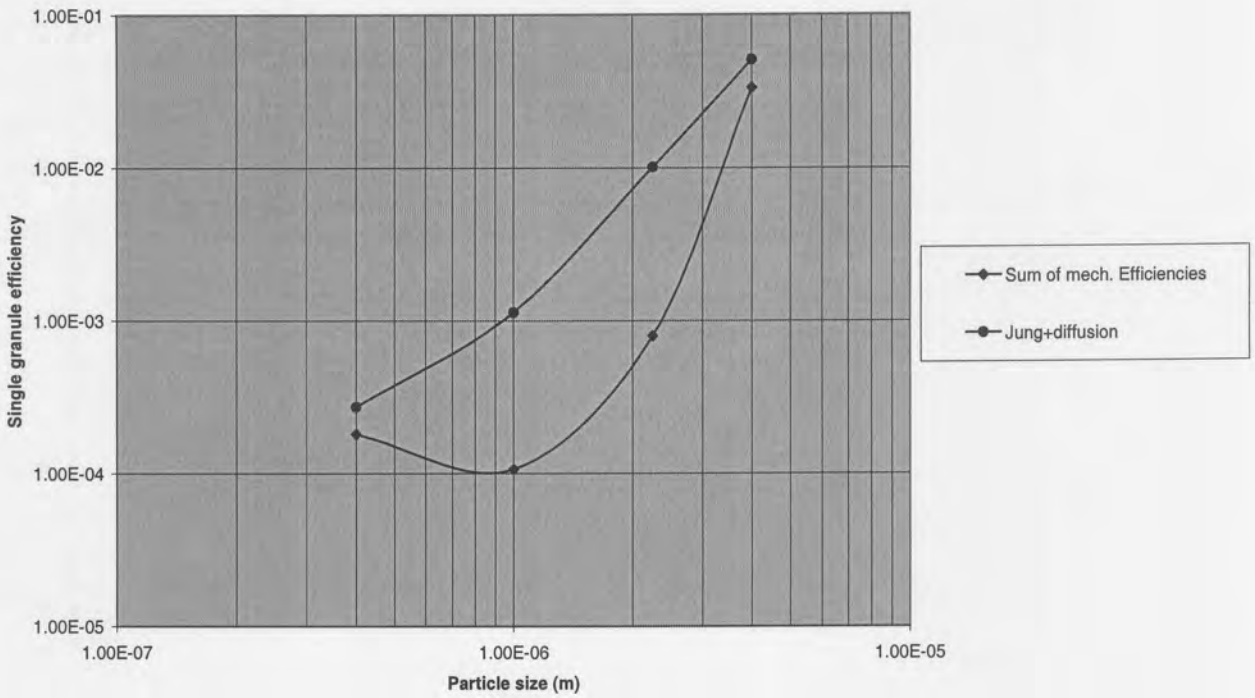

It is clear that, in the particle size range before particle bounce starts to occur (in this work, particles of the order of 3 μm in size), reasonable agreement is obtained. The "sum of mechanical efficiencies" method is probably to be preferred as being derived from fundamental considerations, whereas Jung's values are correlated from experimental values, and are acknowledged by the author to be a "simple" method for allowing for the non-impaction mechanisms.

3.3.4 The effect of granule sphericity.

Little has been published on the effect of particle shape on granule or bed efficiency. D'Ottavio and Goren (*op. cit.),* using pea gravel, have obtained excellent fit of experimental efficiencies to their earlier described model by using an equivalent spherical diameter calculated from pressure drop measurements. Kimura *et al.* (1985) have determined the influence empirically over a wide range of sphericity φ_g, which is defined as in Foust *et al.* (1960) by

$$\varphi_g = \frac{\text{Surface area of sphere with same volume as particle}}{\text{Surface area of particle}} \quad \text{.....(3.15)}$$

The authors apply an empirical correction factor of the form

$$\{1 + K_c N_R (1 - \varphi_g)^{1.5}\} \quad \text{.....(3.16)}$$

to the combined direct interception and diffusion efficiency. $\mathbf{K_c}$ has a value of 5.10^3 in the range of variables tested of φ_g between 0,36 and 0,93 and N_R between 4.10^{-3} and 5.10^{-2}. The latter values are

however an order of magnitude larger than those used in this work, and the D'Ottavio and Goren approach will be used as their values of N_R are very close to those used in this work.

3.3.5 The effect of particle bounce on impaction efficiency.

Equation 3.5 proposed by D'Ottavio and Goren (*op. cit.)* was found to correlate well with experimental values for liquid aerosols. For solid particles, the correlation starts to deteriorate at values of N_{St}^* larger than 0,5 (particle kinetic energy approximately 10^{-4}erg), which is in the middle range of the values used in this work. Yoshida and Tien (1985) ascribe this to "bounce-off of impacting aerosol particles from filter grains" . The phenomenen was described in section 2.4. The value of the ratio of experimental impaction efficiency to predicted efficiency was found to reduce linearly as a function particle kinetic energy (i. e Stokes number) from 1 at approximately 10^{-4} erg (Stokes number of approximately 10^{-2}) to 0,1 at 10^{-2} erg. This slope of the dependency on N_{St} was earlier also given by Dahneke (1971) as negative unity and this was confirmed by Tsiang *et al.*(1982) for fibrous filters in the region of restitution coefficient values occurring in practice.

Yoshida and Tien (*op cit.*) correlate the work of D'Ottavio and Goren and of Tardos *et al.*(1979) in this regard by the equation

$$\frac{(\eta_{0,imp})_{exp}}{(\eta_{0,imp})_{corr}} = 0{,}00318N_{St}^{-1{,}248} \quad \text{.....(3.17)}$$

where the subscripts refer to the experimental values and the values found from equations 3.7 or 3.9, respectively.

It must be mentioned here that the work of Hiller and Löffler (1980) and Löffler (1983) also indicate an inverse relationship with Stokes number (i.e. $\sim N_{St}^{-1{,}09}$) for the adhering fraction of particles. Jung (*op cit.*) uses

$$\frac{(\eta_{0,imp})_{exp}}{(\eta_{0,imp})_{corr}} = 1{,}43(N_{St}^*)^{-1{,}968} \quad \text{.....(3.17a)}$$

on his own experimental correlation. A comparison between the two methods for the filter conditions used in fig 3.1 is shown in fig 3.3 below. The minimum in the "sum of corrected mechanical efficiencies" line has been referred to earlier; the maximum at approximately 4micrometer in both lines is due to the reduction in efficiency as particle bounce sets in with increased values of the Stokes number.

Fig 3.3: Comparison of corrected efficiencies

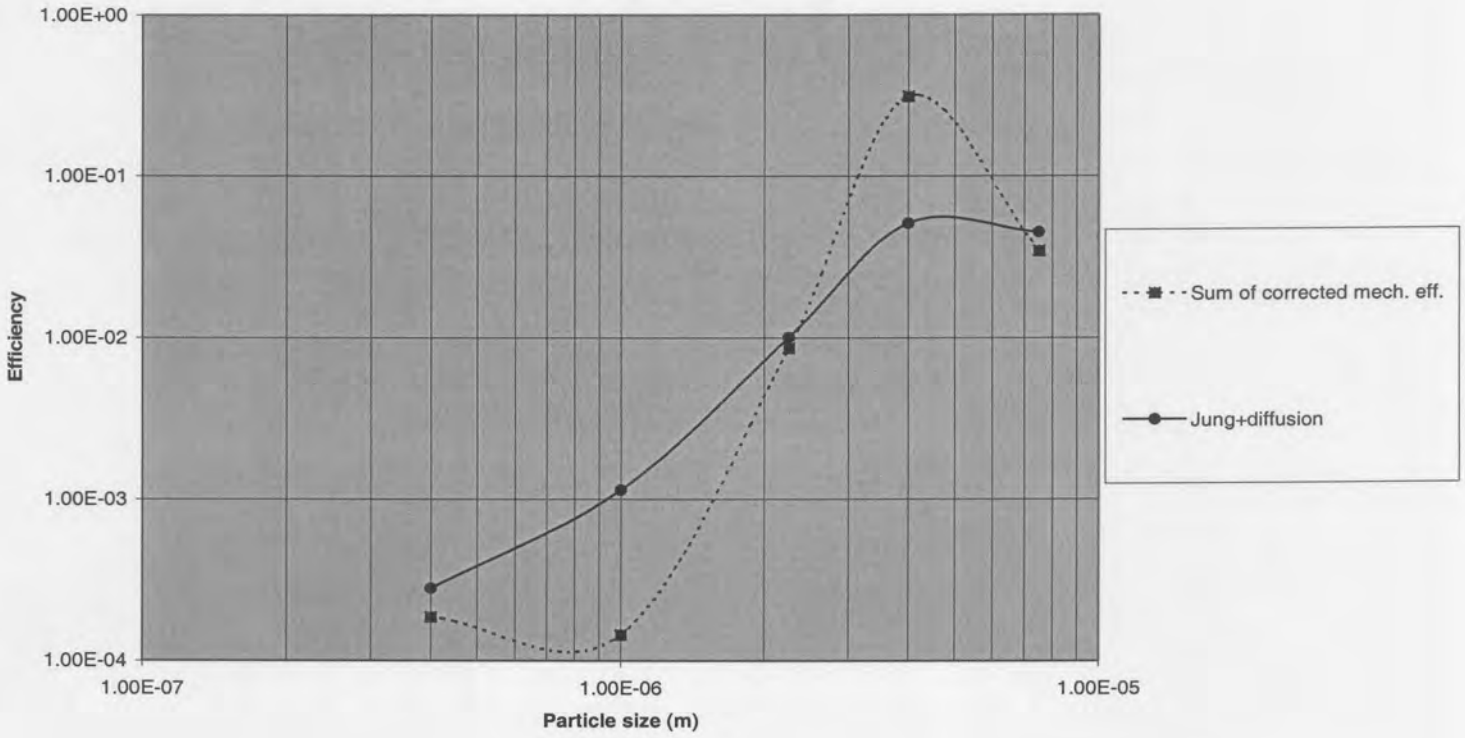

It is clear that, in the particle size range larger than 2 μm, the sum of the values for the individual mechanisms, together with their corrections, do not differ to a great extent from Jung's experimental values. In the lower sizes, as already said, the former values are probably to be preferred, as they were obtained under conditions where the influence of all other mechanisms was minimized, which is not the case for Jung's values.

It has been argued by Coury *et al.*(*op cit.*) that the electrostatic force described below acts at relatively long range, so that it will increase the approach velocity and thus favour "bounce". However, some of the increase in approach velocity is offset by drag in the stagnant zone close to the collector surface, while the very strong attractive force will tend to retain the particles on the collector surface. Electrostatic forces will therefore on balance favour adhesion and may require a modification to the "bounce" corrections described above. It will be determined from the experimental results whether this change is significant.

3.3.6 Electrostatic mechanisms.

It was earlier indicated that the Coulombic and external field forces are dominant in determining the efficiency due to these mechanisms. The efficiency due to these mechanisms was first calculated by Kraemer and Johnstone (1955) for an isolated sphere model and extended by Nielsen and Hill (1976) to generalised flow fields using trajectory analysis. The method is extensively described by Shapiro *et al.*

(1983,1986a, 1986b, 1988) and Tien (1989), and was also used by Wang *et al.* (1986) to describe deposition on single spheres by inertial and electrostatic forces.

It was shown by Self *et al.* (1981) that the charging of the granules in granular beds under practical operating conditions is prevented or at least limited by conduction of current through the bed either through the bulk of the granules but more probably on the surface of the granules. This limits the effect of the Coulombic force, making the external field force dominant.

The descriptions of the efficiency due to the external field force all make use of a parameter which may be interpreted as the ratio of the electrostatic drift velocity $\mathbf{Bq_pE_0}$ to the flow field velocity U_∞.

$$K_E = \frac{Bq_pE_0}{U_\infty} \qquad (3.17)$$

where **B** is the particle mechanical mobility

$$B = C/3\pi/3_{\ p} \qquad (3.18)$$

and E_0 is the effective bed strength, defined as

$$E_0 = E/\varepsilon_m \qquad (3.18a)$$

Nielsen and Hill (1981) used the flow field of Kuwabara (1959) together with the electrostatic field around an isolated single sphere to find

$$\eta_{E,i} = \frac{1+2\varphi_s K_E}{1+K_E[1+2\varphi_s(1-\varepsilon)]} \qquad (3.19)$$

Similarly Dietz (1981) uses the flow fields of Happel (*op cit.*) and Kuwabara (*op cit.*) together with an average potential on the surface of a unit cell in a granular bed defined by the position of the cell in the bed to find

$$\eta_{E,i} = \frac{3\varepsilon_c K_E}{3+\omega+K_E(3\varepsilon_c - 2\omega\omega} \qquad (3.20)$$

which, when the flow field and the electrostatic field are collinear, is independent of the flow field description.. By placing the limiting streamline far upstream instead of at the unit cell boundary, Tardos and Snaddon (1984) find by similar methods

$$\eta_{E,i} = \frac{3\varepsilon_c K_E}{\omega+K_E(\varepsilon_c+2)} \qquad (3.21)$$

In the last two equations, the parameter ω is defined by

$$\omega = 3+\varepsilon(\varepsilon_c - 1) \qquad (3.22)$$

Lastly, Shapiro *et al.* (1986) use an alternative definition of the grazing trajectory or limiting streamline together with the Hashin and Shtrikman (1962) description of the electrostatic properties of granular materials to find

$$\eta_{E,i} = \kappa K_E$$

$$\kappa = \frac{3\varepsilon_m(\varepsilon_c + 2\varepsilon_0)}{(\varepsilon_c + 2\varepsilon_0)(\varepsilon_0 + 2\varepsilon_m) + 2(1-\varepsilon)(\varepsilon_0 - \varepsilon_c)(\varepsilon_m - \varepsilon_0)} \quad \text{.....(3.23)}$$

Figure 3.4 compares the results of single granule efficiency calculations using the methods proposed by the above authors for typical bed conditions using dolomite spheres at an approach velocity of 0,45 meter per second with a particle charging field of 240 kV/m and a field of 100 kV/m applied over the bed. The large difference between the calculation of Nielsen and Hill, who have not allowed for adjacent granules in the field strength calculation, and the granular bed calculation of the other authors is obvious, as is the low efficiency at approximately 1 micrometer particle size. This is because neither of the charging mechanisms provide a high particle charge in this particle size range. The efficiency figures larger than unity for the Nielsen and Hill single collector calculation are due to the fact that particles outside the unit cell boundaries will be attracted by the polarized granule.

Fig 3.4: Comparison of calculated electrostatic efficiency

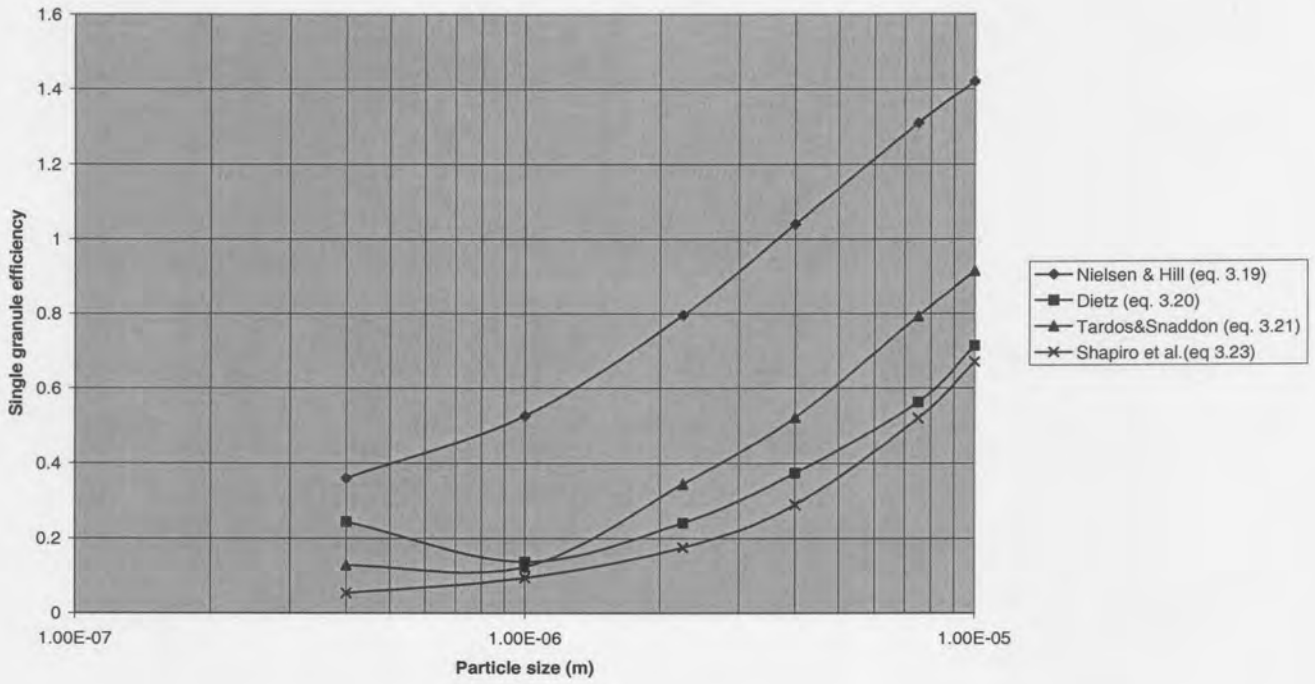

3.4 PARTICLE RELEASE MECHANISMS

Two main effects cause particles to be removed from the granules after capture has taken place. These are drag forces due to gas flow over the granules, and shear forces caused by the movement of the bed.

Both may be described by a re-entrainment coefficient η_R which may mathematically be treated similar to the capture efficiency described in the preceding paragraphs.

3.4.1 Drag forces due to gas flow.

Some theoretical and empirical work has been done by Corn and Silverman (1961) on the ratio of drag forces to adhesive forces on particles collected on wire screens, but at appreciably higher velocities than those used in this work. Only quantitative conclusions could be reached, the main ones being that dust is re-entrained at all velocities, that the rate of re-entrainment is proportional to gas velocity, and that some agglomeration had occurred in the re-entrained dust. A simple model comparing adhesive forces to drag forces underpredicted the rate of re-entrainment by a very large factor. This may be due to the morphology of deposited dust, subsequently identified by a number of investigators (summarised by Jung 1991) as being dendritic. A review of work on particle adhesion and release by Corn (1966) concludes that "at present there is not a satisfactory procedure available for reliably predicting these (adhesive) forces from the physical and chemical nature of the particles or the substrate". It is however clear from the work of Whitby and Liu (1966) that for the particle sizes (larger than 0,1 μm) and electrostatic field strengths (5 kV/cm and larger) under consideration in this work, the electrostatic forces are at least one, and in most cases several, orders of magnitude larger than the other adhesion forces. This means that re-entrainment by gas flow drag can be disregarded for beds over which a strong electrostatic field is applied. Even where particles in such beds become dislodged by gas flow, they will be rapidly re-captured by downstream granules. As an initial approximation therefore, in agreement with the work of Kalinowski and Leith (1983) on co-current moving granular beds, it will be assumed that re-entrainment due to gas drag forces is negligible compared to re-entrainment due to bed movement.

3.4.2 Effect of bed movement

The vertical movement of granular solids has been extensively described in the context of the design of silos for granular materials (Jenike and Shield 1959, Brandt and Johnson 1963, Johanson 1964, Jenike and Johanson 1969, Grossman 1975, Johanson 1994). The granular material used in the filter beds described here and used in practice is classed as non-deformable (Marcus *et al.* 1988). For such materials the magnitude of the internal shear is independent of the rate of shear but dependent on the mean pressure. Under conditions of steady flow near the exit of a conical hopper bottom, the stress field is such that the direction of principal stress is constant along a radial line drawn from the bottom intersection of the sloping walls. Away from the exit, the validity of the radial stress field assumption is dependent on the shape of the container (in particular the transition from parallel to conical), the properties of the solid (such as the angle of repose) and the properties of the interface between the wall of the container and the granular solid, which are characterised by the angle of friction between them.

Where the radial stress field is rendered impossible by a particular combination of these variables, only a conical core within the granular bed moves downward (so-called "core flow" or "funnel flow")

(Johanson 1970). In the case of granular filter beds, funnel flow is to be avoided at all cost, as it would cause part of the bed to be stationary and render continuous filter operation impossible. At the other extreme, where a radial stress field exists together with a low wall friction coefficient, there would be no relative movement between the particles in a moving bed but only between the wall and the layers of particles adjacent to the wall - so-called pure mass flow. In the work described here, the walls (in the form of either a screen, see Chapter 4) have a roughness of the same order of magnitude as the particles and a high relative velocity may be therefore be expected in a number of layers of particles on both sides of the bed, but not between layers of particles in the bulk of the medium. (Although it was shown by Ginestra and Jackson (1985) for bed pressure drops two orders of magnitude larger than those used here that the thickness of these layers on the up- and downstream side of the bed may become unequal to the extent that the bed may become pinned to the downstream retaining screen, equal thicknesses will be assumed here due to the low pressure drop). This has been confirmed by visual studies, using layers of coloured granules by Botha (1995) for screens and Venetian blinds, and by Kuo *et al.* (1998) and Hsiau *et al.*(2000, 2001) for the configuration of the Dorfan Impingio filter. In the latter case, flow visualisation was used for Venetian blind-type bed retaining walls in which the slats of the blind were set at different angles. For angles less than 45° to the vertical, the vertical velocity distribution of the particles in the bed does not vary with bed height and the velocity distribution can be approximated by a parabola with its axis of symmetry at the centre of the bed.

A simple mathematical description of the bed velocity will be tested in this work viz. layers of relative movement at the gas inlet and outlet sides, together with a central core with no relative velocity between granules.

3.5 PARTICLE CHARGING

Particle charging mechanisms are adequately described by the standard texts on electrostatic precipitation (White 1963, White 1984, Bohm 1982). For particles larger than approximately 1 micrometer, the field charging mechanism (i.e. by collision of charged ions moving in an electrostatic field with particles) is dominant and the rate is given by

$$\frac{dq_{p,f}}{dt} = \left(N_0 z q_{s,f} E_0 / 4\varepsilon_0\right)\left(1 - q_{p,f}/q_{p,f,s}\right)^2 \quad \text{.....} \quad \text{.....} \quad \text{...(3.24)}$$

Residence time in practical chargers is usually sufficiently long for the saturation charge to be reached when the charge on the particle repels further charged ions. This saturation charge is given by

$$q_{p,f,s} = 12\pi\left(\frac{\varepsilon_p}{\varepsilon_p + 2}\right) r_p E_0 \varepsilon_0 \quad \text{.....(3.25)}$$

Particles smaller than approximately 1 micrometer acquire a significant additional charge by diffusion charging. The charging rate is given by

$$\frac{dq_{p,d}}{dt} = eN_0 \pi r_p^2 \overline{V} \exp\left(-ne^2/4\pi\varepsilon_0 r_p kT\right) \quad \text{.....(3.26)}$$

In this case there is no saturation charge, the charge collected by diffusion having to be determined from the time that the particle has spent in the electrostatic field.

The simple addition of the charges generated by these mechanisms has been criticized by Zevenhoven (1992) on theoretical grounds. It had however previously been shown by Smith and McDonald (1976) that the refinements suggested by Zevenhoven have a negligible influence at the field strengths normally found in electrostatic precipitators which have been used here.

Equations 3.23 to 3.25 should in principle be applied to particles moving through the pre-charger before the bed and to the particles moving in the electrostatic field in the bed itself. The field strength of the bed may be however be considerably less than that of the pre-charger because of the influence of the granular media on field strength. Under such circumstances, discharging of the particles in the bed (from the higher value reached in the pre-charger)should probably be allowed for.

The considerable influence of the pre-charger on bed efficiency is illustrated in fig 3.5 below. The two curves show for illustrative bed conditions (6cm thick bed of 3mm granules, porosity = 0,49, field of 10^5 V/m applied over bed, di-electric constant of bed material = 5) the total bed efficiency for particles fully charged in a field of 10^6 V/m entering the bed, and particles that are neutral when entering the bed and are incrementally charged by their movement through the collecting field. Dietz's description for electrostatic efficiency was used for this figure, but similar differences are found using the methods of Tardos and Snaddon and of Shapiro (*op cit.)* described in section 3.3.6.

Fig 3.5: Comparative calculated electrostatic bed efficiency

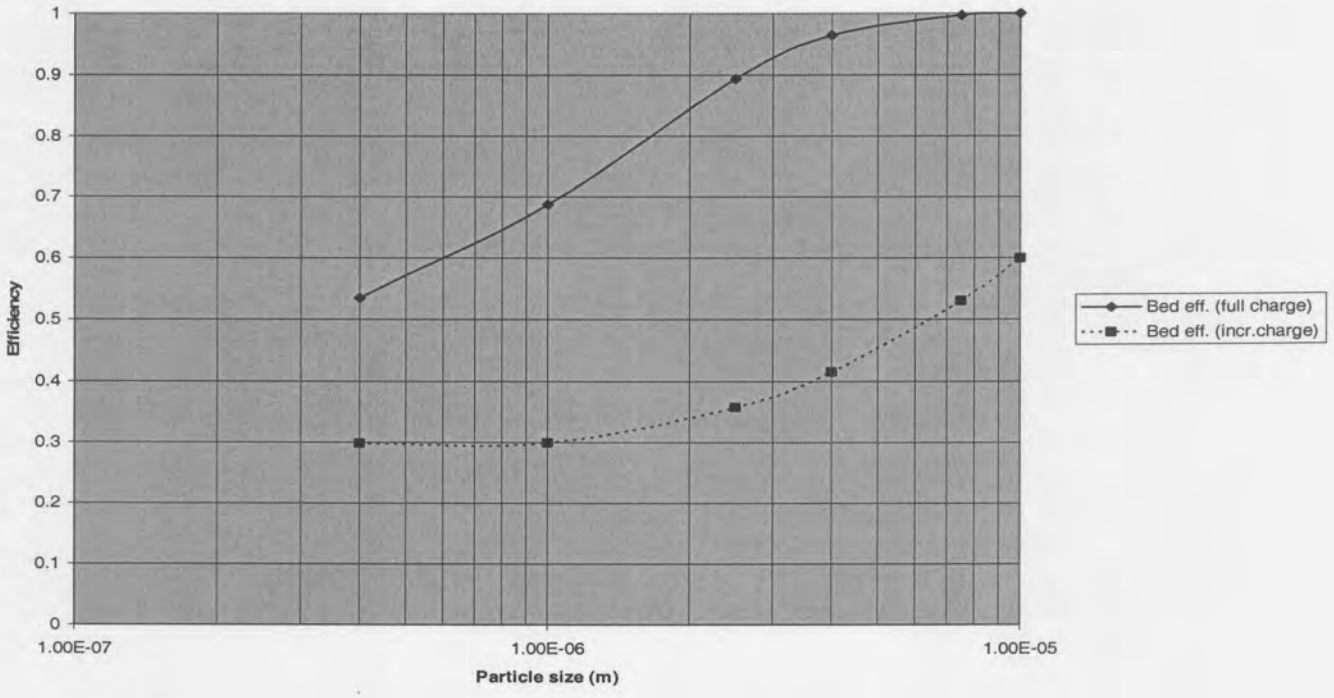

3.6 THE EFFECT OF BED LOADING

The parameter characterising the variation in collecting ability of a granular bed is the filter coefficient λ, which is related to the extent of deposition and is a local function. (Walata *et al.* 1986, Takahashi *et al.* 1986, Tien 1989, Jung 1991, Jung and Tien 1991, 1992, 1993). The change in filter characteristics with bed loading is related to the filter coefficient by the equations

$$F_1 = \frac{\lambda}{\lambda_0} = \frac{\eta}{\eta_0} = 1 + \alpha_1 \sigma^{\alpha_2} \quad \text{.....(3.27)}$$

$$F_2 = \frac{(\partial p/\partial x)}{(\partial p/\partial x)_0} = 1 + \beta_1 \sigma^{\beta_2} \quad \text{.....(3.28)}$$

where equation 3.27 describes the change in efficiency with specific deposit σ (i. e. volume of dust deposited per unit granular bed volume), and equation 3.28 the change in pressure drop. Both equations contain two empirical constants, of which values are given by for monodisperse aerosols by the first and second references above, and for polidisperse aerosols by the remainder, in all cases valid for specific types of materials . The last three references also indicate that the increase in unit collector efficiency due to deposition of a polidisperse aerosol may be described as a linear combination of the

contribution of the individual particle sizes with their volume fraction as the weighing factor, so that for the influence of the *k*th size interval

$$\left(\frac{\eta}{\eta_0}\right)_k = 1 + \sum_{j=1}^{N} \alpha_{1(kj)} \sigma^{\alpha_{2(kj)}} w_k \quad \text{.....(3.29)}$$

where the α_{kj} values denote the influence when particles of type **k** are collected on a granule loaded with particles of type **j** only. In practice, this will require values for each pair of particle sizes, the determination of which falls outside the scope of this work. Jung (*op cit.*) using bidispersed and tridispersed aerosols has however shown that the values can in principle be obtained.

Analysis of experimental results by Takahashi *et al.* (1986) and Jung (*op cit.*) on the effect of N_{St} and N_R of deposited particles indicates an inverse relationship with particle Stokes number to a power somewhat larger than unity for a given granule size through

$$\left[\frac{\eta}{\eta_0} - 1\right]_{\sigma=10^{-3}} = 0{,}09545 N_{St}^{-1.478} N_R^{0.4322} \quad \text{.....(3.30)}$$

$$\alpha_2 = 0{,}4416 N_{St}^{-0{,}3649} N_R^{0{,}2397}$$

For a given granule size and superficial gas velocity, there is a direct relationship between N_R and N_{St} of particles. Correlating the right hand side of eq. 3.30 with N_R number for the glass spheres at 0,453 ms^{-1} will for instance give

$$\left[\frac{\eta}{\eta_0} - 1\right]_{\sigma=10^{-3}} = 0{,}0131 N_{St}^{-1{,}248} \quad \text{.....(3.31)}$$

$$\alpha_2 = 0{,}1468 N_{St}^{-0{,}237}$$

from which α_1 values for each particle size can then be derived from

$$\alpha_1 = \left[\frac{\eta}{\eta_0} - 1\right]_{\sigma=10^{-3}} 10^{3\alpha_2} \quad \text{.....(3.32)}$$

Jung's correlations were obtained (i) for the range of variables $1{,}7.10^{-3} < N_{St} < 3{,}8.10^{-2}$ and $1{,}72.10^{-3} < N_R < 8.10^{-3}$ (ii) for conditions where the deposit and the deposited particle have the same particle size (iii) with specific provision being made for charge neutralisation. They may therefore not be directly applicable to the particles outside this range (0,3 to approx 1,0 micron), or for deposited material of mixed particle size where electrostatic augmentation is applied. Experimental values for particles outside the above range of parameters, and for dust with a mixed particle size, will therefore be compared with Jung's results.

The enhanced cluster model, proposed by Fichman *et al.* (1988b, 1988c), which attempts to describe the morphology of the dust deposits on the granules, yields curves of a similar shape to those given by

eq 3.27 when efficiencies for loaded beds are theoretically calculated using trajectory analysis. This model is independent of dust and collector material, which implies that the empirical constants in eq 3.27 ,eq 3.28 and eq 3.29 will also be applicable to other materials than those for which they were determined. The validity of the latter assumption, as well as the possibility of using single parameters for aerosols containing a large spread of particle sizes, will be tested experimentally.

The application of these equations to electrostatically augmented beds is approached by arguing that the only variable influencing the electrostatic and diffusion collection mechanisms that changes with bed load is ε, the bed porosity. In the range of bed load values investigated here (and of practical concern), the porosity change is so small as to fall within the range of experimental variability. It can therefore be argued that the increase in collection efficiency must be due only to the increase in the impaction and direct interception mechanisms as described by the Walata/Jung model. Electrostatic enhancement can have an influence on these mechanisms by changing the morphology of the deposited dust. Values for α_1 and α_2 calculated using the Jung/Walata model may thus not be applicable to electrostatically augmented beds, but this will be tested experimentally.

Although the effect of changes in characteristics of deposited dust on bed efficiency may in principle be obtained from equations 3.29 to 3.33, this will require experimental values of the single-size and cross-size coefficients of equation 3.29 outside the range of Jung's correlation, and in the presence of electrostatic fields where applicable. It is therefore be useful to develop an approach to the estimation of the parameters in equation 3.27 for a poly-dispersed aerosol of a different particle size distribution than that for which they have been experimentally determined. This is done in the following paragraph.

Deposition of particles on the granules will increase the size of the surface available for the deposition of further particles. The additional surface will depend on the particle size and the morphology of the deposited material; for a given mass and morphology of deposit it can easily be shown that the area of the additional surface is inversely proportional to the particle size of the deposited material. It can then be argued that for the diffusion and direct interception mechanisms, the effect of a given mass of deposit must be inversely proportional to the average particle size of the deposited material. For the impaction mechanism, the relationship would be allied to the change in bed porosity, which is a function of morphology of the deposit. The ratio between the effect of the three "mechanical" mechanisms and the specific bed load should then determine the exponent z in the equation

$$[\frac{\eta}{\eta_0}]_2 = 1 + \left(\frac{d_{p2}}{d_{p1}}\right)^z [\frac{\eta}{\eta_0} - 1]_1 \quad \text{.....(3.33)}$$

Jung (1991) has addressed this problem for monosized deposited particles in the size range 1 to 3 micrometers and has found empirically that the effect of the particle size of the deposited material on the capture of a given size of particle varies between the power -2 for lightly loaded beds (σ = 0,0001) to -1,55 for heavily loaded beds (σ = 0,001).

In a similar manner, the ffect of a change in granule size on the parameters determined at one granule size can be estimated. Such a change will have an effect on both N_{St} and N_R (*cf* equation 3.30). A sensitivity analysis using calculations according to the correlations of Takahashi (op cit) and Jung (op cit) indicates that the value of α_1 will vary with the value of N_R to the power of approximately 2 over the particle size range from 0,3 to 4 micrometer, and this adjustment can be used for each particle size i. e. at constant N_{St} .

The effect of a change in filtration velocity on the loading parameters determined at one value can be similarly estmated. Equation 3.30 indicates a proportionality to N_{St}, and hence to bed velocity, to the power -1,437 at constant particle and granule sizes.

3.7 THE COMBINED USE OF THE EQUATIONS

Although the most appropriate equation to describe each of the mechanisms under the experimental conditions used in this work follow from the experimental work itself, the equations finally used are summarized in Table 3.2 below.

Table 3.2: Summary of equations used.

Mechanism	**Author**	**Equation**
Direct interception	Tardos and Pfeffer (1980)	3.3
N_{Re} correction to interception	Kimura *et al.*(1985)	Table 3.1
Impaction	D'Ottavio and Goren (1983)	3.5
Diffusion	Tardos (1976)	3.14
Particle charging	White (1983)	3.24 and 3.26
Electrostatic capture	Dietz (1981)	3.20
Effect of bed loading	Jung (1991)	3.27

Equations have now been established for all the charging, collection and re-entrainment mechanisms operating in the beds in, both in the layers next to the retaining screens and in the central or bulk zone of the bed. Following Kalinowski and Leith (*op cit.*) and Henriquez and Macias-Machin (1997), these may now be combined using

$$v\frac{\partial m}{\partial y} + U_0 \frac{\partial C_{bed}}{\partial x} = 0 \qquad \text{.....(3.34)}$$

for each element in the bed of size ∂x in the horizontal - and ∂y in the vertical direction, and using element dimensions in each direction to ensure that dust collection and re-entrainment processes are the same throughout the element. In the horizontal direction (parallel to gas flow), this will mean that a number of discrete zones will be used commensurate with the granule flow model being tested, with

the zone velocity calculated for the centre of the zone and the particulate concentration in the bed described by

$$\frac{\partial C_{bed}}{\partial x} = -\lambda x \quad \text{.....(3.35)}$$

with λ representing the filter coefficient, which is directly linked to the unit collector efficiency by

$$\lambda = \frac{1}{\left[\left(\frac{\pi}{6(1-\varepsilon)}\right)^{\frac{1}{3}} d_g\right]} \ln\frac{1}{1-\eta} \cong \left[\frac{6(1-\varepsilon)}{\pi}\right]^{1/3} \frac{\eta}{d_g} \quad \text{.....(3.36)}$$

(Mackie *et al.*1987, Tien, *op cit.*) and

$$\varepsilon = \varepsilon_0 - \frac{m}{\rho_d} \quad \text{.....(3.37)}$$

(Henriquez and Macias-Machin *op cit.*). An Eulerian solution method will be used on the Excel spreadsheet system.

3.8 REFERENCES

Beard, K.V., Grover, S.N. (1974) Numerical collision efficiencies for small raindrops colliding with micron size particles. J. Atmos. Sci. **31** p 543-550

Bohm, J. (1982) *Electrostatic precipitators.* Amsterdam, Elsevier

Botha, J. (1995) Unpublished undergraduate dissertation, Dept. of Chemical Emgineering, University of Pretoria.

Brandt, H.L., Johnson, B.M. (1963) Forces in a moving bed of particulate solids with interstitional fluid flow. AIChE J. **9** (6) p 771-777

Chiang, H.-W., Tien, C. (1982) Deposition of Brownian particles in packed beds. Ch. Eng. Sc. **37** (8) p 1159-1171

Chiang, H.-W., Tien, C. (1985a) Dynamics of deep-bed filtration. Part I: Analysis of two limiting situations. AIChE J. **31** (8) p 1349-1359

Chiang, H.-W., Tien, C. (1985b) Dynamics of deep-bed filtration. Part II: Experiment. AIChE J. **31** (8) p 1360-1371

Choo, C-U., Tien, C. (1993) Transient-state modeling of deep bed filtration. Wat. Sci. Tech. **27** (10) p 101-116

Ciborowski, J. Zakowski, L. (1977) Dust removal in a fluidized bed. I. Use of a fluidized bed in the filtration process. Int. Chem. Eng. **17** (3) p 529-538

Corn, M., Silverman,L. (1961) Removal of solid particles from a solid surface by a turbulent air stream. Ind.Hyg. J. Oct 1961

Corn, M. (1966) Adhesion of particles. Chapter 11 in Davies, C.N.(ed.) *Aerosol Science.* London, Academic Press

Coury, J.T. *et al.* (1987) Capture and rebound of dust in granular bed gas filters. Powder Techn. **50** p 253-265

Dahneke, B. (1971) The capture of aerosol particles by surfaces. J. Colloid and Interface Science **27** (2) p 342-353

Degani, D.D., Tardos, G.I. (1981) Inertial deposition of small particles on a sphere at intermediate and high Reynolds numbers: A time-dependent study. J APCA **31** (9) p 981-986

Dietz, P. (1981) Electrostatic filtration of inertialess particles by granular beds. J. Aerosol Sci. **12** p 27-38

D'Ottavio, T., Goren, L.S. (1983) Aerosol capture in granular beds in the impaction dominated regime. Aerosol Sci. Technol. **2** p 91-107

Fichman, M., Pnueli, D. (1982) More detailed analysis of the effects of inertia on the filtration efficiency of granular bed filters. Israel J. Techn. **20** p 60-70

Fichman, M. *et al.* (1988a) Effect of particle loading on granular bed filtration - the cluster-enhanced filter model. J. Aerosol Sci. **19** (4) p 425-441

Fichman, M. *et al.* (1988b) Effect of particle loading on granular bed filtration - the cluster enhanced filter model. J. Aerosol Sci. **19** p 425-441

Fichman, M. *et al.* (1988c) Effect of particle loading on granular bed filtration – extension of CEF model to polydisperse systems. J. Aerosol Sci. **19** (4) p 443-450

Foust, A.S. *et al.* (1960) *Principles of unit operations.* New York, John Wiley & Sons.

Gal, E. *et al.* (1985) A study of inertial effects in granular bed filtration. AIChE J. **31** (7) p 1093-1104

Ginestra, J.C., Jackson, R. (1985) Pinning of a bed of particles in a vertical channel by a cross flow of gas. Ind. Eng. Chem. Fundam. **24** (2) p 121-128

Grossman, G. (1975) Stresses and friction forces in moving packed beds. ALChE J. **21** (4) p 720-730

Gutfinger, C., Tardos, G.I. (1979) Theoretical and experimental investigation on granular dust filters. Atmos. Env. **13** p 853-867

Happel, J. (1958) Viscous flow in multiparticle systems: slow motion of fluids relative to beds of spherical particles. AIChE J. **4**(2) p 197

Hashin, Z., Shtrikman,S (1962) A variational approach to the theory of the effective magnetic permeability of multiphase materials. J. Appl. Phys. **33**(10) p 3125-3131

Henriquez, V., Macias-Martin, A. (1997) Hot gas filtration using a moving bed heat exchanger-filter (MHEF). Ch. Eng. & Processing **36** p 353-361

Hiller, R., Löffler, F. (1980a) Staub-Reinhalt.Luft **40** p 405-411

Hsiau, S.S. *et al.* (2000) Flow patterns and velocity fields of granules in Dorfan Impingio filters for gas cleanup. Ch. Eng. Sci. **55** p 4481- 4494

Hsiau, S.S. *et al.* (2001) Velocities in moving granular bed filters. Powder Techn. **114** p 205-212

Jackson, S., Calvert,S. (1966) Entrained particle collection in packed beds. AIChE J. **12** (6) p 1075-1078

Jenike, A.W., Johanson, J.R. (1969) On the theory of bin loads. J. Engineering for Industry. Trans. ASME **51** (B2) p339-344

Jenike, A.W., Johanson, J.R . (1970) Solids flows in bins and moving beds. Chem. Eng. Progress.**66** (6) p 31-34

Jenike, A.W., Shield, R.T. (1959) On the plastic flow of Coulomb solids beyond original failure. Trans. ASME **79** (E12) p 599-602

Johanson, J.R. (1964) Stress and velocity fields in the gravity flow of bulk solids. Trans. ASME **84** (E9) p 499-506

Johanson, J.R. (1994) The realities of bulk solid properties testing. Bulk Solids Handling **14** (1) p 133-134

Jung, Y (1991) *Granular filtration of monodispersed and polydispersed aerosols.* Ph. D. dissertation, Syracuse University

Jung, Y., Tien, C. (1991) New correlations for predicting the effect of deposition on collection efficiency and pressure drop in granular filtration. J. Aerosol Sci. **22** (2) p 187-200

Jung, Y., Tien, C. (1992) Increase in collector efficiency due to deposition in polydispersed granular filtration - an experimental study. J. Aerosol Sci. **23** (5) p 525-537

Jung, Y., Tien, C. (1993) Granular filtration of polydispersed aerosols. Filt. & Sep. **30** p 253-259

Kalinowski, T.W., Leith, D. (1983) Aerosol filtration by a co-current moving granular bed: Penetration theory. Environ. Sci. Technol. **17**(1) p 20-26

Kim, H.T. *et al.* (2000) Diffusional filtration of polydispersed aerosol paticles by fibrous and packed-bed filters. Filt. & Sep. **37** (6) p 37-42

Kimura, N. *et al.* (1985) Efficiency of collection of granular bed filters due to diffusion and direct interception. Int. Chem. Eng. **25**(1) p 122-129

Knettig, P., Beeckmans, J.M. (1974) Capture of monodispersed aerosol particles in a fixed and in a fluidized bed. Can. J. Chem. Eng. **52** p 703-706

Kraemer, M.F., Johnstone, H.F.(1955) Collection of aerosol particles in the presence of electrostatic fields. Ind.Eng.Chem. **47** (12) p 2426 *et seq.*

Kuo, J.T. (1998) Stagnant zones in granular moving bed filters for flue gas cleanup. Filt. Sep. **35** (6) p 529-534

Kuwabara, S. (1959) The forces experienced by randomly distributed parallel circular cylinders or spheres in a viscous flow at small Reynolds numbers. J. Phys. Soc. Japan **14** p 527

Lee, K.W. (1981) Maximum penetration of aerosol particles in granular bed filters. J. Aerosol Sci. 12 p 79-87

Löffler, F. (1983) Partikelabscheidung an Tropfen und Fasern. Chem.Ing.Tech. **55** (3) p 171-178

Mackie, R.I. *et al.* (1987) Dynamic modeling of deep-bed filtration. AIChE J **33** (11) p 1761-1775

Marcus, R.D. *et al.* (1988) Solids handling. Ch. 8, p 8.1-8.8 in Gerhatz, W (ed.) Ullmann's Encyclopedia of Industrial Chemistry Vol B7. Weinheim, VCH Verlag.

Neale, G.H., Nader,W.K.(1974) Prediction of transport processes within porous media: Creeping flow relative to a fixed swarm of spherical particles. AIChE J. **20** (3) p 530-538

Nielsen, K.A., Hill, J.C.(1976) Capture of particles on spheres by inertial and electrical forces. Ind.Eng.Chem.Fund. **15** (3) p 157-163

Paretsky, L. *et al.* (1971) Panel bed filters for the simultaneous removal of fly ash and sulfur dioxide. J. APCA **21** (4) p 204-209

Pendse, H., Tien,C.(1982) General correlation of the initial collection efficiency of granular filter beds. AIChE J. **28** (4) p 677-686

Peters, M.H. *et al.* (1982) Simulation of particulate removal in gas-solid fluidized beds. AIChE J. **28** (1) p 39-49

Peters, M.H. *et al.* (1985) A dynamic simulation of particle deposition on spherical collectors. Chem. Eng. Sc. **40** (5) p 723-731

Peukert, W., Löffler, F. (1991) Influence of temperature on particle seperation in granular bed filters. Powder Tech. **68** p 263-270

Pilat, M.J., Prem, A. (1976) Calculated particle collection efficiencies of single droplets including inertial impaction, Brownian diffusion, diffusiophoresis and thermophoresis. Atm Environ. **10** (1) p13-19

Pulley, R.A., Walters, J.K. (1992) The collection of dust particles by falling water droplets. Trans. I. Chem. E. **70** (A) p 354-360

Rajagopalan, R., Tien, C. (1979) Trajectory analysis of deep-bed filtration with the sphere-in-cell porous media model. AIChE J. **22**(3) p 523-533

Ranz, W.E., Wong, J.B. (1952) Impaction of dust and smoke particles. Ind.& Eng. Chem. **44** (6) p 1371-1380

Self, S.A. *et al.* (1981) Electrical augmentation of granular bed filters. Environment International **6** p 397-414

Schlichting, H. (1968) *Boundary Layer Theory* (6^{th} ed) New York, McGraw-Hill

Shapiro, M. *et al.*(1983) Electric forces in aerosol filtration in fibrous and granular filters – a parametric study. Atmos. Environ. **17** (3) p477-484

Shapiro,M. *et al.*(1986a) Electrostatically enhanced granular bed filters. Aerosol Science and Technology **5** p 39-54

Shapiro, M. *et al.*(1986b) The effect of external electrostatic field orientation on aerosol filtration by granular filters. IEEE Trans. on Industrial Applications **IA-22** (2) p 230-234

Shapiro, M. *et al.* (1988) Electrostatic mechanisms of aerosol collection by granular filters: A review. J. Aerosol Sci. **19** (6) p 651-677

Smith, W.B., McDonald, J.R. (1976) Development of a theory for the charging of particles by unipolar ions. Aerosol Sci. **7** p 151-166

Snaddon, R.W.L., Dietz, P.W.(1980) Flow intensification and jetting in packed granular bed filters. General Electric Company Report 80CRD290

Snyder, L.J., Stewart, W.E. (1966) Velocity and pressure profile for Newtonian creeping flow in regular packed beds of spheres. AIChE J. **12**(1) p167

Starr, J.R. (1967) Inertial impaction of particulates upon bodies of simple geometry. Ann. Occup. Hyg. **10** p 349-361

Takahashi, T. *et al.* (1986) Transient behavior of granular filtration of aerosols - effect of aerosol deposition on filter performance. AIChE J. **32**(4) p 684-690

Tardos, G. I. (1974) Deposition of dust particles in a fluidized bed filter . Israel J. Tech. 12, p 184

Tardos, G.I. *et al.* (1976) Diffusional filtration of dust in a fluidized bed. Atmos. Environ. **10** p 389-394

Tardos, G.I. *et al.* (1978) Dust deposition in granular bed filters: theories and experiments. J APCA **28** (4) p 354-363

Tardos, G.I. *et al.* (1979) Experiments on aerosol filtration in granular sand beds. J Coll. Interface Sc.**71** p 616

Tardos, G. I., Pfeffer, R. (1980) Chem.Eng. Comm **4** p 665-669

Tardos, G.I., Snaddon, R.W.L (1984) Separation of charged aerosols in granular beds with imposed electric fields. AIChE Symp. Series 234 **80** p 61-69

Tien, C. (1982) Aerosol filtration in granular media. Chem. Eng. Commun. **17** p 361-382

Tien, C. (1989) *Granular filtration of aerosols and hydrosols.* Boston, Mass. : Butterworths

Tsian, R.C. *et al.* (1982) Dynamics of particle deposition in model fiber filters. Chem. Eng. Sci. **37**(11) p 1661-1673

Walata, S.A. *et al.*(1986) Effect of particle deposition on granular aerosol filtration. Aerosol Sci. Tech. **5** p 23-27

Wang, H.C. *et al.* (1986) Particle deposition on spheres by inertial and electrostatic forces. Aerosol Sci. Tech. **5** p 391-408

Whitby, K.T., Liu, B Y H. (1966) The electrical behaviour of aerosols. Chapter 3 in Davies, C. N. (ed.) *Aerosol Science.* London, Academic Press.

White, H.J. (1963). *Industrial electrostatic precipitation.*, Reading, Mass.: Addison-Wesley

White, H.J. (1984) Control of particulates by electrostatic precipitation *in* Calvert, S., Englund H.M.(eds.) *Handbook of air pollution technology.* New York, J Wiley & Sons

Wilson, E.J., Geankopolis, C.J. (1966) Liquid mass transfer at very low Reynolds numbers in packed beds. Ind. Eng. Chem. Fund.**5**(1) p 9-14

Yoshida, H., Tien,C. (1983) A new correlation of the initial collection efficiency of granular aerosol filtration. AIChE J. **31** (10) p 1752-1754

Zevenhoven, C.A.P. (1992) *Particle charging and granular bed filtration for high temperature application.* Ph.D.dissertation, Technical University of Delft.

CHAPTER 4
EXPERIMENTAL

4.1 APPARATUS

4.1.1 Bed configurations and materials.

For measurements under different condition the following variations in granular bed configuration were used:

- Basic filtration mechanism without electrostatic augmentation: The stationary bed used here consists of a cylindrical section of Perspex or stainless steel 143 mm in diameter and 30 or 60 mm long, flanged at both ends. The granules are retained by stainless steel screens with 0,5 mm dia wire and 2,0 mm square apertures. Air is supplied from the laboratory compressed air supply via a droplet separator and a control valve. Flow is measured by a calibrated rotameter.

  Air is distributed over the face of the filter bed using conical inlet and outlet sections with a 7° included angle to ensure even velocity distribution over the filter face.

  Initial experiments were carried out using uniform glass spheres 3 mm in diameter. Commercial media were simulated by silica sand (Eggo Sand, Brits, NW province), crushed granite (Ready Mix Materials, Rooikraal, Gauteng province) and dolomite chips (Samancor, Lyttelton, Gauteng province) screened on 2,35 mm, 2,75 mm and 3,35 mm screens with rectangular apertures. For the latter two materials, material properties were as follows in table 4.1. Sphericity is defined as the ratio of the surface area of a sphere of volume equal to that of the particle, to that of the particle (Foust *et al.* 1960) and determined by measuring the terminal settling velocity in water.

Table 4.1: Properties of bed materials

	Particle size	Bulk density	Bed porosity	Actual density	Granule sphericity
Crushed granite	2,83-3,36mm	1290-1300 kg m^{-3}	0,48	2480-2600 kg m^{-3}	0,80
Crushed granite	2,28-3,36mm	1320-1380 kg m^{-3}	0,49	2400-2600 kg m^{-3}	0,80
Dolomite chips	2,83-3,36mm	1370-1430 kg m^{-3}	0,45	2550-2760 kg m^{-3}	0,72
Dolomite chips	2,28-3,36mm	1380 kg m^{-3}	0,49	2550-2760 kg m^{-3}	0,72

The relationship between bed porosity and granule sphericity determined by Brown *et al.*(1950) is not followed exactly by the figures in the table, probably due to the inexact results obtained by the measurement of bed porosity in laboratory containers with a ratio of granule diameter to container diameter larger than 0,1 (Leva 1959)

- Moving bed: A schematic diagram of this apparatus is shown in fig 4.1. The bed retaining silo is 500 mm high and 110 mm wide. It is manufactured from Celeron, a fibre-reinforced synthetic resin that is electrically non-conducting and mechanically stable at the temperatures used in this

work (<200°C). Bed thickness is 30 or 60 mm and the active filtration area is 100 mm wide and 200 mm high. The moving bed is retained in the vertical plane by a stainless steel mesh similar to the one in the stationary bed. An isometric sketch of the moving bed is shown in fig 4.1a below. Electrical short circuiting of metal parts such as connecting bolts is eliminated by the use of suitable isolating material.

The bottom of the bed retaining silo is tapered to allow the bed material to rest on a vibrating feeder. Vertical bed movement is controlled by adjustment of the vibrating feeder frequency. As extended experimental runs require re-use of the medium, a pneumatic transport system is used between the vibrating feeder outlet and the top of the apparatus. A separation chamber at the top of the bed allows transport air and dust to exit to the laboratory fume exhaust system, while the medium falls onto the top of the bed for re-use.

Fig 4.1: Experimental moving bed apparatus

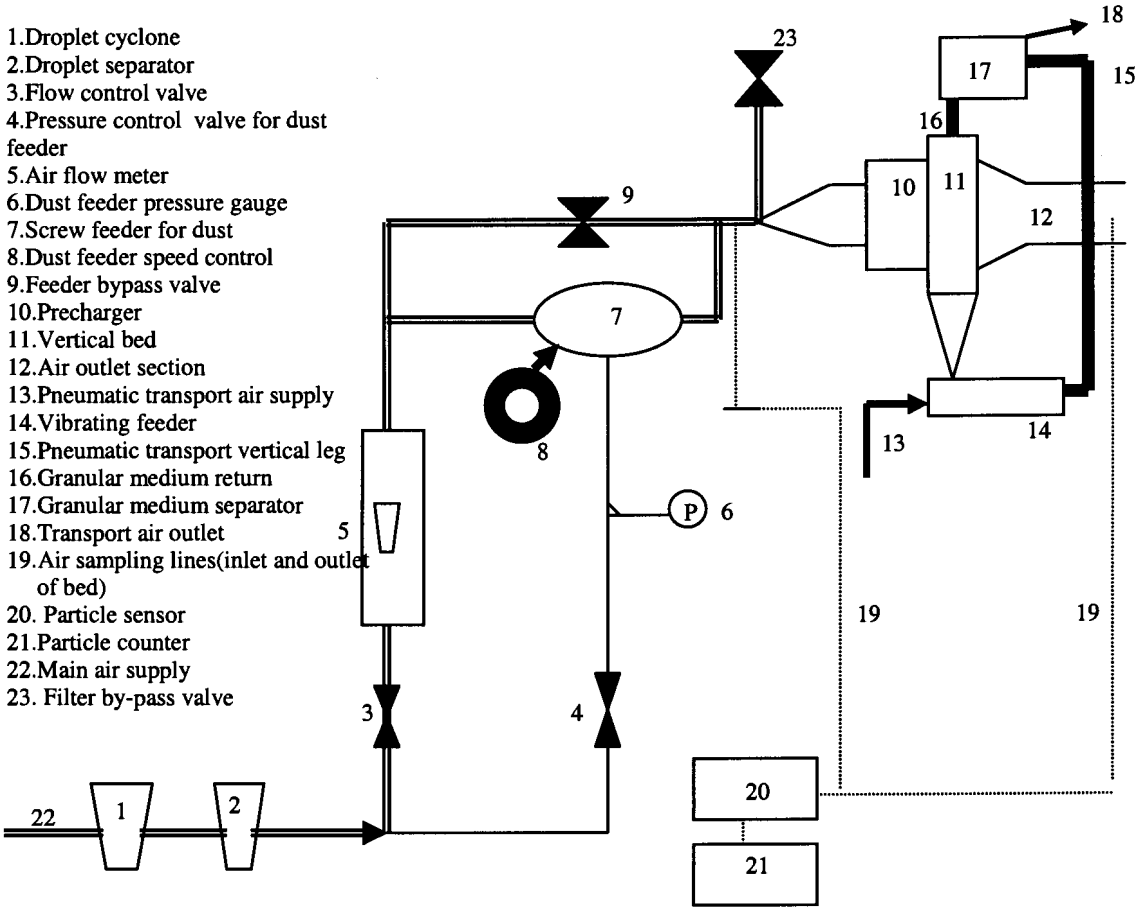

Fig 4.1a: Detail of moving bed.

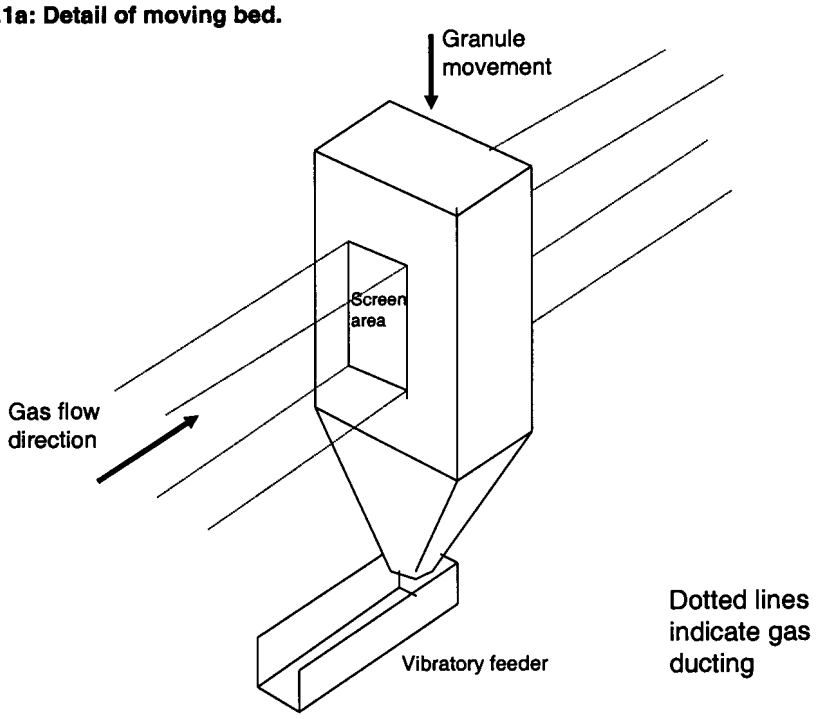

Dolomite and granite gravel screened as indicated in Table 4.2 below were used as filter medium for this part of the work. In order to determine equivalent diameters for the mixed particles, the pressure drop was determined over a static bed of each of the materials, using a flow of dry nitrogen. A bed of 5 mm spherical beads was used as a calibration and check measurement and calculation, using the methods of Ergun (Geiger and Poirier 1973) and Leva (1947,1949). For the 5 mm beads, the methods overpredicted the pressure drop by 32% and 11% respectively at an empty bed linear flow rate of 0,78 meter per second, indicating that the Leva method provides a more accurate prediction at gas velocities used in this work.. In table 4.2, results of both of the methods that were used to back-calculate equivalent particle diameters for the mixed and non-spherical granules are given under E(Ergun) and L(Leva).

Table 4.2 : Equivalent diameters of moving bed granular material

Granite (Rossway, Gauteng)				Dolomite (Rooikraal, Gauteng)			
2,28-3,28 mm		2,80-3,28 mm		2,28-3,28 mm		2,80-3,28 mm	
Porosity 0,438		Porosity 0,480		Porosity 0,480		Porosity 0,463	
E	L	E	L	E	L	E	L
1,84	2,7	1,91	2,8	1,72	2,6	2,20	3,1

Di-electric constants (permittivity values) for the various types of granules and test dusts used were obtained from literature sources (Baumeister *et al.* 1978, Kaye and Laby 1986, Weast 1981, ASI Instruments 2002) as far as possible. The figures are mostly for pure materials, and some values are

obviously repeated from the older to the newer sources. Estimates had to be made using chemical composition where values were not available for specific materials used here.

4.1.2 Electrostatic augmentation.

To investigate the electrostatic mechanism under both static and moving bed conditions, a high voltage direct current source (Hipotronics model 50B) generating a maximum potential of 50 kV was used in conjunction with the apparatus of 4.1.1, connected to the inlet and outlet screens.

4.1.3 Dust feed.

Dust is fed to the air stream on the inlet side of the bed using a variable speed screw feeder. The feed hopper of the screw feeder is pressurised using dry air to prevent reverse flow of the dust through the screw. Between the dust feed point and the bed itself, the "dusty" air passes through a mixing nozzle which provides turbulence for disaggregation and mixing of the individual dust particles (Yamamoto and Suganama 1984). For tests on the non-electrostatic mechanisms, an ionising nozzle was used (20 mCi Polonium 210, 3M Company). This is a source of α radiation to neutralise the tribologically-induced negative charges on particles.

4.1.4 Dust pre-charging.

A particle precharger is installed upstream (in the gas flow direction) of the moving bed. This consists of vertical stainless steel plates with a width of 21 mm in the gas flow direction. This provides a residence time in the pre-charger sufficient for the particles to reach saturation charge by the field charging mechanism at a bed superficial gas velocity of up to 2 meter per second. Two of the plates are arranged against the side walls of the gas flow channel and a third in the centre of the channel, thus providing two charging channels 200 mm high by 50 mm wide, each with a central discharge wire. Stainless steel discharge wires 0,025 mm in diameter are spaced equidistant between the plates. A separate direct current source with a maximum potential of 40 kVwas used to energise the particle precharger.

4.2 TEST DUSTS

For static bed tests, a standard fly ash (no 10: Ultrafine fly ash) was obtained from the Association of Powder Process Industry and Engineering (APPIE) in Japan. The particle size analysis is shown in fig 4.2. The dust has an approximate log-normal distribution with a mass geometric mean particle size of 4,8 micrometer, determined by the standard methods described by Patterson (1984) and de Nevers (1995). Subsequently, a metallurgical alumina powder (Boshoff Alumina) was obtained, with the particle size distribution given in fig 4.2. The mass geometric mean particle size of this dust is 1,8 micrometer. Using the latter dust, frequent blocking of the screw feeder and uneven feeding of the dust

occurred, which was solved by the addition of 5% by mass of a "glidant" in the form of superfine wet-precipitated and reground silica (Degussa Sipernat 220S).

For testing of moving beds, a fine dust from a ferrosilicon furnace bag filter was obtained, as the mechanisms for the fine fraction which in practice is of greater importance would then be emphasized. This material contains approximately 70% silica formed by condensation of fume, with smaller amounts of alumina, magnesia and iron oxides. The particle size analysis of this dust is also shown in fig 4.2. Although the size distribution of this dust deviates somewhat from the log-normal, an approximation of the geometric mean size is 1,3 micrometer.

Fig.4.2: Particle size of test dusts

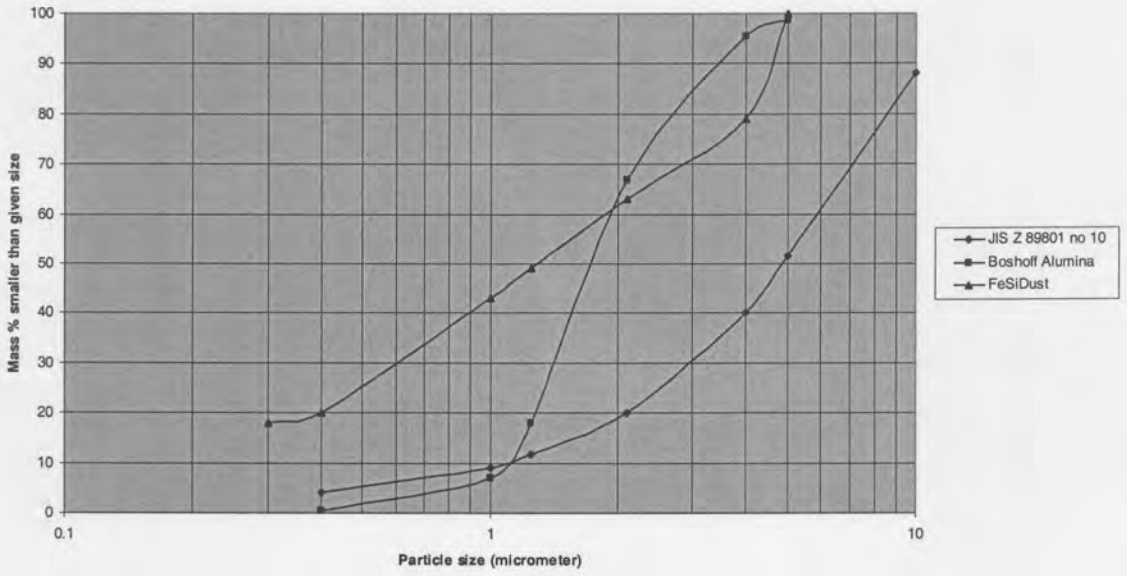

4.3 MEASUREMENT OF PARTICLE CONCENTRATION

Dust concentration on both the inlet and outlet side of the beds were measured using a HIAC/ Royco visible light particle counter, which consists of separate sensor and counter units. In the sensor (Model 1200) a beam of visible light is directed at the gas stream in which the concentration is to be determined. The angle at which the light beam is scattered is a function of particle size. Photodetectors set at different angles measure light impulses generated by particles in the size intervals corresponding to the angles. The Model 4100 counter collects the impulses and reports the number of particles in given size intervals. For this work, the intervals chosen were (in micrometers): 0,3 to 0,5: 0,5 to 1,5; 1,5 to 3,0; 3,0 to 5,0; 5,0 to 10,0 and larger than 10,0. This choice gives a high accuracy in the size range where, under most experimental conditions, a minimum in efficiency may be expected and a high accuracy is required.

For some of the moving bed test work, an APC 300A particle counter (Malvern Instruments) set at 0,3; 0,4; 0,5; 0,7; 1,0; 2,0; and 5,0 micrometer was used. The instrument uses the same principle as the HIAC/Royco machine, but has the the advantage that more channels are available, allowing smaller intervals to be used especially in the smaller particle range. In addition, a filter testing option is available, which allows sequential upstream and downstream samples to be analysed for the direct calculation of efficiency for each size interval.

At extremely high particle concentrations the photodetectors become saturated and the sensor cannot distinguish between individual pulses. For this range of concentrations, a calibrated flow divider (HIAC/Royco) was used. This device accurately divides the sample stream into two portions: approximately. $1/50^{th}$ of the stream is maintained at the sampled concentration, while the balance is passed through an absolute filter. In this manner, the sample gas flow remains constant while the concentration is reduced by a factor of 50.

The particle counter described above operates at a constant gas flow rate. It was therefore not possible to sample the inlet and outlet concentrations isokinetically. This introduces systematic error in the determination of absolute particle concentration which increases with particle size (Hicks 1971, Rouillard 1971) but is relatively small at the particle size and stream flow velocity used in this work. Moreover, the relative values at the in-and outlet of the filter are used for the calculation of efficiency and the error was kept the same for the in-and outlet by using similarly sized sample probes.

4.4 EXPERIMENTAL PROCEDURE

4.4.1 Static bed.

For tests on the static bed apparatus, the granular material is washed with water and dried at 105 °C. After packing the bed, dry clean air is passed through the bed for 30 min. to remove possible residual dust. Air is then passed through the dust feeder section and the dust feeder started at a predetermined feed rate. The dust-laden air is exhausted to the laboratory fume cupboard until the feeder has stabilized. It is then fed to the bed.

Sampling time for in-and outlet concentration is a minute, with a preceding stabilisation time of 30 seconds. At least three concentration readings were taken for each experimental run.

4.4.2 Moving bed.

Before an experimental run, the entire apparatus is blown clean with dried compressed air. The dust feeder is filled with dried dust or a dust/glidant mixture, as appropriate.

For runs at elevated temperature, the air flow is set to the desired value after which the heating elements are switched on until the inlet temperature has stabilised at the required value (approx 30 min.). The bed is then filled with the granular medium and the bed movement initiated with the air flowing, until the outlet temperature has stabilised. The dust feeder is started with the bed bypass filter open until the inlet dust concentration reading has stablised. Flow is then switched to the bed and the dust concentrations at the in-and outlet taken. Wherever possible, ten readings were taken in order to obtain good averages. The particle size intervals were set at the values given earlier.

Runs at room temperature followed the same procedure with the exception of the steps required for heating of the gas and the bed.

4.5 REFERENCES

ASI Instruments: http://asiinstr.com/dc1.html#list Consulted in 2002

Baumeister, T.H. *et al.*(eds) (1978) *Marks' Standard Handbook for Mechanical Engineers*.8th ed. New York, McGraw-Hill

Brown, G.G. and ass. (1950) *Unit Operations* New York, John Wiley, cited in Foust, A.S. *et al.* (1960) *Principles of Unit Operations.* New York, McGraw-Hill

De Nevers, N. (1995) *Air Pollution Control Engineering.* pp 188-192. New York, McGraw-Hill

Foust, A.S. *et al.* (1960) *Principles of Unit Operations.* Corrected 2nd printing p 449-452. New York, John Wiley

Geiger, G.H., Poirier, D R. (1973) *Transport Phenomena in Metallurgy.* New York, Addison-Wesley, cited in Morkel, W.S.T. *Computer-based mathematical model for the prediction of the gas flow and dust distribution in a packed bed.* M Eng Thesis, University of Pretoria 1991

Hicks, R.E. (1971) *Measurement technique and systematic errors in sampling dust laden gas streams.* CSIR Special report CE188, Pretoria

Kaye, G.W.C., Laby, T.H. (1986) *Tables of Physical and Chemical Constants.* 15th ed 2nd printing. London, Longman Scientific

Leva, M (1959).*Fluidization.* New York, McGraw-Hill .cited in Perry, R.H., Green, D.W. (eds) (1984) *Chemical Engineers' Handbook.* New York, McGraw-Hill

Leva, M (1947) Chem Eng Progr 50 p 549, cited in Foust, A.S. *et al.* (1960) *Principles of Unit Operations.* Corrected 2nd printing. New York, John Wiley

Patterson, R.G. (1984) Particulate pollutant characteristics in Calvert, S., Englund,H.M. (eds) *Handbook of Air Pollution Technology.* New York, John Wiley

Rouillard, E.A.A (1971) *Experimental errors in sampling dust laden gas streams.* CSIR Special report CE189, Pretoria.

Weast, R. C.(1981) *CRC Handbook of Chemistry and Physics* CRC Press, Boca Raton.

Yamamoto, H., Suganama, A. (1984). Dispersion of airborne aggregated dust by an orifice. Int. Chem Eng. **24** (2) p 338-345

CHAPTER 5
RESULTS

5.1 STATIC BED

5.1.1 Confirmation of basic theory

The experimental apparatus was first tested using a 3 cm thick bed of 3 mm glass spheres without electrostatic augmentation (Kornelius *et al.* 1987). Experimental results are given in Table A1. In fig 5.1 below, experimental results are compared to the "corrected sum of mechanical efficiencies" prediction for which details are given in Chapter 3. The calculated efficiencies are neglible for particles smaller than 1 micrometer and only become significant for particles larger than 2 micrometer. From 2 micrometer, particle bounce becomes limiting and bed efficiency decreases. It is obvious t hat the experimental efficiencies are much higher than predicted values, even by orders of magnitude for the smaller particle sizes. The most obvious explanation is the phenomenen first recorded by Pilney and Erickson (1968) viz. that tribo-electric charging of particles (i.e. generation of an electrostatic charge without imposition of an electric field) may considerably enhance capture efficiency.

Fig 5.1: Capture efficiency of 3 cm static glass bead bed for JIS fly ash

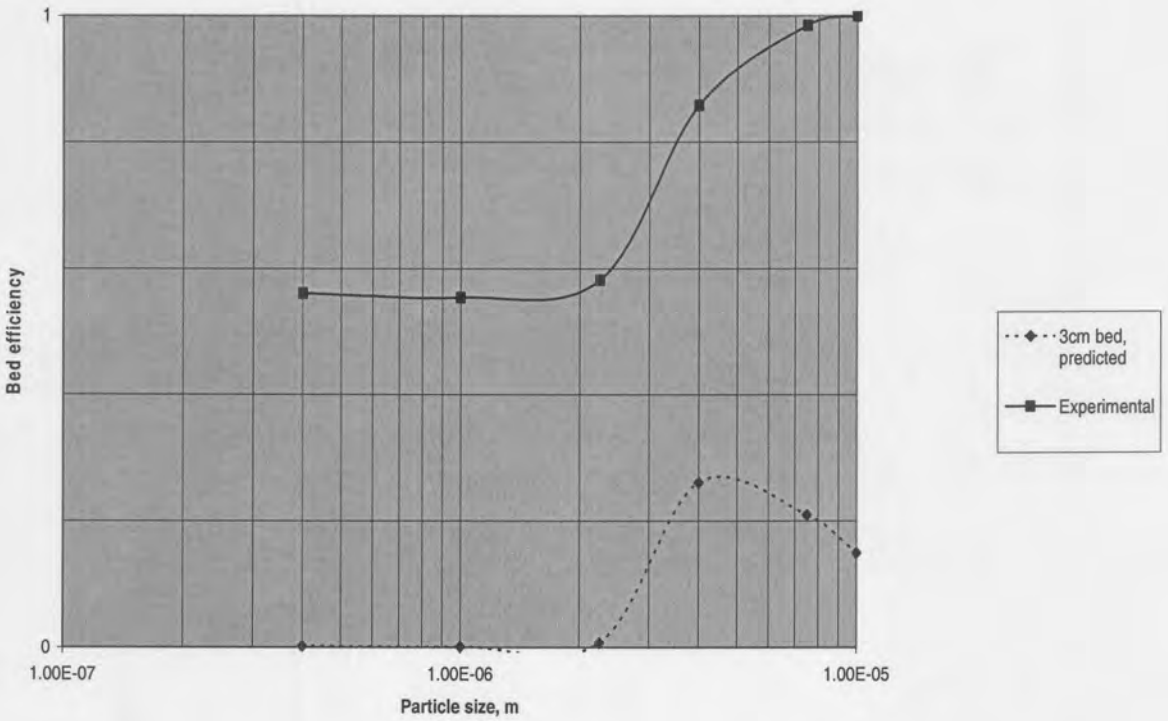

Two phenomena may explain the anomalies in efficiency shown in fig. 5.1. For the smaller particle sizes (< approximately 3μm), the accumulation of tribo-electrically charged particles in the bed may cause a field to be set up around the granules. In this field, the collection of charged particles will be enhanced. For the larger particles, the presence of charges will enhance retention of particles on the granules and educe the effect of "bounce" on particle collection efficiency.

The next set of experiments was aimed at testing the basic theory for static beds with an applied field, but eliminating the tribo-electrically induced particle charges. Experimental results were obtained by the introduction of the ionising nozzle (described in section 4.1.3) upstream of the bed and downstream of the particle feed point to neutralise particle charges that might have been produced by friction effects in the connecting ductwork. This is the only condition for which no assumption or measurement of particle charges upstream of the bed is required.

To test the influence of (i) the model used to describe electrostatic efficiency (Tardos and Snaddon 1984, Dietz 1981, or Shapiro *et al.* 1988 as described in section 3.3.6), (ii) the effect on "particle bounce" of an applied electrostatic field over the bed and (iii) the appropriate value of the ion density used in particle charge calculations, an objective function or the sum of relative least squares of deviations $\Sigma[(\eta_{exp}-\eta_{th})/(\eta_{th})]^2$ (the "error sum") was calculated for a number of different combinations of the variables, and the minimum value of the sum taken as indicating the best representation. It should be noted that this sum is "artificially" high where a zero experimental value occurs for a non-zero theoretical value, as the contribution of that point to the sum is always unity.

The value of the ion density in the granular bed deserves some comment. This value is commonly assumed to be an average of the order of 10^{12} to 5.10^{13} per cubic meter in a normal electrostatic precipitator (White 1963, 1984). The value for a granular bed could not be found in the available literature, and would be extremely complicated to determine directly. Its effect thus has to be found indirectly by the change in calculated collection efficiency and, as will be shown below, this may cause considerable uncertainty. In the results presented in figs. 5.2 to 5.4, there was no direct correlation between the value of the applied field and the ion density that produced the least value of the error sum.

Results from Tables A2 to A4 are compared to calculations in figs. 5.2 to 5.4 below for three values of potential applied to a 3 cm static bed of spherical glass granules without a pre-charger, (i.e. using the in-bed charging mechanism described in section 3.5) capturing alumina dust. When calculating the time available for the in-bed charging process ,and hence the actual particle charge, the actual gas velocity in the bed calculated by dividing superficial velocity by bed porosity (rather than the superficial velocity of 0,453 ms^{-1}) was used. The minimum total value for the error sum for the three cases is found with the Dietz description of the electrostatic efficiency, K_1 in equation 3.2 taken equal to $(1-\varepsilon)/\varepsilon$ and an ion density of the order of 10^8 per cubic meter. Varying the ion density by an order of magnitude away from the value at which the lowest error sum is found in most cases increases the error sum by less than 20%, indicating that the results are relatively insensitive to the ion density value. The potential shown in the figure legends is the value applied across the bed; the equivalent field strength in the bed was calculated using the method of Hashin and Shtrikman (1962).

The lines fitted to the experimental points have been added for graphical clarity, as are all the lines shown on the graphs of this chapter, and have no physical significance. The exceedence of a value of unity for

the capture efficiency at appriximately 6 micrometer in particle size is therefore a phenomenen merely caused by the curve-fitting routine within the Excel software package.

It is clear from the high experimental values found for the larger particles (> 4 micrometer) that particle bounce-off has been eliminated, or at least reduced to negligible proportions, by the strong adhesion forces between granules and captured particles created by the applied field.

Fig 5.2: 3 cm static glass bead bed, alumina dust, no precharger

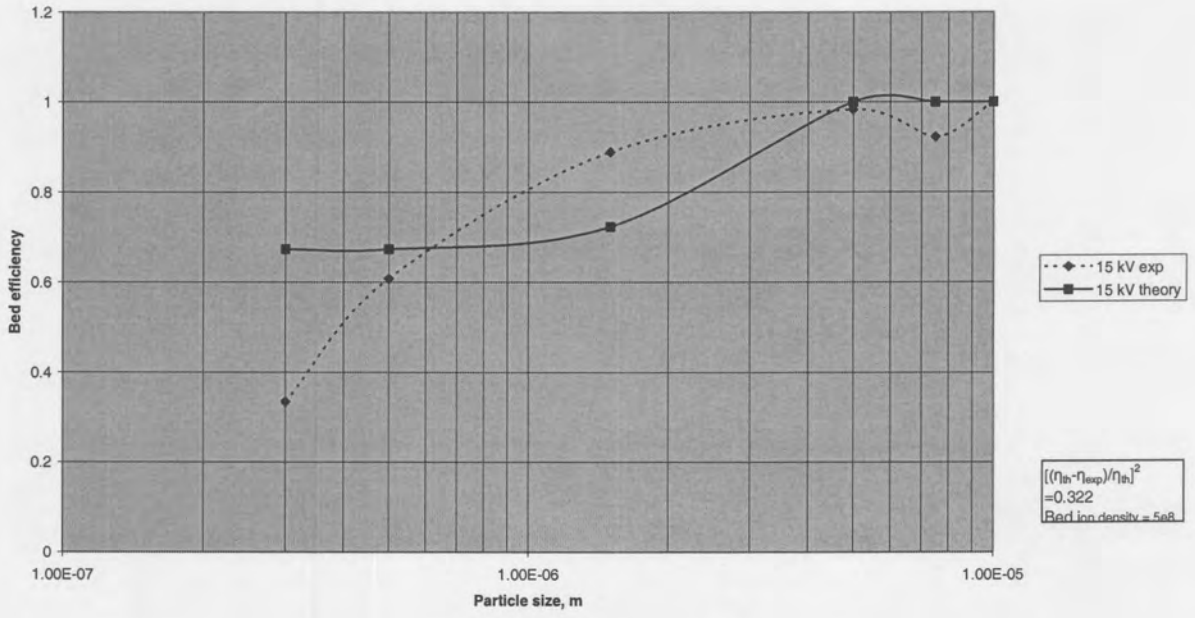

Fig 5.3: 3 cm static glass bead bed, alumina dust, no precharger.

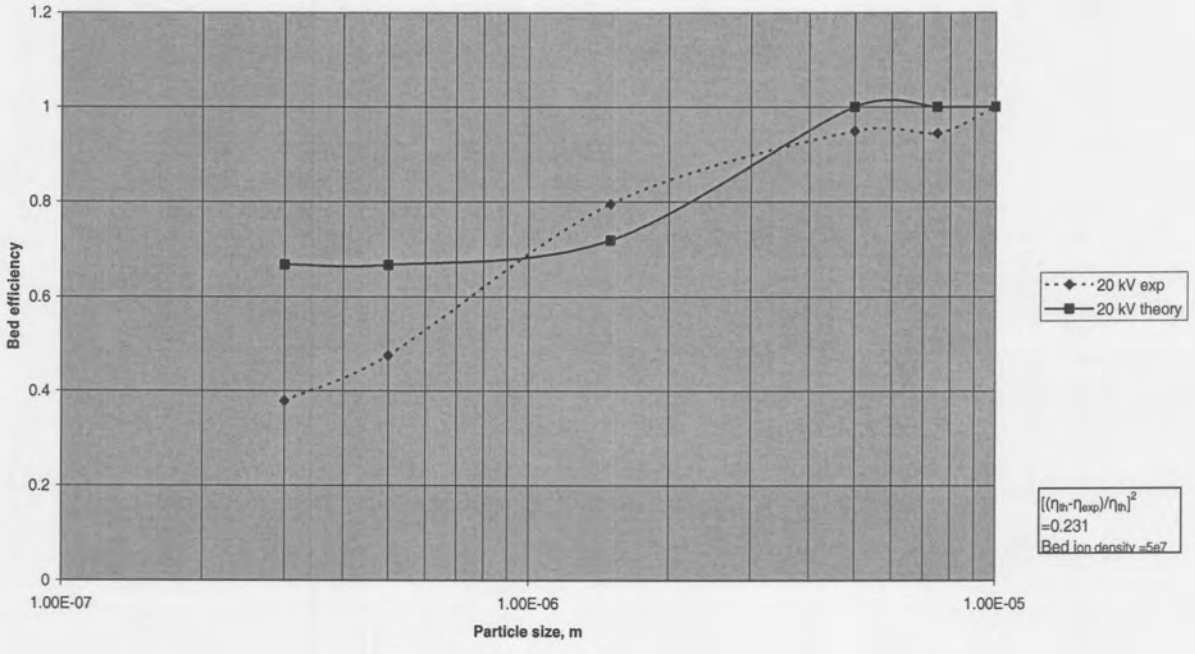

Fig. 5.4: 3 cm static glass bead bed,alumina dust, no precharger

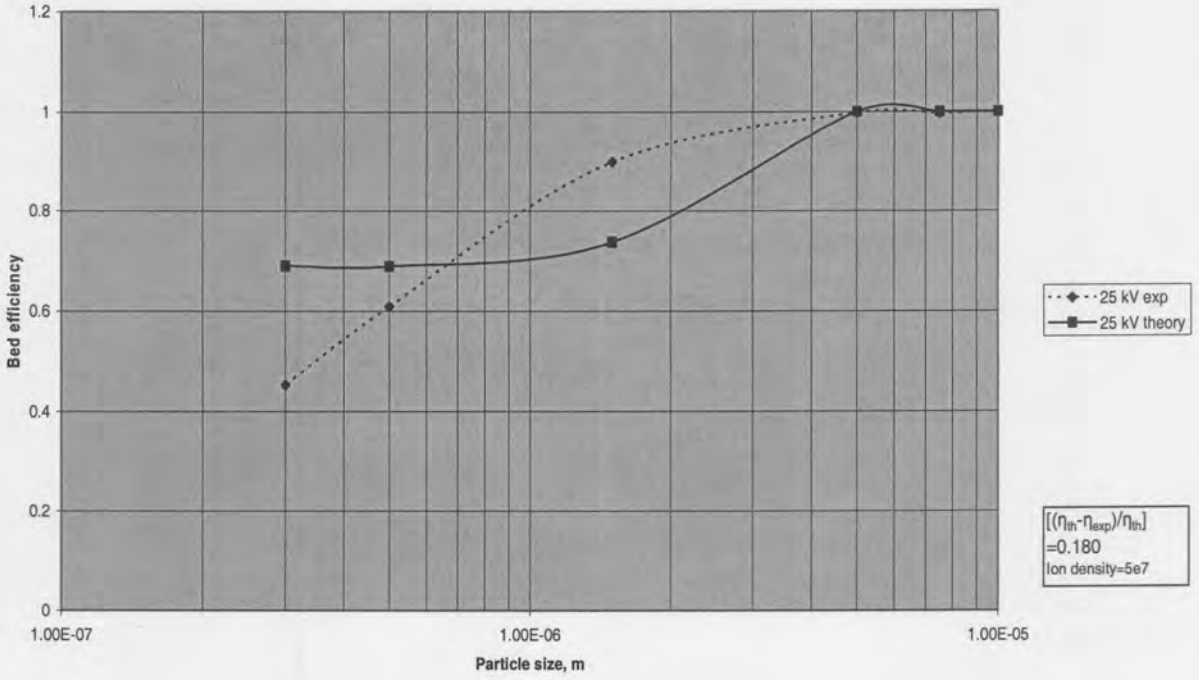

The increase of experimental efficiencies with the log of the particle size between 0,3 and 1,5 micrometer while the calculated efficiencies are fairly constant in this size range, which is found throughout the results in this section, cannot be adequately explained. It is well known that electrostatic particle collection efficiencies go through a minimum in this size range and all the calculational procedures described in section 3.3.6 show the same tendency. The monotonous increase in efficiency is therefore at odds with the physical mechanisms in a clean bed. In addition, the single granule efficiencies in this size range are all sufficiently small for the addition of efficiencies of the individual mechanisms (as used in the calculations for the results reported here), rather than multiplication of penetrations, not to cause a meaningful difference. The discrepancy might arise if particles were to behave differently under test and measurement conditions, for instance agglomerating under conditions in the test bed, but reporting as individual particles under high shear conditions in the measuring cell of the light diffraction type instruments used here. This tendency is however not apparent in later results under similar circumstances. It may therefore be due either to the presence of the ionising nozzle under clean bed conditions, as the phenomenon is not found in later experiments on bed loading or where the nozzle is absent, or more likely to the effect of the bed being loaded with dust during the measurement, a phenomenen which is investigated in detail in section 5.1.2 .

Figs. 5.5 to 5.7 similarly show a comparison between predicted values and experimental values (from table A5 to A7) for a static bed of silica sand capturing alumina dust for three values of applied potential. The Leva equivalent particle size calculation (see section 4.1.1, table 4.2), the Dietz electrostatic efficiency description and a much lower ion density of only 6.10^4 to 4.10^5 per cubic meter gave the minimum error sum. No obvious explanation for the low ion density value offers itself, although the value

is obviously influenced by the porosity and by the dielectric constant of the bed material. This is indicated by the results of fig 5.8, where dolomite chips (dielectric constant 7.4) instead of silica sand (dielectric constant 2.5) were used under otherwise similar values of the variables. (Experimental data from table A8) In this case, an ion density of approximately 10^7 per cubic meter provides the best fit to the data. A summary of the pertinent variables is given in table 5.1 below.

Fig 5.5 : 3 cm static silica sand bed, alumina dust, no precharger

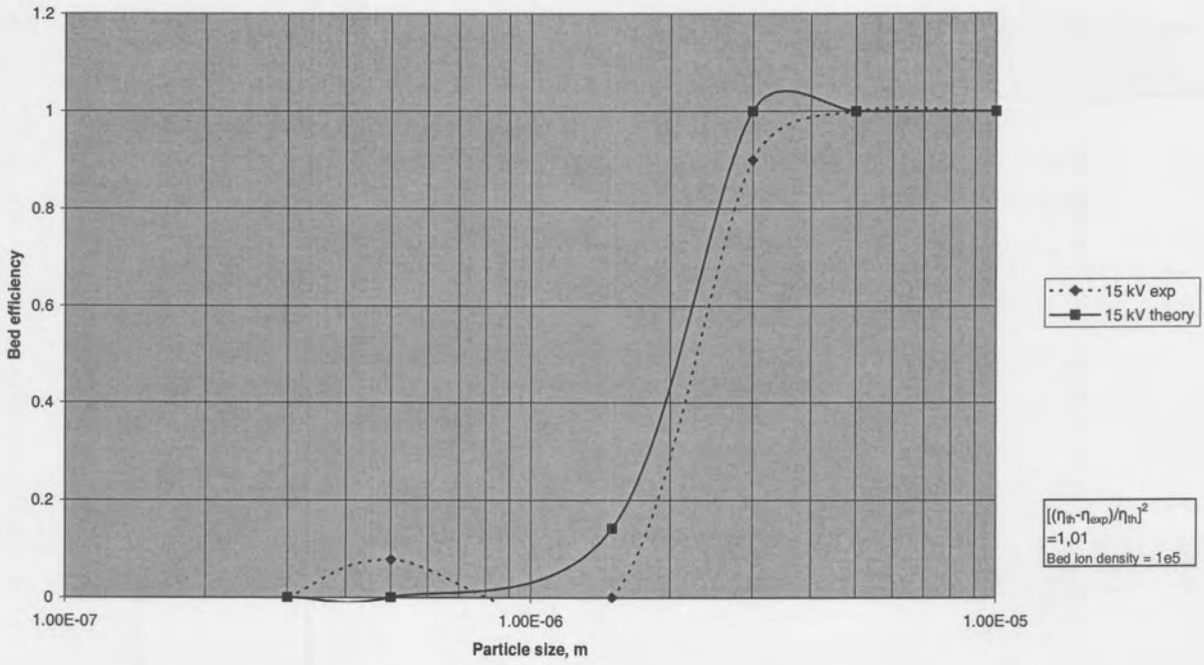

Fig 5.6 : 3 cm static silica sand bed, alumina dust, no precharger.

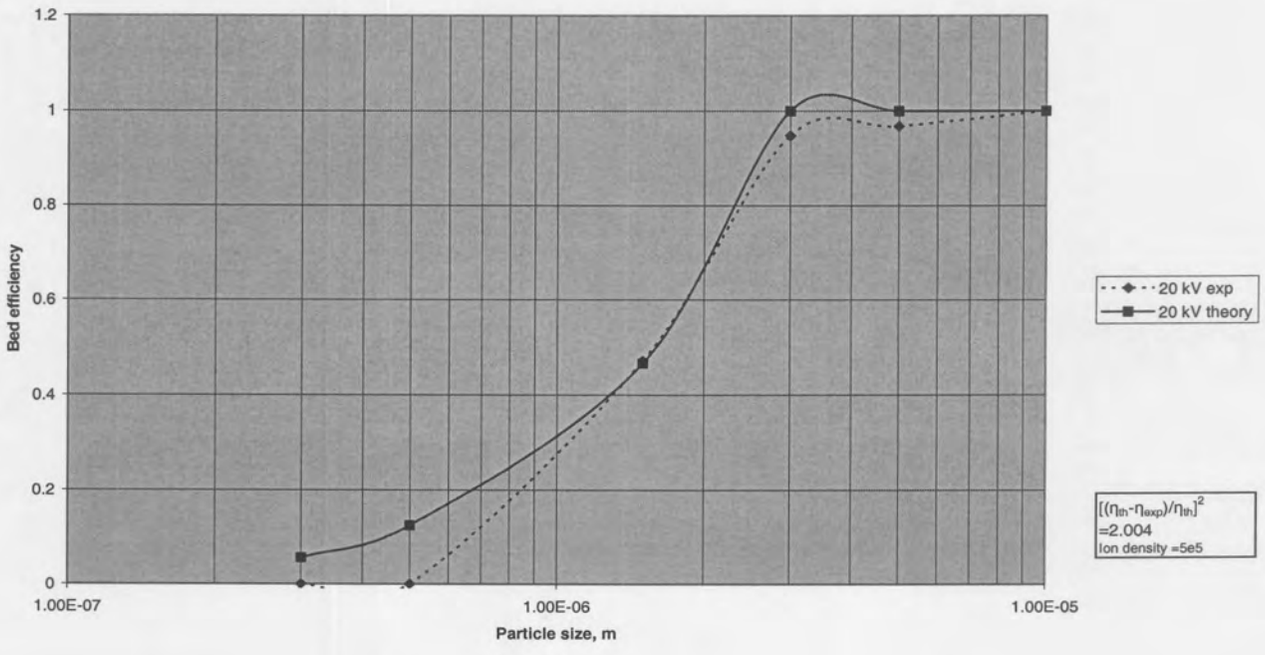

Fig. 5.7: 3 cm static silica sand bed, alumina dust, no precharger

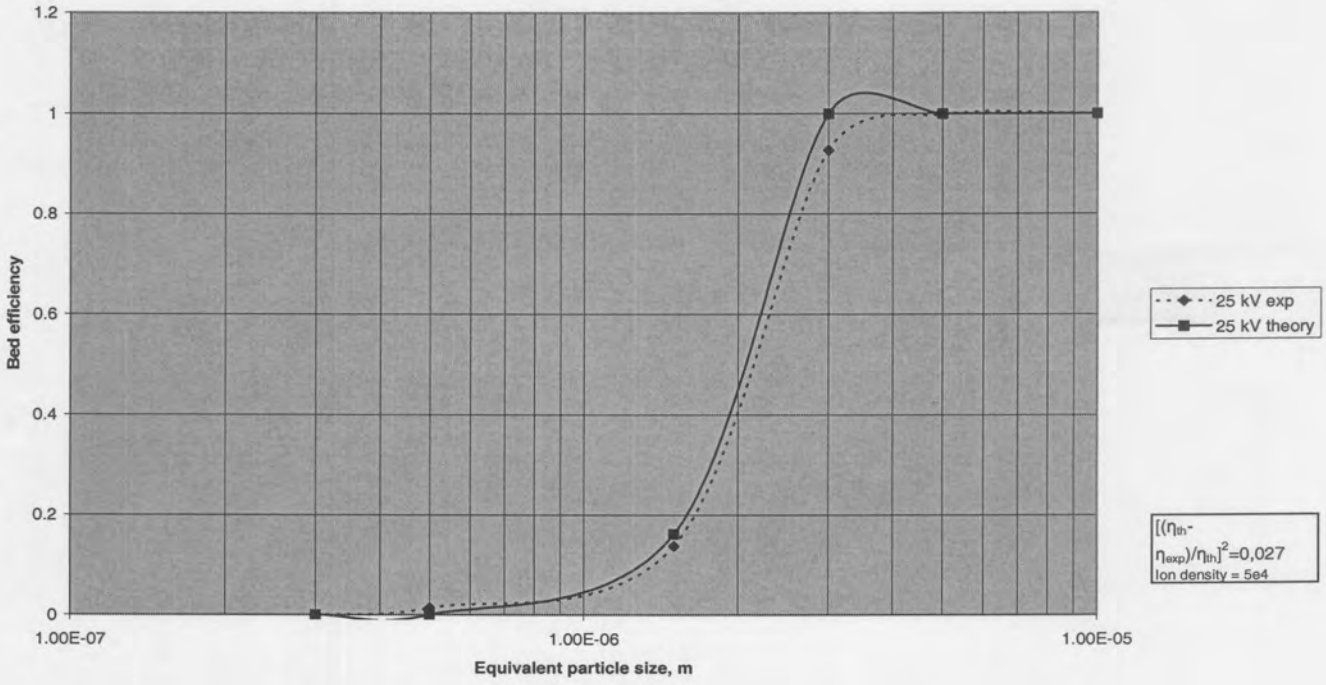

Fig 5.8: 3 cm static dolomite chip bed, alumina dust, no precharger

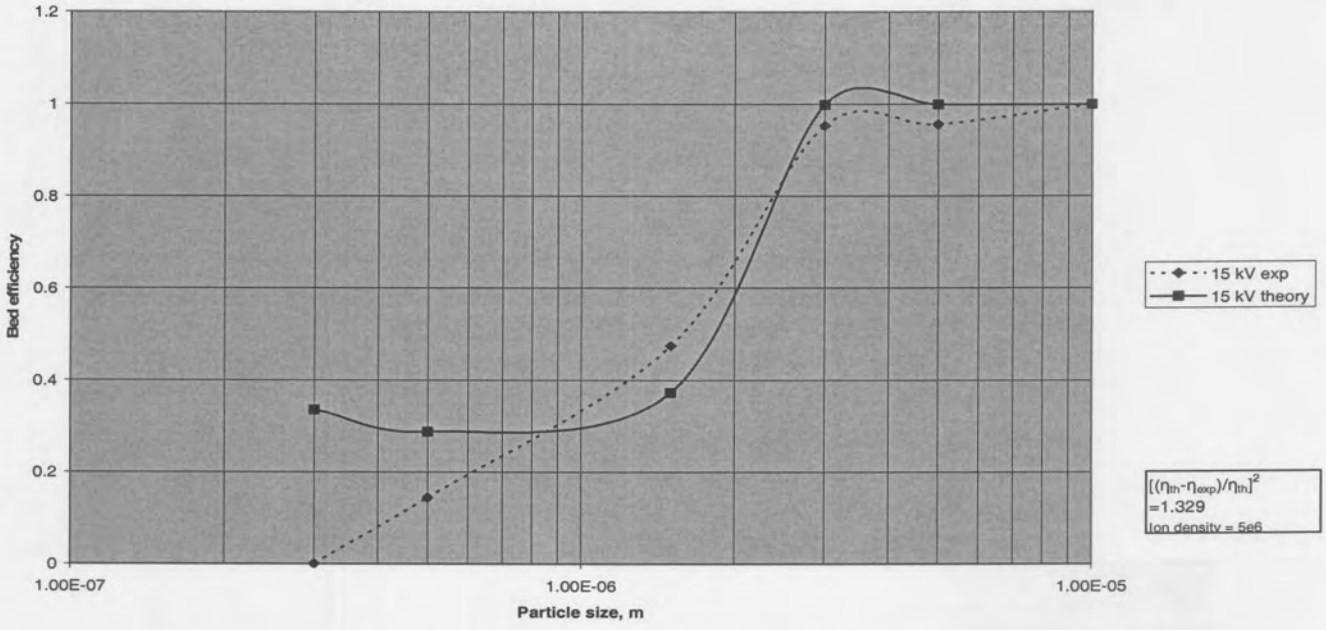

Table 5.1: 3 cm static bed variables for best experimental fit.

Bed material	Bed porosity	Granule sphericity	Dielectric constant	Effective di-electric const	Ion density@ 15kV (m^{-3})
Glass beads	0,38	1	3,8	2.413	5.10^8
Silica sand	0,48	0,80	2.5	1.663	4.10^5 to 6.10^4
Dolomite chips	0.463	0,72	7.4	3.312	5.10^6 to 2.10^7

The low and erratic value of the ion density required for a good model fit leads to the conclusion that, although the results can be fairly well represented by the proposed calculation procedure, the presence of the ionising nozzle in the gas circuit leads to conditions considerably removed from those that would be found under typical operating conditions and that results obtained for clean beds under these experimental conditions would not materially contribute to a practical design strategy.

5.1.2 The influence of bed loading.

5.1.2.1 Single granule efficiency enhancement factors directly from experimental results.

As an analytical solution of the differential equation linking bed loading as a function of bed depth with change in efficiency proved impossible, an alternative method of describing this effect was sought. It has been shown by Walata *et al.* (1986) that the parameters in equation 3.27 to 3.29 can in principle be obtained experimentally by the use of filter beds thin enough for the dust deposition to be considered uniform through the thickness of the bed, or by finding the values at different bed thcknesses and extrapolation of the results to zero bed thickness. Using these methods, they demonstrate that the value of α_2 varies little with bed height. It was subsequently shown by Jung (1991) that the assumption of uniform deposition may be valid for beds consisting of up to 18 layers of unit cells or collecting elements (depending on the superficial bed velocity) provided that the value of σ , the specific deposition volume, is below 10^{-3} . A method of finding the parameters α_1 and α_2 would then be to determine change in bed efficiency with time (and thus bed loading under conditions of uniform dust feed rate), plot $\log(\eta/\eta_0-1)$ against $\log \sigma$ and determine α_2 from the slope of the line. This value of α_2 could then be back-substituted into equation 3.27 together with the experimental value of η/η_0 at the lowest experimental value of σ (provided that this value is lower than the upper limit given above) to determine a value of α_1 . Alternatively, the intercept on the vertical axis could be used to provide an estimate for α_1.

To determine the feasibility of this technique for beds with applied fields, the efficiency history of static beds with applied fields (but using the ionising nozzle to eliminate tribo-electric charging of particles before entering the bed) was determined (Kamffer and Kornelius 1988, Kornelius and Kamffer 1989). A typical set of results is given in fig 5.9 below. Experimental values are given in Tables A6 and A9 to A.14

The parameter in fig. 5.9 is the bed load in cubic meter of alumina dust per cubic meter of bed i.e. the specific bed loading value. The values for specific deposition volume σ obviously depend on the actual and bulk density of the deposited dust; for a bulk density of 2500 kg m^{-3} the lowest value shown corresponds to a specific deposition volume of 0, 00018. This value is well within the range for which uniform deposition is a good approximation. Applying the extrapolation technique described above to these results leads to figures similar to 5.10 below, with linear least squares lines fitted to some of the data sets. It should be noted that the low correlation coefficient occurs for the larger particle size, where the high efficiency or low penetration values increase the uncertainty of the measureents (*cf.* section 5.2.3)

Fig 5.9: Efficiency history for 3cm glass bead static bed, 20 kV applied potential

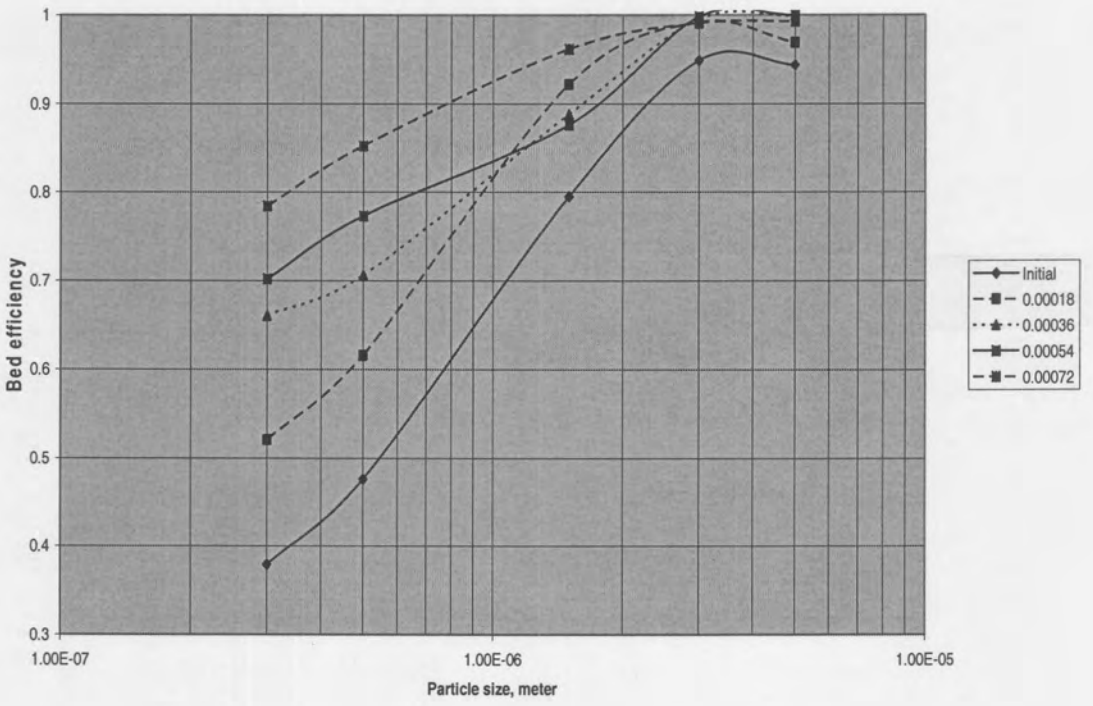

Fig.5.10: Graphic determination of loading parameters

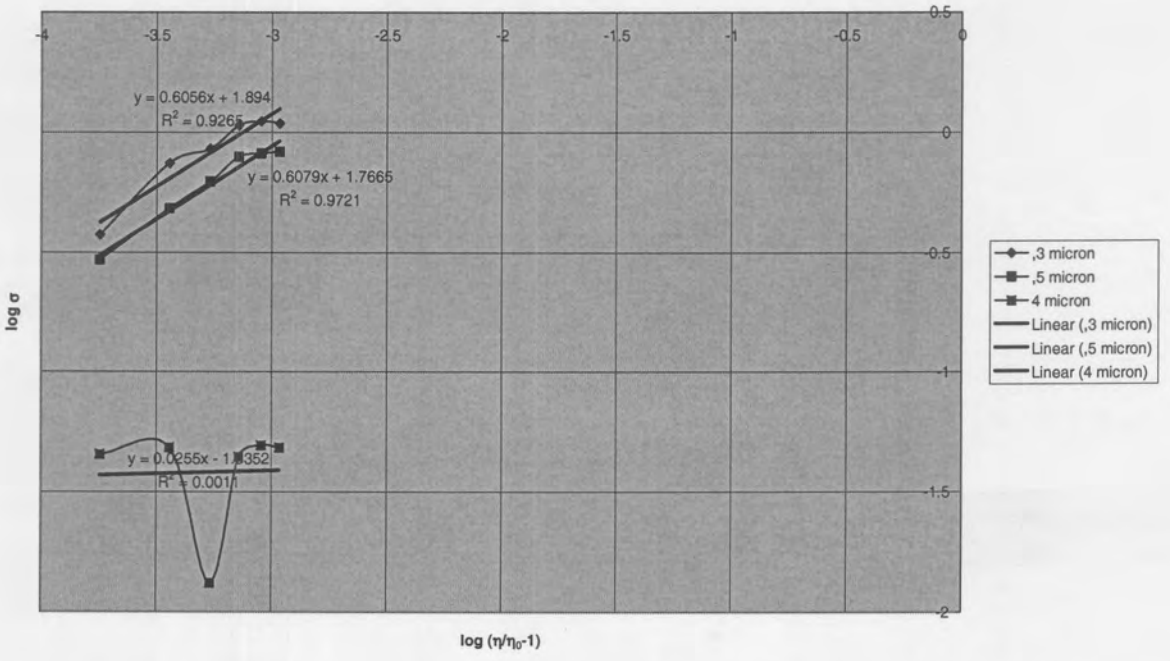

The conclusion can be drawn that the calculation technique described above will yield usable results for poly-dispersed dust in electrostatically augmented beds, especially if used on smoothed data.

Values for α_1 and α_2, calculated as described above (intercept method) for the cases where the initial collection efficiency was not zero, are shown in table 5.2 below for a number of operational parameters. (Data in tables A2, A4, A7, A8 and A15 to A38) The values shown under R^2 are those of the correlation coefficient, indicating how well the experimental values fit the chosen model. A value of 0 indicates no correlation with the model, while a value of 1 indicates that the model describes the experimental values exactly. The values obtained here are obviously applicable only to the experimental conditions for which they were determined, including the electrostatic augmentation.

Due to the sensitivity of the results to the value of η_0, a sensitivity analysis was done. The bold figures in table 5.2 indicate those sets of results where adjustment of the η_0 value (as might be required where measurement of the "clean" bed results took some time to stabilise) improved the correlation coefficient to larger than 0,8.

Table 5.2: Experimental values of bed loading parameters

Particle	Dolomite 5kV/cm			Glass 5kV/cm			Glass 6,7kV/cm			Glass 8,3 kV/cm			Sand 8,3 kV/cm		
size(μm)	α_1	α_2	R^2	α_1	α_2	R^2	α_1	α_2	R^2	α_1	α_2	R^2	α_1	α_2	R^2
0,3	**4931**	**0,953**	**0,869**	**11,83**	**0,579**	**0,836**	140	0,606	0,927	**161,1**	**0,853**	**0,585**	**1614**	**0,848**	**0,918**
0,5	480	0,695	0,907	**13,5**	**0,579**	**0,831**	20,5	0,608	0,972	**53,1**	**0,45**	**0.860**	485	0,477	0,605
1,5	36	0,526	0,881	0,35	0,008	0,001	0,017	-0,75	0,129	13e6	2,387	0,653	64	0,485	0,560
3,0	**4.9**	**0,465**	**0,839**	2,1	0,454	0,671	0,018	-0,09	0,01	0,51	-0,06	0,043	0	-0,99	0,310
5,0	**2,88**	**0,572**	**0,820**	0,02	0,068	0,337	1,96	0,473	0,53	0,01	-0.03	0,005	0,02	-0,23	0,595
10,0				0,02	-0,14	0.558									

Blank spaces indicate that too few valid experimental points were available for the calculation. These all occur for the largest particle size, where the effect of load is negligible and where the high efficiency values increase the uncertainty of the experimental values.

A number of conclusions can be drawn from the figures in this table:

- Comparison to the values of Walata *et al.*(1986) and Jung (1991) indicates that the order of magnitude of the α_2-values is similar (literature values from 0,315 to 1,152 for particle sizes of 1 to 4 micrometer). Where the experimental values in this work are outside that range, the correlation coefficient R^2 has a low value, indicating that the experimental values do not fit the Walata/Jung model very well.
- Although the experimental values for α_1 in this work vary too much for a systematic comparison to be made, the values for deposits of mixed particle sizes obtained here are generally much smaller than those cited in Walata (*op cit.*) and Jung (*op cit.*) for monodisperse particles, in some cases by several orders of magnitude (values obtained by the cited authors range between 10^2

range between 10^2 and 10^6). The α_1 values do however systematically decrease with particle size, indicating that the influence of bed loading becomes less important for the larger particles.

5.1.2.2 Correlation of single granule efficiency enhancement factors for electrostatically augmented beds.

Following the argument in section 3.6 that bed loading only affects the direct interception and impaction mechanisms, an alternative to the analysis in 5.1.2.1 is to calculate values for α_1 and α_2 applicable to the direct interception and impaction mechanisms only under varying experimental conditions. The first step in this analysis was to calculate values for the efficiency increase at a number of bed load values from the Jung correlations (Jung *op. cit.*) for comparison with experimental values. The calculated values are shown in Table 5.3 below for the operating parameters of fig. 5.9

Table 5.3: Calculated values for the Jung parameters and for increase in bed efficiency

Particle			Jung value for α_1	Jung value for α_2	Efficiency increase	
Size, μm	N_{St}	N_R			σ=0.00054	σ=0,00108
0,3	$1{,}89.10^{-4}$	$1{,}00.10^{-4}$	$1{,}34.10^{6}$	1,120	12200	21200
0,5	$4{,}45.10^{-4}$	$1{,}67.10^{-4}$	$1{,}10.10^{5}$	0,914	1790	3120
1,5	$3{,}29.10^{-4}$	$5{,}00.10^{-4}$	83,6	0,569	5,28	8,46
3,0	$1{,}25.10^{-2}$	$1{,}00.10^{-3}$	5,49	0,415	1	1

Jung's correlations were obtained (i) for the range of variables $1{,}7.10^{-3}<N_{St}<3{,}8.10^{-2}$ and $1{,}72.10^{-3}<N_R<8.10^{-3}$ (ii) for conditions where the deposit and the deposited particle have the same particle size (iii) with specific provision being made for charge neutralisation. They may therefore not be directly applicable to the particles outside this range (0,3 to approx 1,0 micron), or for deposited material of mixed particle size where electrostatic augmentation is applied. This is indicated in figure 5.11 below, which was calculated as follows using the experimental results given in table A3 and A9 to A14 and graphically depicted in fig 5.9:

- Single granule efficiency due to all mechanisms was calculated for each particle size from the "no load" experimental bed efficiency
- Increase in single granule bed efficiency was calculated for different bed loads from equations 5.2 to 5.4 using Jung's correlations applied to equation 3.7 for impaction and equation 3.4 with the Kimura correction for interception (sample results given in table 5.3)
- The results were added to the "no load"single granule experimental efficiency and the resultant total single granule efficiency calculated.

From the results depicted in fig 5.11, it is clear that the effect of bed loading using the constants as determined from Jung's correlations is not well estimated, especially in the middle range of particle size. The probable reason is that the correlations of equations 5.2 to 5.4 do not allow for the electrostatic field which may have a major impact on the morphology of the deposits; in addition, the experimental work was carried out with deposits of mixed particle size..

Fig 5.11: Jung's predictions for the effect of bed loading:3 cm bed of glass beads, alumina dust, 20 kV applied over bed, charge neutraliser but no precharge

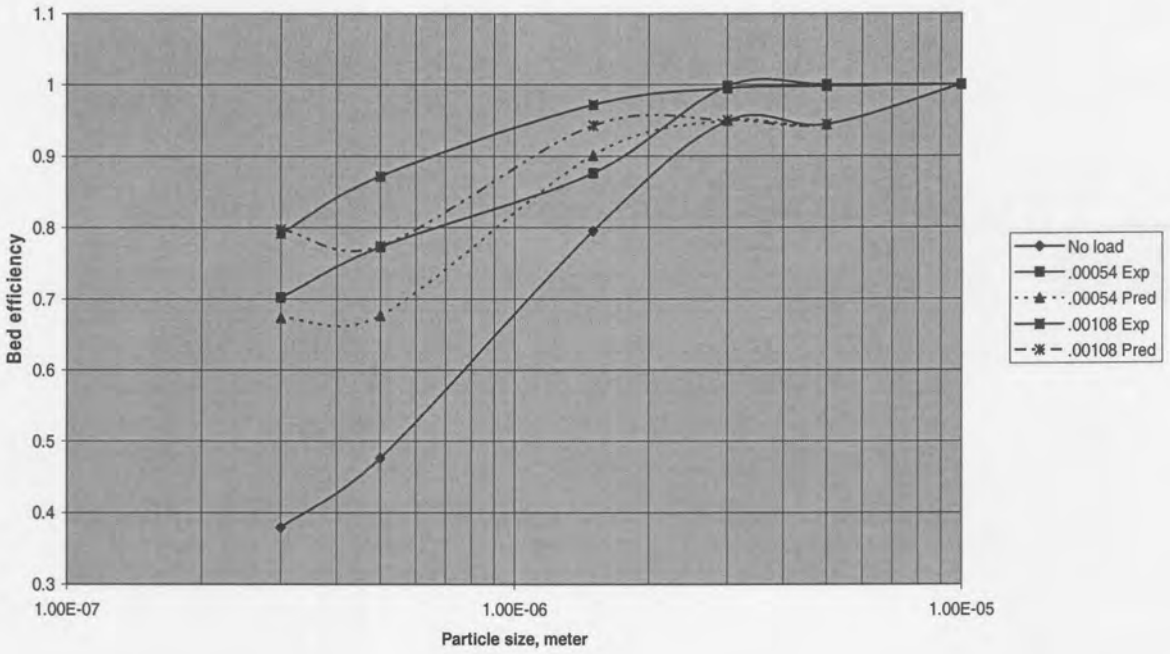

Improved estimates for the change in bed efficiency with increase in bed load under applied electrostatic field were therefore determined as follows:

- Single granule efficiency due to all mechanisms was calculated for each particle size from the "no load" experimental bed efficiency.
- Equation 3.4 with the Kimura correction and equation 3.7 were used to calculate single granule efficiencies for the interception and impaction mechanisms.
- The objective function $\Sigma[\eta_{\sigma i,exp}/\eta_{0,exp}-\eta_{\sigma i,calc}/\eta_{0,exp}]^2$ proposed by Walata *et al.* (*op cit.*) was minimised for values α_1 and α_2 for each particle size with equation 3.27 applied to the single granule interception and impaction mechanisms by the univariant search method described by Beveridge and Scheckter (1970). In this function, $\eta_{0,exp}$ denotes the clean bed single granule experimental efficiency value, $\eta_{\sigma i,exp}$ the experimental single granule value for the *i*th bed loading value and $\eta_{\sigma i,calc}$ the single granule total efficiency calculated from

$$\eta_{\sigma i,calc} = \eta_{0,exp} + \eta_{imp,int}\,\alpha_{1,i}\,\sigma_i^{\alpha_{2,i}} \quad \text{.....(5.1)}$$

The values in table 5.4 below were obtained.

Table 5.4: Experimental values for bed load parameters

	Glass 6,7 kV/cm				Dolomite 5 kV/cm			
Particle size micrometer	α_1	α_2	Efficiency increase factor for σ =		α_1	α_2	Efficiency increase factor for σ =	
			0,00054	0,00108			0,00054	0,00108
0,3	$1,19.10^6$	0,58	15151	22643	**$1,81.10^6$**	**0,66**	12620	19941
0,5	$5.18.10^5$	0,68	3108	4979	$2,1.10^5$	0,57	2882	4279
1,5	880	0,69	5,90	8,90	945	0,63	9,26	13,78
3	12	0,56	1,18	1,26	**9,7**	**0,57**	1,13	1,20

The figures in bold were obtained on the modified data which were indicated similarly in table 5.2. As the results described so far were obtained at one superficial velocity only, α_1 can not be correlated with N_{St} and N_R independently; for this velocity, it does correlate with $N_{St}^{-2,86}$. Using the correlation between N_{St} and N_R at this specific velocity, Walata's (*op. cit.*) equation for α_1 has a dependency on $N_{St}^{-3,27}$ for particles of a single size (2 µm) for varying granule sizes, indicating a similarity in trend. Similarly, the results of Takahashi *et al.* (*op.cit.*) indicate a correlation with $N_{St}^{-3,.8}$ for constant N_R .

As there is no clear correlation between the calculated α values and the variables of field strength and collector type, an average value for α_2 of 0,617 and the average of the above α_1 values for each particle size was used on the results depicted in fig 5.9 to obtain the results shown in figure 5.12 below.

Fig.5.12: Influence of bed load using experimentally determined load parameter

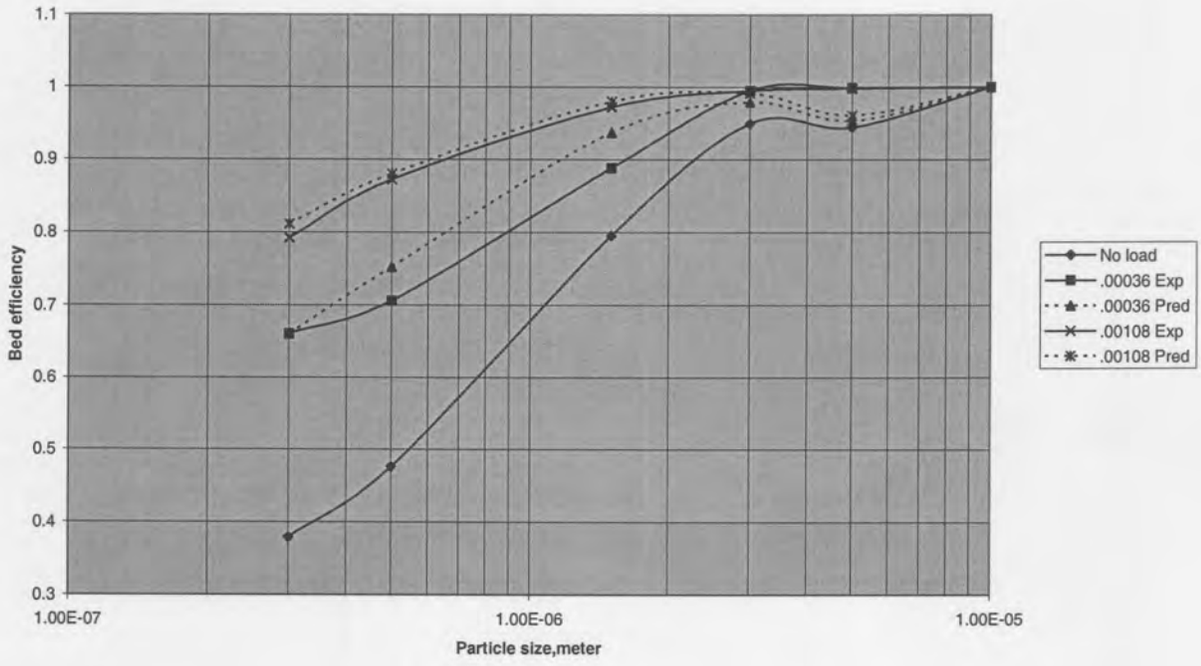

It is clear that the prediction is much improved from that depicted in fig 5.11. Even better results can of course be obtained if the experimental constants obtained for each collector type and particle size shown in table 5.4 are used.

5.2 MOVING BED

5.2.1 The influence of bed movement

The influence of bed movement was initially tested using the data shown in tables A39 to A43 of Appendix A. The bed consisted of a 6 cm thick bed 2,8 mm dolomite chips with 10kV applied over the bed. JIS fly ash was used as test dust and bed velocities of 0,25 and 0,5 mh^{-1} were used at a constant filtration velocity of 0,4 ms^{-1}. The bed loading parameters for dolomite given in table 5.4 were adjusted for the average dust particle size (mass mean geometric diameter) of the deposited dust and for the change in granule size using the methods of section 3.6. This resulted in the efficiency increase factors given in table 5.5 below. The variation with vertical bed velocity is caused by the variation in bed load, which for a constant inlet dust concentration is determined by both filtration velocity and vertical bed velocity.

Table 5.5: Single granule efficiency enhancement factors due to bed load, 2, 6 mm dolomite bed and JIS fly ash.

Particle size, micron	Gas temperature 20 °C		Gas temperature 100 °C	
	Bed vel. 0,25 mh^{-1}	Bed vel. 0,5 mh^{-1}	Bed vel. 0,25 mh^{-1}	Bed vel. 0,5 mh^{-1}
0,3	4502	2869	6031	3843
0,5	523	334	700	446
1,5	3,35	2,50	4,14	3,01
5,0	1,02	1,015	1,03	1,02

Bed movement was then allowed for by assuming a linear relationship between re-entrainment efficiency (section 3.4) and vertical bed velocity over the two layers of granules at the inlet and the outlet of the bed (adjacent to the retaining grids). In this configuration, the velocity of the two moving layers relative to adjacent layers (a static grid on one side and the fully moving bed on the other), and therefore the assumed re-entrainment efficiency, is equal. A sensitivity analysis indicated that calculating with the assumption of only one moving layer on either side of the bed did not improve the model fit. The minimisation of the "error sum" described in section 5.1 was again used to find the values of the re-entrainment efficiencies for the varying conditions described. Figure 5.13 indicates the results achieved when the same re-entrainment efficiency is assumed for all particle sizes. It is clear that there is a systematic deviation related to particle size when this assumption is made.

Fig 5.13: Effect of bed movement, filtr.velocity 0,4 m/s 20 deg C

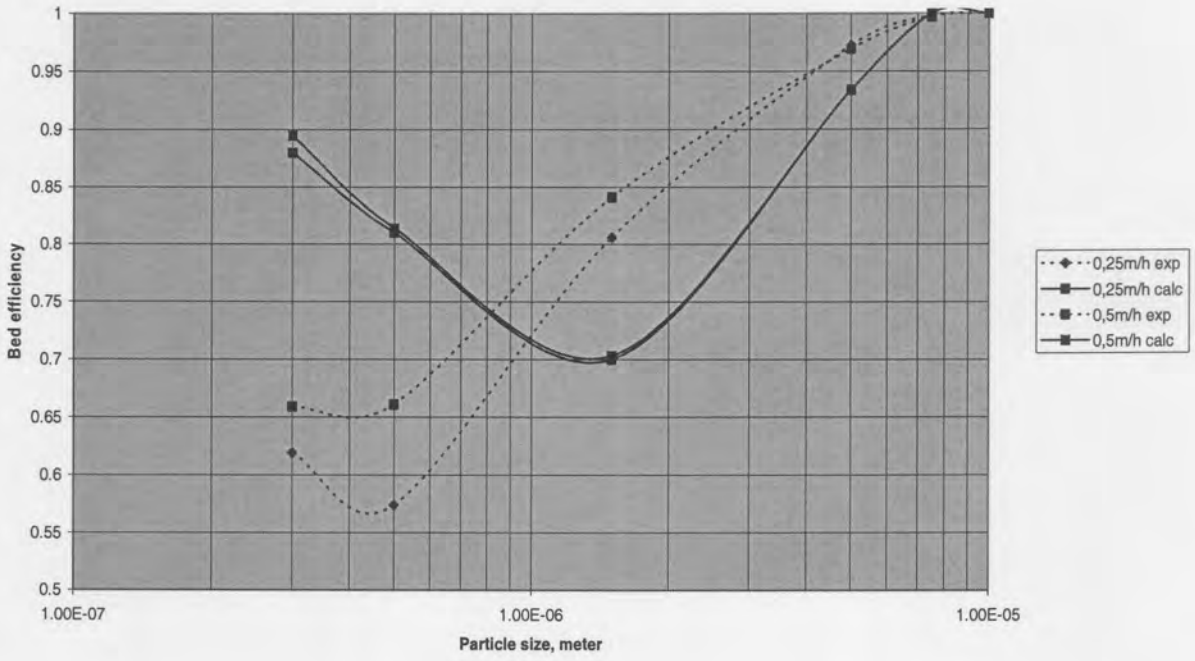

It is clear that the re-entrainment efficiency must be determined as a function of particle size. Hence, by minimisation of the "error sum" for each particle size seperately, a particle size-specific re-entrainment or release efficiency was found. Results are given in table 5.6 below.

Table 5.6: Variation of re-entrainment efficiency with particle size

Particle size, micron	Gas temperature 20 °C		Gas temperature 100 °C	
	Bed vel. 0,25 mh^{-1}	Bed vel. 0,5 mh^{-1}	Bed vel. 0,25 mh^{-1}	Bed vel. 0,5 mh^{-1}
0,3	0,37	0,34	0,27	0,30
0,5	0,30	0,26	0,19	0,25
1,5	0,10	0,07	0,04	0,09
5,0	0	0	0	0

The results at 20 °C are counter-intuitive, in the sense that re-entrainment efficiency decreases with increasing bed velocity. This is of course due to the fact that the experimental efficiency results at this temperature show the same tendency. However, even for the results at 100 °C the effect of bed velocity on release efficiency is much less than proportional. The results of section 5.2.4 will be used to further clarify this relationship.

5.2.2 The influence of the pre-charger

It is obvious from equations 3.24 and 3.26 that the electrostatic charge on particles increases with time spent in an electric field (although not in linear proportion) and from equation 3.17 that single granule collection efficiency due to the electrostatic mechanism is a linear function of particle charge. One

method of increasing the particle charge would be to increase charged bed thickness; this would simultaneously increase the "mechanical" efficiencies for the larger particle sizes. The pressure drop would however also rise. A separate precharger, constructed like a normal plate-type industrial electrostatic precipitator installed upstream of the granular bed provides the means of increasing particle charge while retaining the advantages of a thin bed, and the next set of experiments were carried out on this configuration (Kornelius 1991, Kornelius and von Reiche 1993). A static 6 cm. thick bed, using 2,3 to 2,8 mm dolomite (Leva equivalent diameter 2,7 mm) was initially used in conjunction with the precharger described in section 4.1.4.

JIS fly ash was used as test dust. The effect of bed loading was calculated for by applying the methods discussed in section 3.6 to the parameters of table 5.4 to allow for the change in particle size of the deposited material and the change in filtration velocity.

As only one high voltage source was available at the time, this was used for both the precharger and the bed, but due to the relative dimensions and because the effective field in the bed is the nominal value divided by the effective dielectric constant of the granular medium (Hashin and Shtrikman, 1962), this provided a much stronger charging field to the precharger than the collecting field across the bed. This results in particles entering and moving through the bed having a much higher charge than would result from charging in the bed itself. Strictly speaking, a slow discharge of the particle should therefore occur as it moves through the bed. To simplify calculations, no charging or discharging of the particles in the bed itself was however allowed for in the calculations described below. The ionising nozzle was not used, but for calculation purposes zero charge was assumed for the particles entering the precharger.

Figures 5.14 and 5.15 show the calculated and experimental results (tables A44 to A49 in Appendix A) for filtration velocities of 0,25 ms^{-1} and 0,75 ms^{-1} respectively and at different field strengths. All of the calculated results were obtained at assumed ion densities of 10^{15} in the precharger, which can be considered normal for the high field strengths applied here. Again, the error sum, and hence the calculated efficiencies, were relatively insensitive for ion densities one order of magnitude away from the value at which the minimum error sum was obtained. It should be noted that figure 5.14 has an expanded vertical scale starting at an efficiency of 0,7.

Fig 5.14: Effect of precharger, filtr. velocity 0,25 m/s

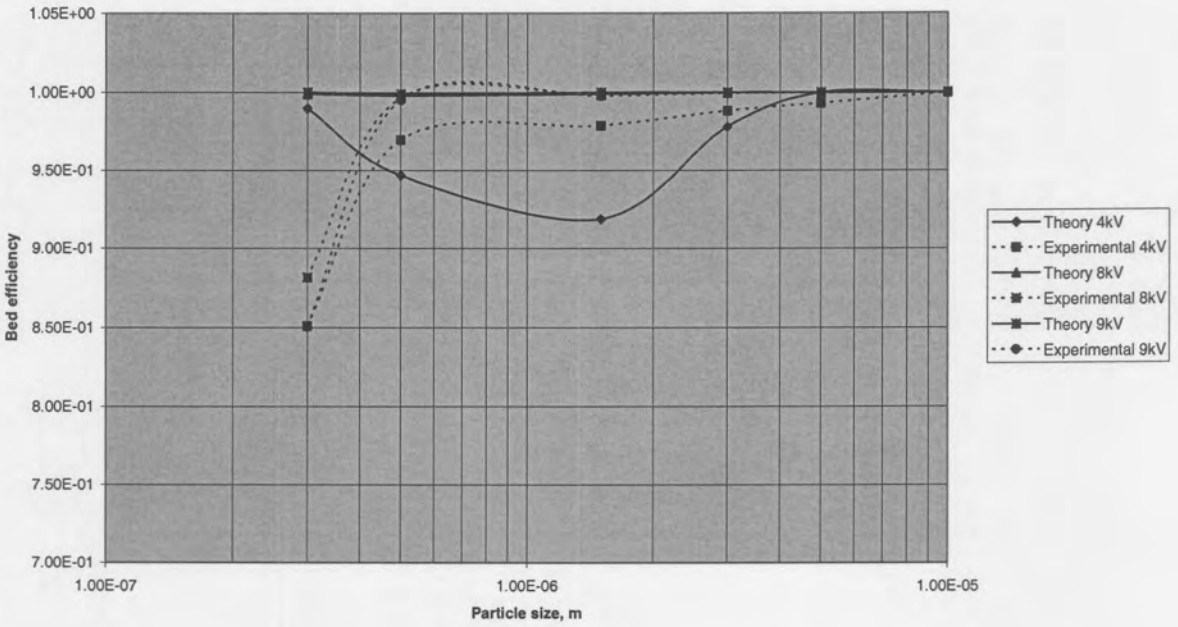

Figure 5.15:Effect of precharger, filtr. velocity 0,75 m/s

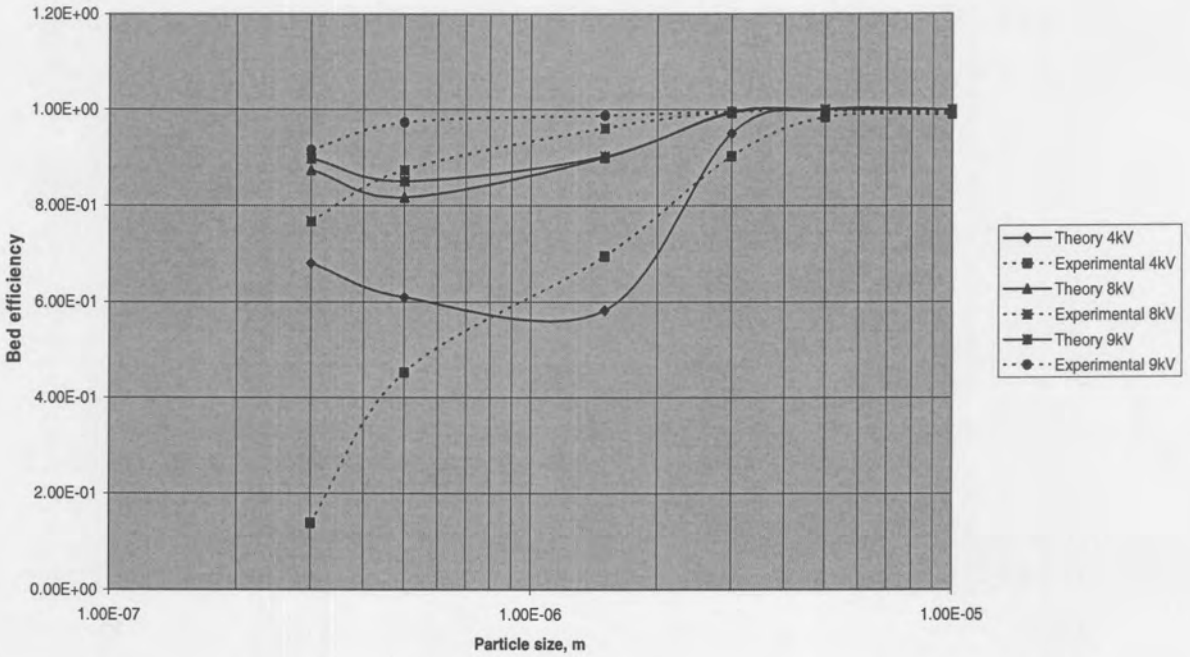

Although there is some discrepancy especially in the lower particle sizes, the trend of the impact of the pre-charger is reasonably predicted

5.2.3 The influence of bed movement with the precharger

This effect was tested for with a 6 cm thick bed of 2,7 mm dolomite chips using JIS fly ash. The experimental design allowed for two levels of pre-charger voltage (5 kV and 8 kV), two levels of bed voltage (5 kV and 10 kV), two levels of filtration velocity (0,24 ms^{-1} and 0,68 ms^{-1}) and three levels of vertical bed velocity (0,55 mh^{-1}, 1,05 mh^{-1} and 2,1 mh^{-1}). Valid results were obtained at all but two of the combinations.

To obtain values for the re-entrainment efficiency under the above experimental conditions, the previously described calculation methods for the efficiency of pre-charged beds, allowing for the influence of bed loading,,were used. The corrections of section 3.6 for particle size of deposited dust, granule size and filtration velocity were applied to the loading parameters of table 5.4 . The variation in bed load with filtration velocity and bed velocity, due to the constant dust feed rate, was again allowed for. The resultant calculated bed loadings and efficiency enhancement factors are shown in tables 5.7 below.

Table 5.7.1: Bed dust loadings (m^3 dust per m^3 bed), 6 cm bed, 2,7 mm dolomite chips, 20 °C; JIS fly ash

Filtration velocity 0,24 ms^{-1}			Filtration velocity 0,68 ms^{-1}		
BV 0,55 mh^{-1}	BV 1,05 mh^{-1}	BV 2,12 mh^{-1}	BV 0,55 mh^{-1}	BV 1,05 mh^{-1}	BV 2,12 mh^{-1}
$2,3.10^{-4}$	$1,13.10^{-4}$	$5,5.10^{-5}$	$6,5.10^{-4}$	$3,0.10^{-4}$	$1,58.10^{-4}$

Table 5.7.2: Single granule efficiency enhancement figures for conditions of table 5.7.1

	Filtration velocity 0,24 ms^{-1}			Filtration velocity 0,68 ms^{-1}		
Particle size,μm	BV 0,55 mh^{-1}	BV 1,05 mh^{-1}	BV 2,12 mh^{-1}	BV 0,55 mh^{-1}	BV 1,05 mh^{-1}	BV 2,12 mh^{-1}
0,3	26025	16398	10389	10710	6480	4271
0,5	6316	3976	2518	2599	1571	1035
1,5	16,8	11,0	7,31	7,50	4,94	3,59
3,0	1,19	1,12	1,06	1,08	1,05	1,03
5,0	1	1	1	1	1	1
10,0	1	1	1	1	1	1

BV=vertical bed velocity

A value for the re-entrainment efficiency for the two upstream and two downstream particle layers, assuming the same velocity and hence the same re-entrainment efficiency for each of the layers, was then calculated by minimising the objective function or "error sum" for each particle size. The results in table 5.8 were obtained, using the "addition of efficiencies" approach. The sensitivity of the results to this calculational approach was tested by re-calculating results using the "multiplication of penetration" approach. It was found that only the results for the largest two particle sizes were influenced in the sense that values even larger than those in the table were obtained. This is because a single mechanism (impaction) is dominant for these particle sizes and approaches unity. Any uncertainty in the experimental

Table 5.9: Re-entrainment efficiencies for operating conditions of table 5.7.1

Bed potential 5 kV											Bed potential 10 kV										
Precharger potential 5 kV					Precharger potential 8 kV						Precharger potential 5 kV					Precharger potential 8 kV					
FV 0,24		FV 0,68			FV 0,24			FV 0,68			FV 0,24		FV 0,68			FV 0,24			FV 0,68		
BV	BV	BV	BV	BV	BV	BV	BV	BV	BV	BV	BV	BV	BV	BV	BV	BV	BV	BV	BV	BV	BV
1,05	2,12	0,55	1,05	2,12	0,55	1,05	2,12	0,55	1,05	2,12	1,05	2,12	0,55	1,05	2,12	0,55	1,05	2,12	0,55	1,05	2,12
,174	,217	,0545	,0714	,029	,243	,219	,202	,012	,049	-	,374	,426	,11	,11	,065	,498	,405	,44	,124	,125	,058
,13	,196	,049	,043	,004	,207	,187	,17	,016	,015	-	,328	,378	,099	,076	,057	,443	,368	,403	,115	,055	,038
,112	,164	,060	,030	,007	,188	,213	,212	,058	,044	,012	,331	,361	,118	,062	,065	,479	,430	,442	,162	,102	,072
,157	,190	,700	,705	0,69	,264	,330	,326	,782	,73	,731	,453	,444	,82	,76	,78	,640	,619	,594	,916	,84	,81
,645	,88	2,27	2,30	2,29	,66	,785	,699	2,35	2,37	2,36	1,22	,87	2,40	2,41	2,43	1,14	1,16	1,14	2,56	2,51	2,50
2,14	2,97	2,40	2,57	2,46	3,10	-	-	2,55	2,74	2,63	3,43	3,39	2,72	2,83	2,69	3,73	3,79	3,88	2,92	3,01	2,85

Table 5.10. Re-entrainment efficiencies independent of vertical bed velocity, for operating conditions of table 5.7.1

FV = Filtration velocity in ms^{-1}, BV= bed velocity in mh^{-1}

Particle size, µm	Bed potential 5 kV				Bed potential 10 kV			
	Precharger potential 5 kV				Precharger potential 8 kV			
	FV 0,24		FV 0,68		Precharger potential 5 kV		Precharger potential 8 kV	
0,3	0,200	0,051	FV 0,24	FV 0,68	FV 0,24	FV 0,68	FV 0,24	FV 0,68
0,5	0,163	0,032	0,221	0,031	0,400	0,095	0,448	0,102
1,5	0,138	0,032	0,188	0,016	0,353	0,072	0,405	0,069
3,0	0,174	0,698	0,204	0,038	0,346	0,082	0,450	0,112
5,0	0,760	2,29	0,307	0,748	0,448	0,790	0,618	0,855

determination of penetration, which for very low values exceeds the measured value and can only result in an overestimate of the penetration (an experimental negative penetration value being impossible), will result in false and abnormally high re-entrainment efficiency values. The values in the last two rows of the table are therefore included for completeness, but can be disregarded for design purposes.

Two preliminary conclusions can be drawn from this table

- For the range of vertical bed velocities tested, there is no statistically significant correlation between the vertical bed velocity and the re-entrainment efficiency (all other factors being constant). The mere fact that the bed moves seems to cause re-entrainment, the magnitude of which is determined by operating parameters other than the vertical velocity. For the analysis that follows, the average value of the re-entrainment efficiency at the three vertical bed velocities for each set of variables of pre-charger potential, bed potential and filtration velocity has been used. These are shown in table 5.9
- There is a clear distinction in behaviour between the smaller particles up to 1,5 μm, for which the electrostatic mechanism dominates and the intermediate range for which mechanical and electrostatic mechanism are of the same order of magnitude. The collection efficiency for particles of 5 μm and larger, for which the dominating mechanism is impaction, is so close to unity that experimental values determined here are unreliable. For design purposes however the re-entrainment efficiency may be taken as zero for these very large particles.

Due to the fact that operating variables were tested only at two levels for each vertical bed velocity value, it is not possible to obtain predictive models. Nevertheless, conclusions can be drawn about the relative influence of the parameters and the relationship between the re-entrainment efficiency and parameters which can be calculated from the independent variables. Some heuristics for use of the empirical parameters for design at other than the experimental conditions can also be deduced..

5.2.3.1 For the smaller particles.

Figure 5.16 below shows the re-entrainment efficiency as a function of particle size for different operating parameters for the smaller particle sizes. In this graph, the values for the 5 kV precharger potential and the 8 kV precharger potential have been averaged as they generally are within 25% of each other and show the same trend. The figure indicates that, similar to the electrostatic efficiency, the re-entrainment efficiency is not a strong function of particle size. It is however strongly influenced by the filtration velocity and the potential over the bed. When the line is continued to 3 micrometer particle size, as in Fig 5.17, the deviation from the above trend presumably caused by the increasing impaction efficiency, which at the higher filtration velocity exceeds the electrostatic efficiency, becomes clear. In the latter figure, the efficiency value less than zero in the lowermost line is an artifact of the curve-fitting procedure and has no physical significance.

The operating parameters are given in the box to the right of the figure, with the bed potential first and the filtration velocity second.

Fig.5.16: Re-entrainment efficiency of small particles under different operating conditions

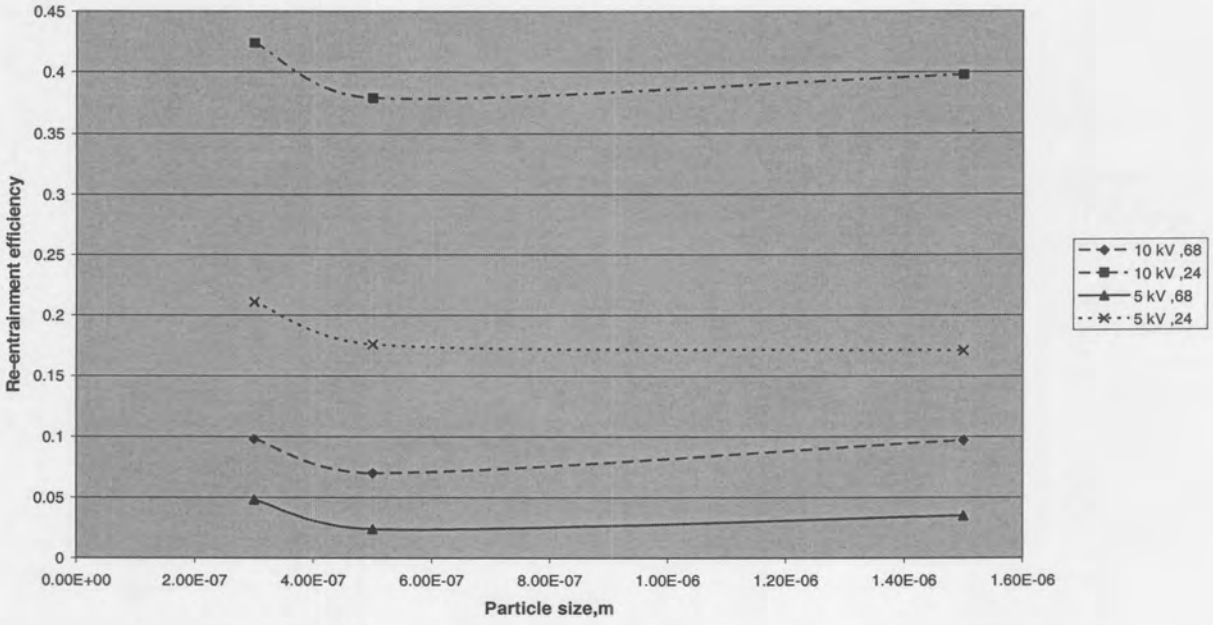

Fig. 5.17. Re-entrainment efficiency of small and medium as function of operating parameters

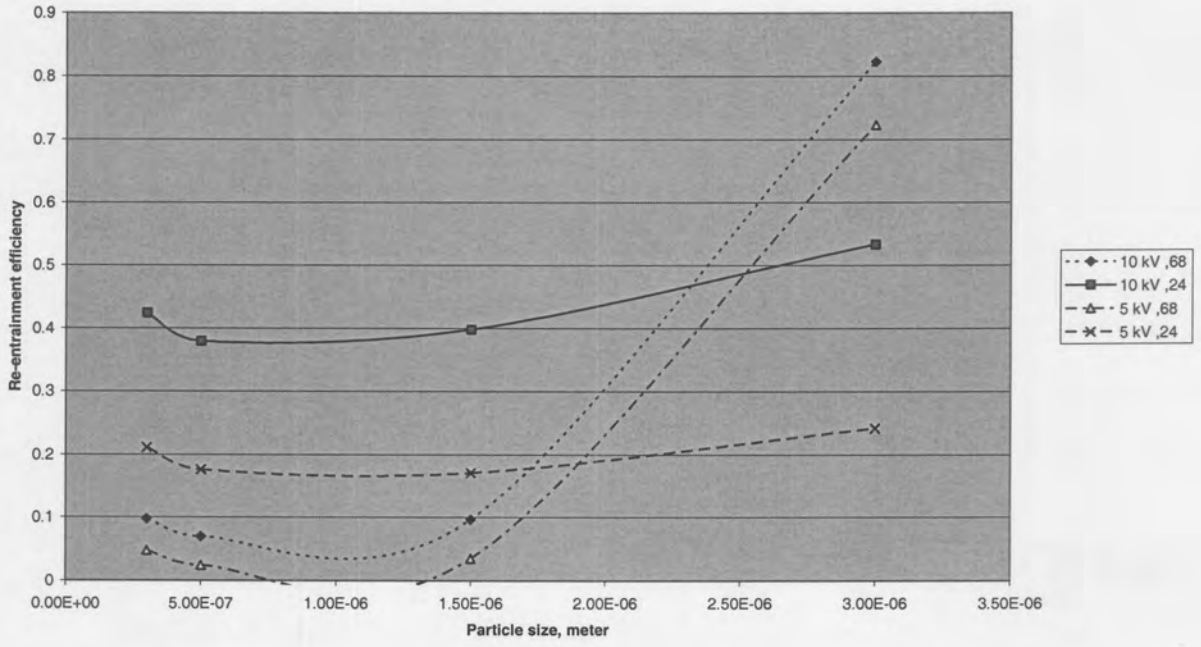

The relationship between the calculated single granule electrostatic efficiency and the re-entrainment efficiency for the particle sizes up to 1,5 µm is illustrated by table 5.10, where he proportionality constant between re-entrainment efficiency and electrostatic efficiency as determined by the operating parameters, is shown.

Table 5.10: Ratio of re-entrainment efficiency to electrostatic efficiency as function of operating parameters (both single granule values).

	Bed potential 5 kV				Bed potential 10 kV			
Particle size, μm	Precharger potential 5 kV		Precharger potential 8 kV		Precharger potential 5 kV		Precharger potential 8 kV	
	FV 0,24	FV 0,68	FV 0,24	FV 0,68	FV 0,24	FV 0,68	FV 0,24	FV 0,68
0,3	2,32	1,70	1,33	1,05	2,40	1,61	2,49	1,59
0,5	2,02	1,14	1,21	0,50	2,26	1,30	2,31	1,10
1,5	1,44	0,94	1,12	0,89	1,89	1,24	1,97	1,34

The higher ratios in the columns corresponding to the lower filtration velocity are probably due to the fact that the deposited dust is less compacted (*vide* the higher re-entrainment efficiency factors at the lower filtration velocity , table 5.7.2) and therefore more easily dislodged. The average ratio of the re-entrainment efficiency at 0,24 ms^{-1} filtration velocity to that at 0,68 ms^{-1} is 1,58 and does not vary appreciably with electrostatic parameters while the ratio between the efficiency enhancement factors due to bed loading at 0,24 and 0,68 ms^{-1} is constant at 2,43 and is also not influenced by bed or precharger potential.

Because re-entrainment efficiency results were obtained at only two values of bed potential, it is not possible to provide a predictive model for the efficiencies as a function of operating parameters. The empirical values found here must therefore be used for design; estimates at other than the above velocities and/or bed loads may however be made by interpolation using the above ratios. As an approximation, for a given set of operating parameters the same re-entrainment efficiency could be used for all particle sizes between 0,3 and 1,5 μm without introducing major error. These results differ from those in section 5.2.1, where the precharger was not used, and this is an indication of improvement in efficiency obtained through the use of the pre-charger.

5.2.3.2 For the largest particles

For particles approaching 10 μm in size, impaction is the overwhelming capture mechanism at all filtartion velocities of practical interest and the influence of the electrostatic mechanism is merely to reduce the effect of "particle bounce" to negligible values. The single granule impaction efficiency exceeds 0,95 for all the variables tested here. Measured penetration values are much smaller than the experimental and measurement uncertainty and can therefore be taken as zero.

5.2.3.3 For the intermediate particles.

In the size range between 1,5 and 10 μm, efficiency is influenced by both mechanical and electrostatic parameters. Attempts at correlating efficiency with operating parameters for particles in this size range

were made using using a variety of equations with two and three parameters. Amongst these were Freudich, Langmuir and logistics-type equations as well as combinations of simpler mathematical forms. (Silva and Silva 2002) Because the number of experimental points for each set of operating variables is small, good correlation is easily obtained, especially using three parameters. No single form of equation does however fit data for the different experimental series equally well, indicating that the good correlation is mathematical in nature, rather than through the representation of common physical phenomena. It is therefore recommended that interpolation be used for the intermediate particle sizes until such time as more experimental data elucidate the relationship in this size range.

5.3 REFERENCES

Beveridge, G.S., Scheckter, R S. (1970) *Optimization: Theory and practice.* McGraw-Hill, New York

Dietz, P. (1981) Electrostatic filtration of inertialess particles by granular beds. J. Aerosol Sci. **12** p 27-38

Fichman, M. *et al.* (1981) A modified model for the deposition of dust in a granular bed filter. Atm. Env. **15** (9) p 1669-1674

Hashin, Z., Shtrikman,S (1962) A variational approach to the theory of the effective magnetic permeability of multiphase materials. J. Appl. Phys. **33**(10) p 3125-3131

Jung, Y (1991) *Granular filtration of monodispersed and polydispersed aerosols.* Ph. D. dissertation, Syracuse University

Kamffer, L., Kornelius, G.(1988) Gasfiltrasie deur elektrostatiese gruisbeddens. SAIChE 5th National Meeting, Pretoria. Paper G3

Kornelius, G. *et al.*(1987) Gasfiltrasie deur gruisbeddens met aanwending van 'n elektriese veld. SA Journal for Clean Air **7** (3) p 15-20

Kornelius, G., Kamffer L. (1989) *Finale verslag: Elektrostatiese gruisbedfilters vir filtrasie van vliegas uit warm gasstrome.* Unpublished report to the SA Council for Scientific and Industrial Research, Pretoria

Kornelius, G. (1991) Elektrostatiese gruisbeddens vir gasfiltrasie: Die invloed van partikellading op doeltreffendheid. SAIChE 6th National Meeting, Durban. Paper I1

Kornelius, G., von Reiche, F.V.K. (1993) Gravel bed filters with electrostatic augmentation: Laboratory and plant experience. CHISA 1993, Prague

Shapiro, M. *et al.* (1988) Electrostatic mechanisms of aerosol collection by granular filters: A review. J. Aerosol Sci. **19** (6) p 651-677

Silva, W., Silva P.S.(2002) LAB Fit V 6.6 software. www.extensao.hpg.com.br Consulted Nov. 2003

Takahashi, T. *et al.* (1986) Transient behavior of granular filtration of aerosols - effect of aerosol deposition on filter performance. AIChE J. **32**(4) p 684-690

Tardos, G.I., Snaddon, R.W.L (1984) Separation of charged aerosols in granular beds with imposed electric fields. AIChE Symp. Series 234 **80** p 61-69

Walata, S.A. *et al.*(1986) Effect of particle deposition on granular aerosol filtration. Aerosol Sci. Tech. **5** p 23-27

White, H.J. (1963). *Industrial electrostatic precipitation.*, Reading, Mass.: Addison-Wesley

White, H.J. (1984) Control of particulates by electrostatic precipitation *in* Calvert, S., Englund H.M.(eds.) *Handbook of air pollution technology.* New York, J Wiley & Sons

CHAPTER 6
CONCLUSIONS

6.1 RATIONALE FOR USE OF PRECHARGER

The purpose of the work described in this thesis was to establish design methods for the design of electrostatically augmented gravel bed filters. The logic for using the configuration described here, *viz.* a thin vertically moving bed with electrostatic augmentation preceded by a separate wire and plate type precharger is as follows:

6.1.1 The calculation methods described in the literature for the fluid dynamic mechanisms of particle capture in gravel bed filters adequately descibe the phenomena of impaction, direct capture and diffusion. These are also the mechanical phenomena that are most directly of interest for the particle size that must most commonly be removed from gas streams in industrial air pollution control practice. However, in the particle size range and under operating conditions of most practical interest, electrostatic phenomena are rarely absent and these may cause gross underestimates of filter efficiency to be made if they are not taken into account.

6.1.2 The magnitude of naturally occurring electrostatic charges is not easy to predict and is influenced by a large number atmospheric, operating and other variables in a presently unpredictable manner. This does not allow the use of naturally occurring charges only in industrial processes. Particle charging in a controlled and predictable manner is therefore required.

6.1.3 For thick granular beds (thickness in excess of a hundred or so granule diameters) in-bed charging (obtained by the application of a direct current between the inlet and outlet screens) is sufficient to obtain such particle charges, but at the cost of increased bed pressure drop. Furthermore, the rate of particle charging is reduced by the fact that the effective field strength, which in this case is both the charging and capturing field, is considerably reduced from the nominal value by the presence of the granules.

6.1.4 To retain the pressure drop advantages of a thin bed, and to obtain more rapid charging than can be obtained within the bed, the function of charging particles and providing a capturing field should be separated. The provision of a corona discharge apparatus upstream of gravel bed filters allows a much higher effective field strength for particle charging, resulting in both more rapid charging and a higher final charge. This leads to considerably enhanced capture in beds as thin as 10 granule diameters.

6.2 CONCLUSIONS ON BED LOAD PARAMETERS

The parameters describing the increase in filtration efficiency that occurs due to the deposition of dust in an electrostatically augmented filter found in this study differ from those described in the literature for the fluid mechanical capture mechanisms. Because the parameters were determined for one type of dust only, it was not possible to determine whether this is due to the use of dusts of varying particle sizes, the change in deposit morphology due to electrostatic effects, or to both. Methods are however proposed to allow the use of the parameters determined in this work for dusts with different particle size distributions, for granules of a different size and for different filtration velocities.

6.3 CONCLUSIONS ON RE-ENTRAINMENT OF PARTICLES DUE TO BED MOVEMENT

The re-entrainment of dust due to bed movement is independent of vertical bed velocity for the range of parameters used in this work. The mechanism of re-entrainment of particles into the gas stream due to bed movement differs over the range of particle sizes. For particles smaller than 1,5 μm, for which the dominant capture mechanism is electrostatic, there is a close link between the electrostatic capture efficiency and the re-entrainment efficiency. For those particles with an impaction capture efficiency close to unity (in this work, those approaching 10 μm in size) the penetration can be regarded as zero and re-entrainment is negligible. It did not prove possible to develop predictive equations for the re-entrainment efficiency using the results of this study. This is due to the large number of variables which influence the particle capture and release phenomena. However, empirical results using the simple "two moving layers" model, as well as a number of heuristics allowing estimates of the magnitude of the re-entrainment efficiency at operating conditions other those at which the experimental values were obtained. This allows for rational design at least in the range of the variables investigated in this work.

6.4 DESIGN PROCEDURE OUTLINE

The following design procedure for a gas filtration apparatus using this configuration follows from the investigation described in chapters 3 to 5 of this work.:

6.4.1 Particles larger than 10 μm in size should be removed using standard mechanical collectors (cyclones or where applicable a settling chamber and cyclone in series).

6.4.2 Determine the spherical equivalent diameter of the selected gravel medium using the method of Leva, as well as the required physical, hydraukic and electrostatic properties of the granular medium. (Particle density, bed porosity, substance di-electric constant and effective bed di-electric constant).

6.4.3 Determine the particle size distribution, and the physical and electrostatic properties of the dust to be filtered and calculate a geometric mean particle size on a mass basis.

6.4.4 From the required gas flow rate and the particle concentration leaving the pre-cleaner develop a configuration envelope within the following restrictions, assuming at this stage 100% capture:

- Filtration velocity of the order of 0,5 ms^{-1}, final value not to exceed 1mh^{-1}
- Vertical bed velocity not exceeding 2 mh^{-1}
- Not thinner than 10 granule diameters
- Bed volume loading can now be calculated, should not exceed 0,001. If it does, the value should be reduced to below this by increasing the vertical bed velocity or reducing the filtration velocity
- Assume bed field strength of 250 kV/m as initial estimate.
- Assume pre-charger field strength of 100 kV/m

6.4.5 Calculate the enhancement factors due to bed load at the configurations within the envelope using the empirical factors determined in Chapter 5 for a reference dust, adjust for differences in granule size, filtration velocity and dust particle size from the reference dust.

6.4.6 Design a wire and plate type precharger using standard design methods having a sufficient retention time to achieve 90% of saturation charge in a field strength of the order of 4 00 kV/m.

6.4.7 Capture efficiencies can now be calculated using the methods of Chapter 3 and 5. Re-entrainment efficiencies for those particles with an impaction efficiency less than 50% of the electrostatic efficiency can be found by interpolation of the values from table 5.10. For particles with a single granule impaction efficiency larger than 0,9 , the re-entrainment efficiency can be assumed to be zero. For particles intermediate between the above, interpolation on a log scale of particle size may be used.

6.4.8 Capture efficiencies for the particle sizes can now be compared to design specifications.

- If the required efficiency for the smaller particles (<1,5 micrometer) is obtained but not for the larger particles, filtration velocity may be increased to obtain better impaction efficiency, while increasing the pre-charger length proportionally in order to maintain similar electrostatic charges on the smaller particles.
- If efficiency for the larger particles meets specified value but small particles are undercaptured, bed velocity is kept constant while increasing pre-charger length or pre-charger field strength. A practical

upper limit is 200 kV/m before sparking between discharge electrode and plate starts to occur. Alternatively, bed field strength may be increased, although this is not as effective due to the lower effective field strength obtained in the granular medium.

- If efficiency is too low across the particle spectrum, a combination of the above must be attempted.

6.5 FURTHER RESEARCH RECOMMENDED

6.5.1 Large-scale filters will probably not use the bed retaining screen configuration used in this work. Confirmation of the re-entrainment efficiencies found here for other bed retaining screen configurations should be sought.

6.5.2 Although there is a correlation between re-entrainment efficiency and electrostatic capture efficiency for particles with a low impaction efficiency, the nature of the relationship is not clear and this needs further investigation.

6.5.3 The re-entrainment efficiency in the region where electrostatic efficiency and impaction efficiency are of the same order should be further investigated.

6.5.4 The tentative method proposed for applying the bed load efficiency increase parameters found at one set of operating parameters to other values of operating parameters needs to be confirmed. In addition, it needs to be determined whether the mass weighted geometric average particle size is a good representative value for dusts of mixed particle size.

Appendix A

1. Static bed results, 3 cm thick bed

Table A1		Table A2		Table A3	
3 mm glass spheres, 0 kV		3 mm glass spheres, 15 kV over bed, no precharge		3 mm glass spheres, 20 kV over bed, no precharge	
JIS fly ash		Boshoff alumina, charge neutraliser		Boshoff alumina, charge neutraliser	
Filtration velocity 0,453 ms^{-1}		Filtration velocity 0,453 ms^{-1}		Filtration velocity 0,453 ms^{-1}	
Particle size,µm	Efficiency, %	Particle size,µm	Efficiency, %	Particle size,µm	Efficiency, %
0,3	56,1	0,3	33,4	0,3	37,9
0,5	55,4	0,5	60,8	0,5	47,6
1,5	58,2	1,5	88,9	1,5	79,5
3,0	85,7	3,0	98,3	3,0	94,9
5,0	98.5	5,0	92,3	5,0	94,4
10,0	100,0	10,0	100,0	10,0	100,0
Table A4		Table A5		Table A6	
3 mm glass spheres, 25 kV over bed, no precharge		3 mm silica sand granules, 15 kV over bed, no precharge		3 mm silica sand granules, 20 kV over bed, no precharge	
Boshoff alumina, charge neutraliser		Boshoff alumina, charge neutraliser		Boshoff alumina, charge neutraliser	
Filtration velocity 0,453 ms^{-1}		Filtration velocity 0,453 ms^{-1}		Filtration velocity 0,453 ms^{-1}	
Particle size,µm	Efficiency, %	Particle size,µm	Efficiency, %	Particle size,µm	Efficiency, %
0,3	46,7	0,3	0	0,3	0
0,5	60,5	0,5	7,8	0,5	0
1,5	48,7	1,5	0	1,5	47,2
3,0	99,6	3,0	89,9	3,0	94,8
5,0	100,0	5,0	99,9	5,0	96,8
10,0	100,0	10,0	100,0	10,0	100,0
Table A7		Table A8		Table A9	
3 mm silica sand granules, 25 kV over bed, no precharge		3 mm dolomite chips, 15 kV over bed, no precharge		3 mm glass spheres, 20 kV over bed, no precharge	
Boshoff alumina, charge neutraliser		Boshoff alumina, charge neutraliser		Boshoff alumina, charge neutraliser, 10 minutes load	
Filtration velocity 0,453 ms^{-1}		Filtration velocity 0,453 ms^{-1}		Filtration velocity 0,453 ms^{-1}	
Particle size,µm	Efficiency, %	Particle size,µm	Efficiency, %	Particle size,µm	Efficiency, %
0,3	0	0,3	0	0,3	52,1
0,5	1,4	0,5	14,4	0,5	61,6
1,5	13,8	1,5	47,5	1,5	92,2
3,0	92,6	3,0	95,3	3,0	99,2
5,0	99,8	5,0	95,6	5,0	96,9
10,0	100,0	10,0	100,0	10,0	100,0

Table A10		Table A11		Table A12	
3 mm glass spheres, 20 kV over bed, no precharge		3 mm glass spheres, 20 kV over bed, no precharge		3 mm glass spheres, 20 kV over bed, no precharge	
Boshoff alumina, charge neutraliser, 20 minutes load		Boshoff alumina, charge neutraliser, 30 minutes load		Boshoff alumina, charge neutraliser, 40 minutes load	
Filtration velocity 0,453 ms^{-1}		Filtration velocity 0,453 ms^{-1}		Filtration velocity 0,453 ms^{-1}	
Particle size,µm	Efficiency, %	Particle size,µm	Efficiency, %	Particle size,µm	Efficiency, %
0,3	66,1	0,3	70,2	0,3	78,4
0,5	70,6	0,5	77,3	0,5	85,2
1,5	88,8	1,5	87,6	1,5	96,2
3,0	99,5	3,0	99,8	3,0	99,1
5,0	99,9	5,0	100,0	5,0	99,3
10,0	100,0	10,0	100,0	10,0	100,0
Table A13		Table A14		Table A15	
3 mm glass spheres, 20 kV over bed, no precharge		3 mm glass spheres, 20 kV over bed, no precharge		3 mm silica sand granules, 25 kV over bed, no precharge	
Boshoff alumina, charge neutraliser, 50 minutes load		Boshoff alumina, charge neutraliser, 60 minutes load		Boshoff alumina, charge neutraliser, 10 minutes load	
Filtration velocity 0,453 ms^{-1}		Filtration velocity 0,453 ms^{-1}		Filtration velocity 0,453 ms^{-1}	
Particle size,µm	Efficiency, %	Particle size,µm	Efficiency, %	Particle size,µm	Efficiency, %
0,3	80,1	0,3	79,2	0,3	4,0
0,5	86,5	0,5	87,2	0,5	15,1
1,5	85,3	1,5	97,2	1,5	29,0
3,0	97,0	3,0	99,5	3,0	88,1
5,0	99,6	5,0	99,8	5,0	97,6
10,0	100,0	10,0	100,0	10,0	100,0
Table A16		Table A17		Table A18	
3 mm silica sand granules, 25 kV over bed, no precharge		3 mm silica sand granules, 25 kV over bed, no precharge		3 mm silica sand granules, 25 kV over bed, no precharge	
Boshoff alumina, charge neutraliser, 20 minutes load		Boshoff alumina, charge neutraliser, 30 minutes load		Boshoff alumina, charge neutraliser, 40 minutes load	
Filtration velocity 0,453 ms^{-1}		Filtration velocity 0,453 ms^{-1}		Filtration velocity 0,453 ms^{-1}	
Particle size,µm	Efficiency, %	Particle size,µm	Efficiency, %	Particle size,µm	Efficiency, %
0,3	19,7	0,3	32,4	0,3	33,7
0,5	38,1	0,5	32,7	0,5	29,6
1,5	55,0	1,5	61,2	1,5	60,6
3,0	93,2	3,0	93,9	3,0	93,6
5,0	97,8	5,0	97,0	5,0	93,3
10,0	100,0	10,0	100,0	10,0	100,0

Table A19		Table A20		Table A21	
3 mm silica sand granules, 25 kV over bed, no precharge		3 mm silica sand granules, 25 kV over bed, no precharge		3 mm glass spheres, 15 kV over bed, no precharge	
Boshoff alumina, charge neutraliser, 50 minutes load		Boshoff alumina, charge neutraliser, 60 minutes load		Boshoff alumina, charge neutraliser, 10 minutes load	
Filtration velocity 0,453 ms^{-1}		Filtration velocity 0,453 ms^{-1}		Filtration velocity 0,453 ms^{-1}	
Particle size,µm	Efficiency, %	Particle size,µm	Efficiency, %	Particle size,µm	Efficiency, %
0,3	31,1	0,3	40,0	0,3	61,9
0,5	31,4	0,5	46,7	0,5	79,4
1,5	50,7	1,5	54,4	1,5	91,8
3,0	90,5	3,0	92,8	3,0	99,5
5,0	94,6	5,0	96,0	5,0	99,7
10,0	100,0	10,0	100,0	10,0	100,0
Table A22		Table A23		Table A24	
3 mm glass spheres, 15 kV over bed, no precharge		3 mm glass spheres, 15 kV over bed, no precharge		3 mm glass spheres, 15 kV over bed, no precharge	
Boshoff alumina, charge neutraliser, 20 minutes load		Boshoff alumina, charge neutraliser, 30 minutes load		Boshoff alumina, charge neutraliser, 40 minutes load	
Filtration velocity 0,453 ms^{-1}		Filtration velocity 0,453 ms^{-1}		Filtration velocity 0,453 ms^{-1}	
Particle size,µm	Efficiency, %	Particle size,µm	Efficiency, %	Particle size,µm	Efficiency, %
0,3	66,3	0,3	69,2	0,3	67,3
0,5	81,6	0,5	82,5	0,5	81,8
1,5	95,7	1,5	96,1	1,5	95,6
3,0	99,4	3,0	99,6	3,0	98,2
5,0	99,6	5,0	99,8	5,0	98,5
10,0	100,0	10,0	100,0	10,0	100,0
Table A25		Table A26		Table A27	
3 mm glass spheres, 15 kV over bed, no precharge		3 mm glass spheres, 15 kV over bed, no precharge		3 mm glass spheres, 25 kV over bed, no precharge	
Boshoff alumina, charge neutraliser, 50 minutes load		Boshoff alumina, charge neutraliser, 60 minutes load		Boshoff alumina, charge neutraliser, 10 minutes load	
Filtration velocity 0,453 ms^{-1}		Filtration velocity 0,453 ms^{-1}		Filtration velocity 0,453 ms^{-1}	
Particle size,µm	Efficiency, %	Particle size,µm	Efficiency, %	Particle size,µm	Efficiency, %
0,3	69,2	0,3	61,2	0,3	45,3
0,5	85,5	0,5	76,5	0,5	60,9
1,5	96,8	1,5	94,3	1,5	89,9
3,0	99,6	3,0	98,3	3,0	99,8
5,0	97,8	5,0	98,6	5,0	99,7
10,0	100,0	10,0	100,0	10,0	100,0

Table A28		Table A29		Table A30	
3 mm glass spheres, 25 kV over bed, no precharge		3 mm glass spheres, 25 kV over bed, no precharge		3 mm glass spheres, 25 kV over bed, no precharge	
Boshoff alumina, charge neutraliser, 20 minutes load		Boshoff alumina, charge neutraliser, 30 minutes load		Boshoff alumina, charge neutraliser, 40 minutes load	
Filtration velocity 0,453 ms^{-1}		Filtration velocity 0,453 ms^{-1}		Filtration velocity 0,453 ms^{-1}	
Particle size,µm	Efficiency, %	Particle size,µm	Efficiency, %	Particle size,µm	Efficiency, %
0,3	59,7	0,3	64,2	0,3	60,8
0,5	71,7	0,5	77,8	0,5	75,0
1,5	86,6	1,5	95,9	1,5	96,6
3,0	99,1	3,0	99,7	3,0	99,8
5,0	99,7	5,0	100,0	5,0	99,9
10,0	100,0	10,0	100,0	10,0	100,0
Table A31		Table A32		Table A33	
3 mm glass spheres, 25 kV over bed, no precharge		3 mm glass spheres, 25 kV over bed, no precharge		3 mm dolomite chips, 15 kV over bed, no precharge	
Boshoff alumina, charge neutraliser, 50 minutes load		Boshoff alumina, charge neutraliser, 60 minutes load		Boshoff alumina, charge neutraliser, 10 minutes load	
Filtration velocity 0,453 ms^{-1}		Filtration velocity 0,453 ms^{-1}		Filtration velocity 0,453 ms^{-1}	
Particle size,µm	Efficiency, %	Particle size,µm	Efficiency, %	Particle size,µm	Efficiency, %
0,3	63,6	0,3	68,3	0,3	16,6
0,5	78,7	0,5	82,1	0,5	29,8
1,5	78,7	1,5	95,3	1,5	66,3
3,0	99,8	3,0	99,4	3,0	90,3
5,0	100,0	5,0	77,8	5,0	96,7
10,0	100,0	10,0	100,0	10,0	100,0
Table A34		Table A35		Table A36	
3 mm dolomite chips, 15 kV over bed, no precharge		3 mm dolomite chips, 15 kV over bed, no precharge		3 mm dolomite chips, 15 kV over bed, no precharge	
Boshoff alumina, charge neutraliser, 20 minutes load		Boshoff alumina, charge neutraliser, 30 minutes load		Boshoff alumina, charge neutraliser, 40 minutes load	
Filtration velocity 0,453 ms^{-1}		Filtration velocity 0,453 ms^{-1}		Filtration velocity 0,453 ms^{-1}	
Particle size,µm	Efficiency, %	Particle size,µm	Efficiency, %	Particle size,µm	Efficiency, %
0,3	37,9	0,3	41,3	0,3	42,7
0,5	49,9	0,5	48,7	0,5	56,7
1,5	75,8	1,5	74,2	1,5	90,2
3,0	93,1	3,0	92,4	3,0	97,6
5,0	98,6	5,0	99,4	5,0	99,4
10,0	100,0	10,0	100,0	10,0	100,0

Table A37		Table A38	
3 mm dolomite chips, 15 kV over bed, no precharge		3 mm dolomite chips, 15 kV over bed, no precharge	
Boshoff alumina, charge neutraliser, 50 minutes load		Boshoff alumina, charge neutraliser, 60 minutes load	
Filtration velocity 0,453 ms^{-1}		Filtration velocity 0,453 ms^{-1}	
Particle size,µm	Efficiency, %	Particle size,µm	Efficiency, %
0,3	53,0	0,3	53,0
0,5	66,8	0,5	66,8
1,5	91,7	1,5	91,7
3,0	97,1	3,0	97,1
5,0	99,4	5,0	99,4
10,0	100,0	10,0	100,0

2. Moving bed results, 6 cm thick bed

Table A39		Table A40		Table A41	
2,8 mm dolomite chips, 10 kV over bed, no precharge		2,8 mm dolomite chips, 10 kV over bed, no precharge		2,8 mm dolomite chips, 10 kV over bed, no precharge	
JIS fly ash, 20 °C Bed velocity 0 mh^{-1}		JIS fly ash, 20 °C Bed velocity 0,25 mh^{-1}		JIS fly ash, 20 °C Bed velocity 0,50 mh^{-1}	
Filtration velocity 0,4 ms^{-1}		Filtration velocity 0,4 ms^{-1}		Filtration velocity 0,4 ms^{-1}	
Particle size,µm	Efficiency, %	Particle size,µm	Efficiency, %	Particle size,µm	Efficiency, %
0,3	91,7	0,3	61,9	0,3	65,9
0,5	90,0	0,5	57,4	0,5	66,1
1,5	94,8	1,5	80,6	1,5	84,1
3,0	98,6	3,0	97,2	3,0	96,9
5,0	99,6	5,0	99,8	5,0	99,7
10,0	100,0	10,0	100,0	10,0	100,0
Table A42		Table A40		Table A43	
2,8 mm dolomite chips, 10 kV over bed, no precharge		2,8 mm dolomite chips, 10 kV over bed, no precharge		2,8 mm dolomite chips, 10 kV over bed, no precharge	
JIS fly ash, 100 °C Bed velocity 0 mh^{-1}		JIS fly ash, 100 °C Bed velocity 0,25 mh^{-1}		JIS fly ash, 100 °C Bed velocity 0,50 mh^{-1}	
Filtration velocity 0,4 ms^{-1}		Filtration velocity 0,4 ms^{-1}		Filtration velocity 0,4 ms^{-1}	
Particle size,µm	Efficiency, %	Particle size,µm	Efficiency, %	Particle size,µm	Efficiency, %
0,3	88,0	0,3	74,3	0,3	65,9
0,5	87,9	0,5	72,5	0,5	58,7
1,5	92,2	1,5	83,3	1,5	77,9
3,0	97,8	3,0	94,8	3,0	95,0
5,0	99,8	5,0	99,5	5,0	99,6
10,0	100,0	10,0	100,0	10,0	100,0

Table A44		Table A45		Table A46	
2,7 mm dolomite chips, 4 kV over bed and precharger		2,7 mm dolomite chips, 8 kV over bed and precharger		2,7 mm dolomite chips, 9 kV over bed and precharger	
FeSi dust 20 °C Bed velocity 0 mh^{-1}		FeSi dust 20 °C Bed velocity 0 mh^{-1}		FeSi dust 20 °C Bed velocity 0 mh^{-1}	
Filtration velocity 0,25 ms^{-1}		Filtration velocity 0,25 ms^{-1}		Filtration velocity 0,25 ms^{-1}	
Particle size,µm	Efficiency, %	Particle size,µm	Efficiency, %	Particle size,µm	Efficiency, %
0,3	85,08	0,3	88,16	0,3	85,03
0,5	96,95	0,5	99,65	0,5	99,52
1,5	97,88	1,5	99,83	1,5	99,78
3,0	98,83	3,0	99,95	3,0	99,97
5,0	99,32	5,0	99,98	5,0	99,99
10,0	100	10,0	100	10,0	100
Table A47		Table A48		Table A49	
2,7 mm dolomite chips, 4 kV over bed and precharger		2,7 mm dolomite chips, 8 kV over bed and precharger		2,7 mm dolomite chips, 9 kV over bed and precharger	
FeSi dust 20 °C Bed velocity 0 mh^{-1}		FeSi 2dust 20 °C Bed velocity 0 mh^{-1}		FeSi dust 20 °C Bed velocity 0 mh^{-1}	
Filtration velocity 0,75 ms^{-1}		Filtration velocity 0,75 ms^{-1}		Filtration velocity 0,75 ms^{-1}	
Particle size,µm	Efficiency, %	Particle size,µm	Efficiency, %	Particle size,µm	Efficiency, %
0,3	13,77	0,3	76,70	0,3	91,54
0,5	45,29	0,5	87,40	0,5	97,28
1,5	69,44	1,5	96,08	1,5	98,72
3,0	90,27	3,0	99,54	3,0	99,60
5,0	98,39	5,0	99,84	5,0	99,79
10,0	99,01	10,0	99,80	10,0	99,32
Table A50		Table A51		Table A52	
2,7 mm dolomite chips, 8 kV over precharger, 5 kV over bed		2,7 mm dolomite chips, 8 kV over precharger, 10 kV over bed		2,7 mm dolomite chips, 8 kV over precharger, 5 kV over bed	
JIS fly ash, 20 °C Bed velocity 0,515 mh^{-1}		JIS fly ash, 20 °C Bed velocity 0,515 mh^{-1}		JIS fly ash, 20 °C Bed velocity 0,515 mh^{-1}	
Filtration velocity 0,24 ms^{-1}		Filtration velocity 0,24 ms^{-1}		Filtration velocity 0,68 ms^{-1}	
Particle size,µm	Efficiency, %	Particle size,µm	Efficiency, %	Particle size,µm	Efficiency, %
0,3	60,09	0,3	29,58	0,3	60,54
0,5	63,76	0,5	47,24	0,5	61,03
1,5	81,01	1,5	74,31	1,5	72,98
3,0	92,99	3,0	92,79	3,0	92,51
5,0	97,05	5,0	97,26	5,0	95,92
10,0	97,40	10,0	99,11	10,0	99,61

Table A53	
2,7 mm dolomite chips, 8 kV over precharger, 5 kV over bed	
JIS fly ash 20 °C Bed velocity 0,515 mh^{-1}	
Filtration velocity 0,68 ms^{-1}	
Particle size,µm	Efficiency, %
0,3	80,66
0,5	79,39
1,5	81,03
3,0	87,33
5,0	95,28
10,0	99,17

Table A54	
2,7 mm dolomite chips, 5 kV over precharger, 10 kV over bed	
JIS fly ash 20 °C Bed velocity 0,515 mh^{-1}	
Filtration velocity 0,68 ms^{-1}	
Particle size,µm	Efficiency, %
0,3	67,46
0,5	70,17
1,5	80,58
3,0	92,11
5,0	97,00
10,0	98,59

Table A55	
2,7 mm dolomite chips, 8 kV over precharger, 10 kV over bed	
JIS fly ash 20 °C Bed velocity 0,515 mh^{-1}	
Filtration velocity 0,68 ms^{-1}	
Particle size,µm	Efficiency, %
0,3	68,81
0,5	71,32
1,5	80,78
3,0	90,07
5,0	94,98
10,0	99,05

Table A56	
2,7 mm dolomite chips, 5 kV over bed and precharger	
JIS fly ash 20 °C Bed velocity 1,05 mh^{-1}	
Filtration velocity 0,24 ms^{-1}	
Particle size,µm	Efficiency, %
0,3	18,30
0,5	25,50
1,5	56,47
3,0	78,83
5,0	77,61
10,0	100,00

Table A57	
2,7 mm dolomite chips, 8 kV over precharger, 5 kV over bed	
JIS fly ash 20 °C Bed velocity 1,05 mh^{-1}	
Filtration velocity 0,24 ms^{-1}	
Particle size,µm	Efficiency, %
0,3	58,80
0,5	64,75
1,5	72,52
3,0	81,78
5,0	81,17
10,0	100,00

Table A58	
2,7 mm dolomite chips, 5 kV over precharger, 10 kV over bed	
JIS fly ash 20 °C Bed velocity 1,05 mh^{-1}	
Filtration velocity 0,24 ms^{-1}	
Particle size,µm	Efficiency, %
0,3	72,04
0,5	74,13
1,5	84,38
3,0	93,29
5,0	96,83
10,0	98,27

Table A59	
2,7 mm dolomite chips, 8 kV over precharger, 10 kV over bed	
JIS fly ash, 20 °C Bed velocity 1,05 mh^{-1}	
Filtration velocity 0,24 ms^{-1}	
Particle size,µm	Efficiency, %
0,3	72,83
0,5	76,67
1,5	87,11
3,0	94,33
5,0	97,09
10,0	98,02

Table A60	
2,7 mm dolomite chips, 5 kV over precharger, 5 kV over bed	
JIS fly ash, 20 °C Bed velocity 0 mh^{-1}	
Filtration velocity 0,24 ms^{-1}	
Particle size,µm	Efficiency, %
0,3	35,43
0,5	54,51
1,5	75,62
3,0	89,61
5,0	93,90
10,0	94,68

Table A61	
2,7 mm dolomite chips, 8 kV over precharger, 5 kV over bed	
JIS fly ash, 20 °C Bed velocity 0 mh^{-1}	
Filtration velocity 0,68 ms^{-1}	
Particle size,µm	Efficiency, %
0,3	57,82
0,5	74,00
1,5	78,39
3,0	92,02
5,0	93,16
10,0	90,32

Table A62		Table A63		Table A64	
2,7 mm dolomite chips, 5 kV over precharger, 10 kV over bed		2,7 mm dolomite chips, 8 kV over precharger, 10 kV over bed		2,7 mm dolomite chips, 5 kV over precharger, 5 kV over bed	
JIS fly ash 20 °C Bed velocity 1,05 mh^{-1}		JIS fly ash 20 °C Bed velocity 1,05 mh^{-1}		JIS fly ash 20 °C Bed velocity 2,12 mh^{-1}	
Filtration velocity 0,68 ms^{-1}		Filtration velocity 0,68 ms^{-1}		Filtration velocity 0,24 ms^{-1}	
Particle size,µm	Efficiency, %	Particle size,µm	Efficiency, %	Particle size,µm	Efficiency, %
0,3	59,07	0,3	59,75	0,3	33,68
0,5	72,47	0,5	84,50	0,5	31,42
1,5	87,87	1,5	88,78	1,5	66,99
3,0	95,69	3,0	95,23	3,0	90,50
5,0	96,52	5,0	97,54	5,0	94,35
10,0	92,87	10,0	96,41	10,0	94,06
Table A65		Table A66		Table A67	
2,7 mm dolomite chips, 8 kV over precharger, 5 kV over bed		2,7 mm dolomite chips, 5 kV over precharger, 10 kV over bed		2,7 mm dolomite chips, 8 kV over precharger, 10 kV over bed	
JIS fly ash 20 °C Bed velocity 2,12 mh^{-1}		JIS fly ash 20 °C Bed velocity 2,12 mh^{-1}		JIS fly ash 20 °C Bed velocity 2,12 mh^{-1}	
Filtration velocity 0,24 ms^{-1}		Filtration velocity 0,24 ms^{-1}		Filtration velocity 0,24 ms^{-1}	
Particle size,µm	Efficiency, %	Particle size,µm	Efficiency, %	Particle size,µm	Efficiency, %
0,3	-14,60	0,3	23,64	0,3	43,24
0,5	37,42	0,5	36,89	0,5	54,06
1,5	66,40	1,5	75,11	1,5	84,87
3,0	90,97	3,0	92,36	3,0	96,24
5,0	99,55	5,0	96,73	5,0	97,27
10,0	95,17	10,0	96,40	10,0	93,61
Table A68		Table A69		Table A70	
2,7 mm dolomite chips, 5 kV over precharger, 5 kV over bed		2,7 mm dolomite chips, 8 kV over precharger, 5 kV over bed		2,7 mm dolomite chips, 5 kV over precharger, 10 kV over bed	
JIS fly ash, 20 °C Bed velocity 2,12 mh^{-1}		JIS fly ash, 20 °C Bed velocity 2,12 mh^{-1}		JIS fly ash, 20 °C Bed velocity 2,12 mh^{-1}	
Filtration velocity 0,68 ms^{-1}		Filtration velocity 0,68 ms^{-1}		Filtration velocity 0,68 ms^{-1}	
Particle size,µm	Efficiency, %	Particle size,µm	Efficiency, %	Particle size,µm	Efficiency, %
0,3	60,17	0,3	76,92	0,3	76,03
0,5	70,26	0,5	79,75	0,5	75,99
1,5	79,20	1,5	84,08	1,5	84,96
3,0	88,74	3,0	89,40	3,0	92,10
5,0	94,80	5,0	94,34	5,0	95,53
10,0	98,90	10,0	97,94	10,0	99,10